Going Deep – The Past, Present, and Future of Neural Networks in Structural Biology

Jens Meiler

UNIVERSITÄT LEIPZIG

and

VANDERBILT UNIVERSITY

are partner universities: www.leipzig.vanderbilt.edu

Computational Structural and Chemical Biology in the Meiler Lab

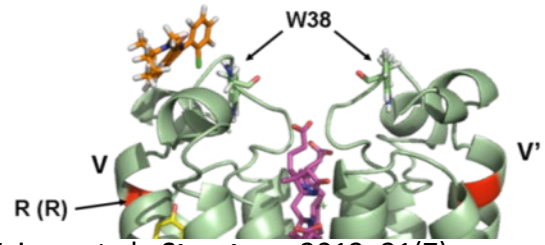

Weiner, et al., **Structure**, 2013, 21(7)

Protein structure prediction de novo and from limited experimental data

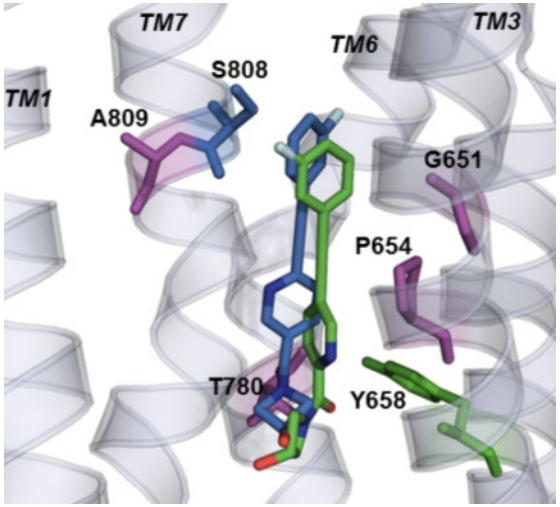

Dong, et al., **PLoS ONE**, 2013, 8(7)

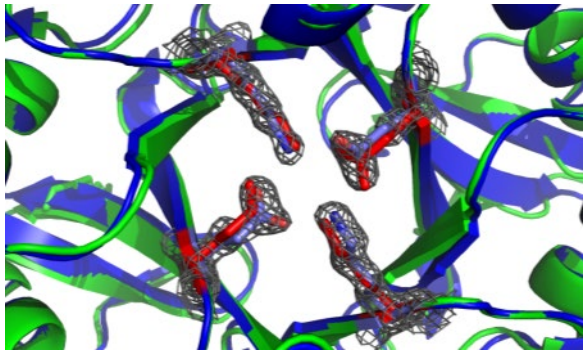

Fortenberry, et al., **JACS**, 2011, 133(45)

Design of large protein scaffolds, antibodies, and protein/ligand interfaces

Merging ligand- and structure-based computer-aided drug discovery

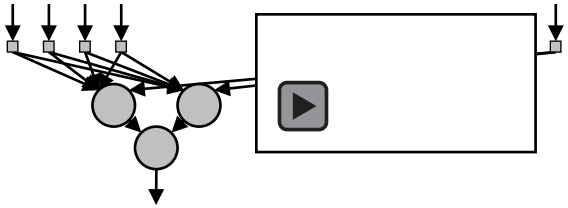

Muller, et al., **ChemMedChem**, 2012, 7(3)

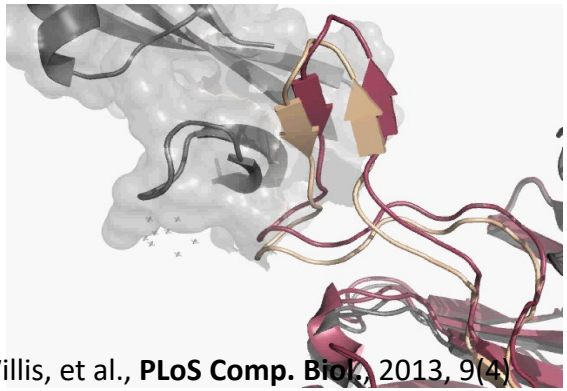

Willis, et al., **PLoS Comp. Biol.**, 2013, 9(4)

Alexander et al., **NSMB**, 2014, 21(1)

The (Inverse) Protein Folding Problem Holy Grail of Comp. Structural Biology

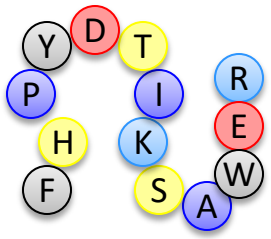

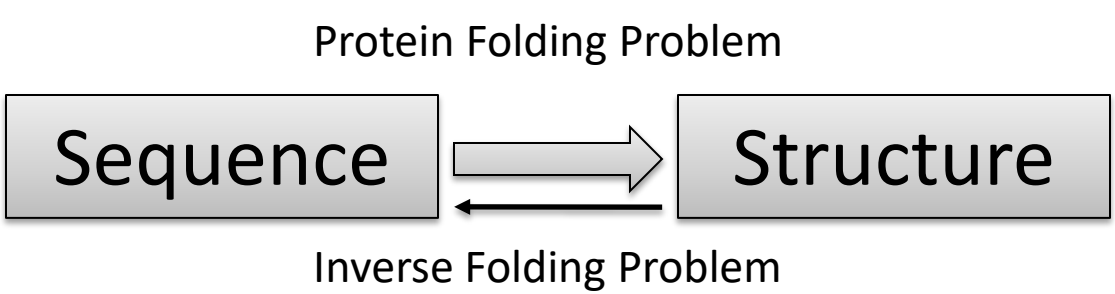

- Given a protein's AA sequence, what is its 3-dimensional fold , and how does it get there?
- Assume 100 conformations for each amino acid in a 100 amino acid protein ⇨ 10^{200} possible conformations!
- Cyrus Levinthal's paradox of protein folding,1968.

Rosetta: A Unified Framework for Tackling Molecular Modeling

A. Leaver-Fay, et al.; "ROSETTA3: an object-oriented software suite …"; Methods Enzymol; 2011; Vol. 487 p. 545-74.
J. K. Leman, et al.; "Macromolecular modeling and design in Rosetta: recent methods and frameworks"; Nat Methods; 2020; Vol. 17 (7): p. 665-680.

Rosetta: A Unified Framework for Tackling Molecular Modeling

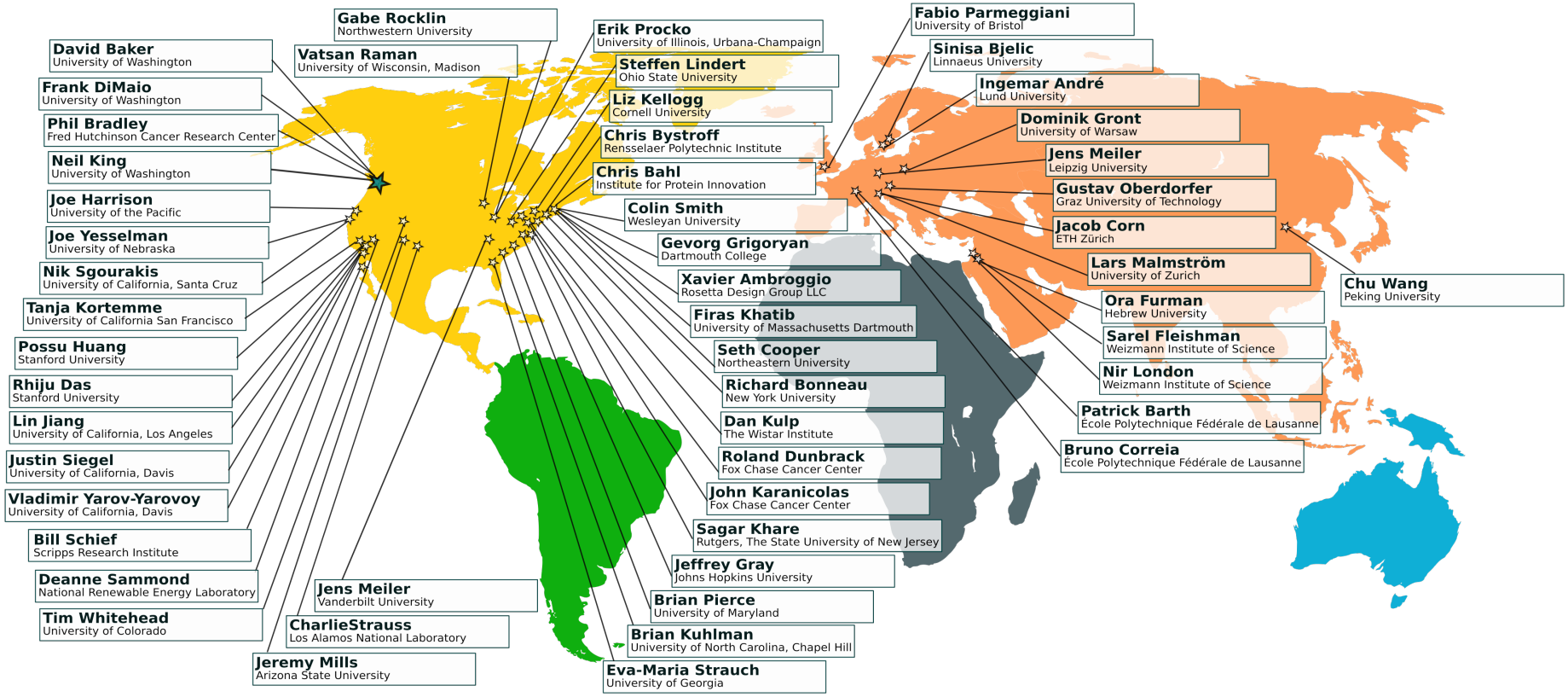

A. Leaver-Fay, et al.; "ROSETTA3: an object-oriented software suite …"; Methods Enzymol; 2011; Vol. 487 p. 545-74.
J. K. Leman, et al.; "Macromolecular modeling and design in Rosetta: recent methods and frameworks"; Nat Methods; 2020; Vol. 17 (7): p. 665-680.

Peptide Bond Formation and Folding of Protein Tertiary Structure

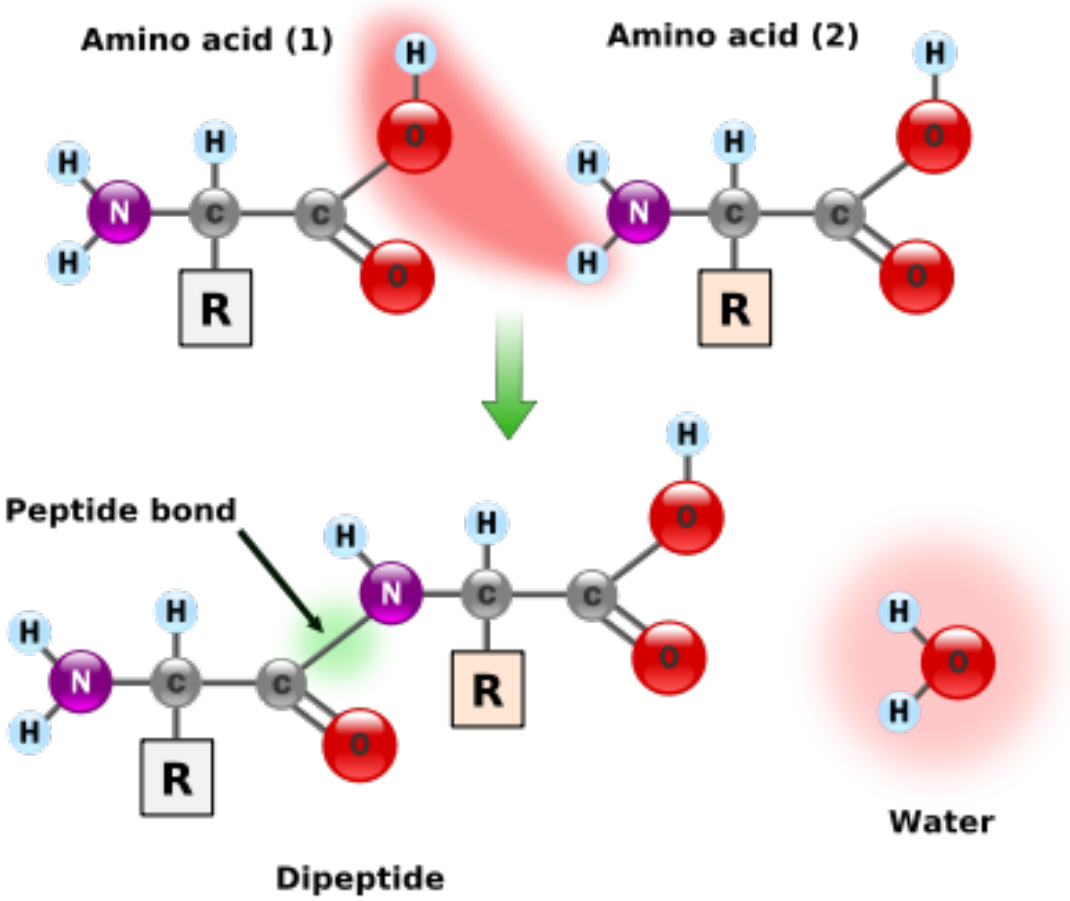

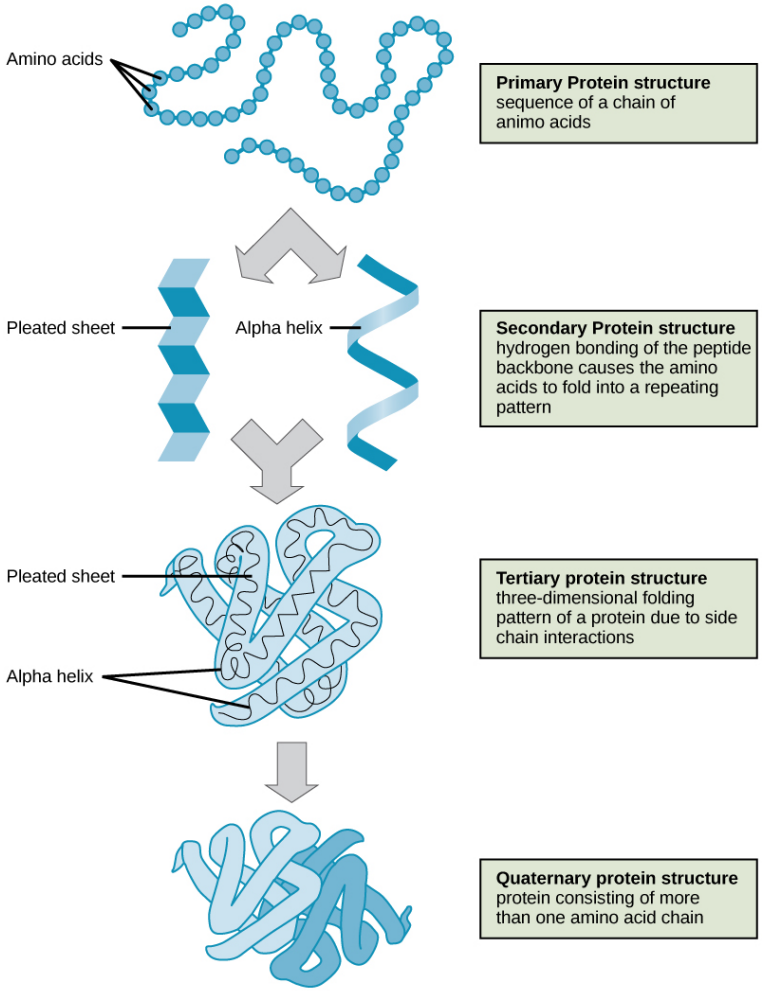

Protein Folding is Driven by the Minimization of Free Energy

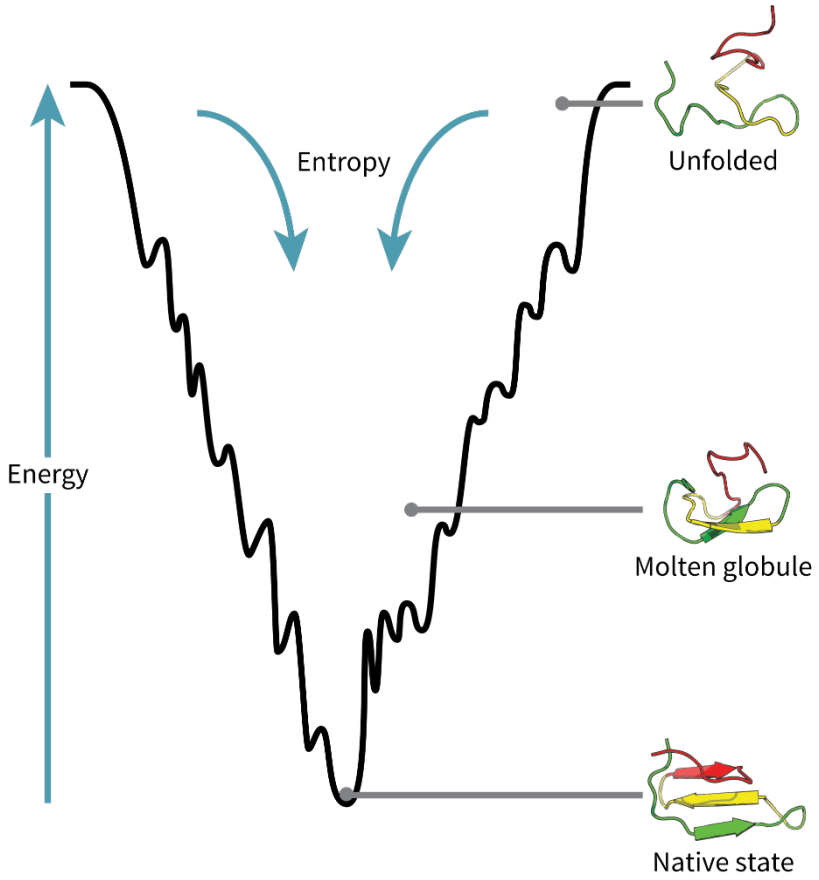

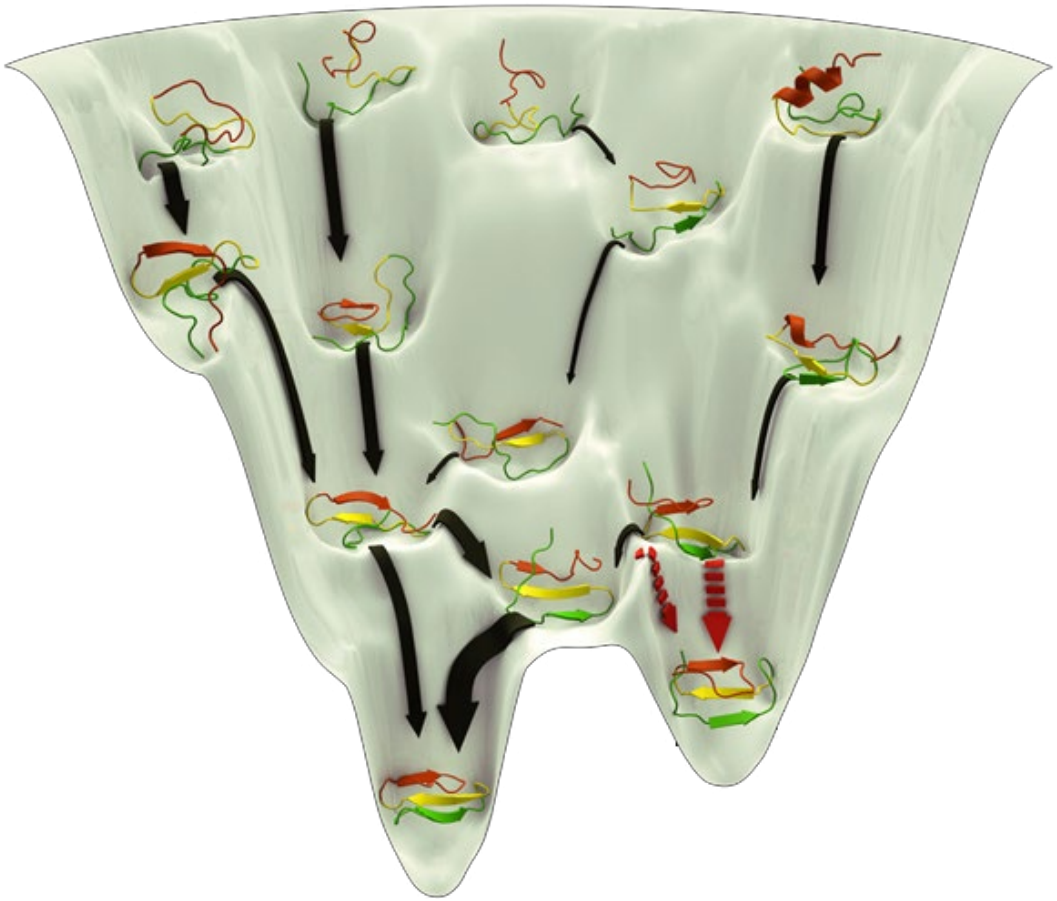

Thomas Splettstoesser (www.scistyle.com)

Protein Tertiary Structure is Tied to Function

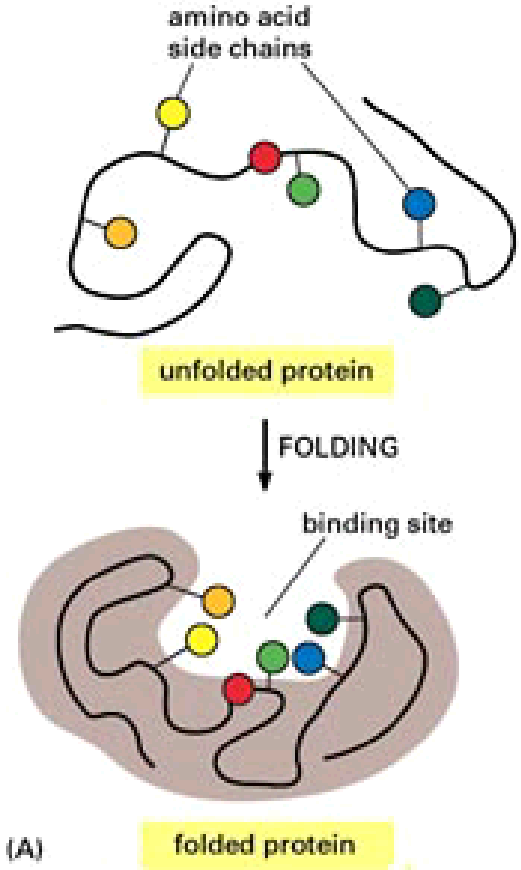

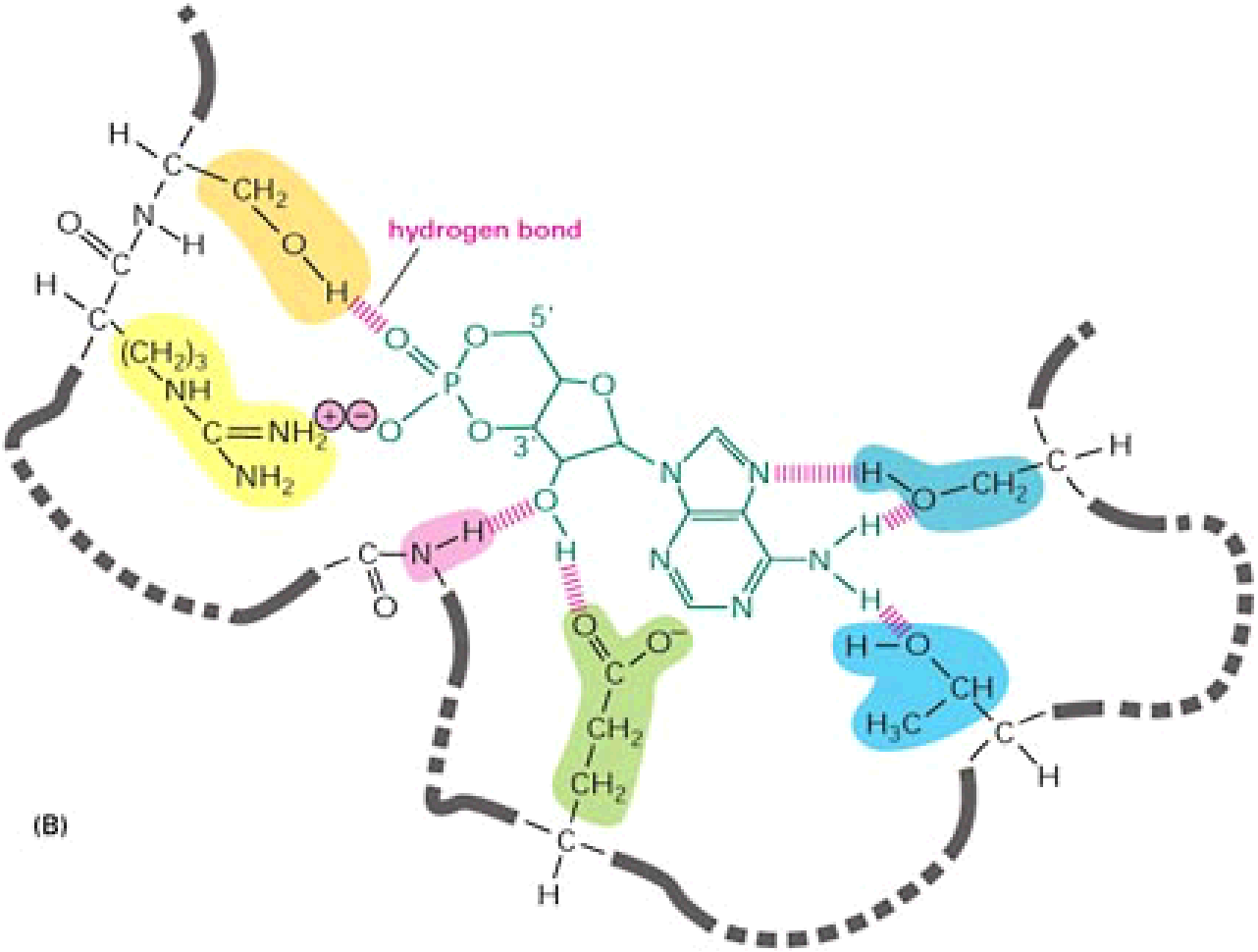

Did AlphaFold “solve” the Protein Folding Problem?

PROTEINFALTUNG VORHERSAGBAR?

Künstliche Intelligenz macht ernst im Biolabor

VON JOACHIM MÜLLER-JUNG - AKTUALISIERT AM 01.12.2020 - 16:42

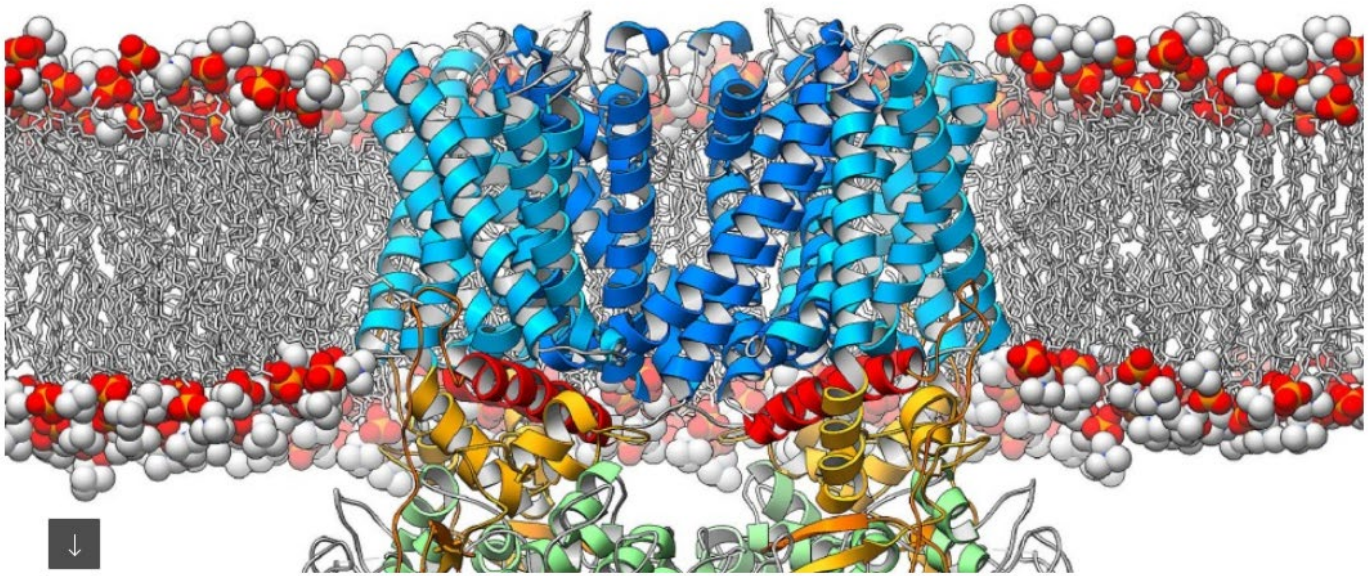

Lebenswissenschaftler verneigen sich. Doch hat DeepMind mit seiner lernenden Maschine „AlphaFold“ wirklich ein Jahrzehnte altes Problem der Biologie gelöst, wie behauptet wird? Eine Umfrage unter unabhängigen Experten.

Critical Assessment of protein Structure Prediction (CASP) – established 1994

- CASP is a community-wide, worldwide experiment for protein structure prediction taking place every two years since 1994.
- CASP provides research groups with an opportunity to objectively test their structure prediction methods and delivers an independent assessment of the state of the art in protein structure modeling to the research community and software users.
- Even though the primary goal of CASP is to help advance the methods of identifying protein three-dimensional structure from its amino acid sequence many view the experiment more as a “world championship” in this field of science.
- More than 100 research groups from all over the world participate in CASP on a regular basis and it is not uncommon for entire groups to suspend their other research for months while they focus on getting their servers ready for the experiment and on performing the detailed predictions.

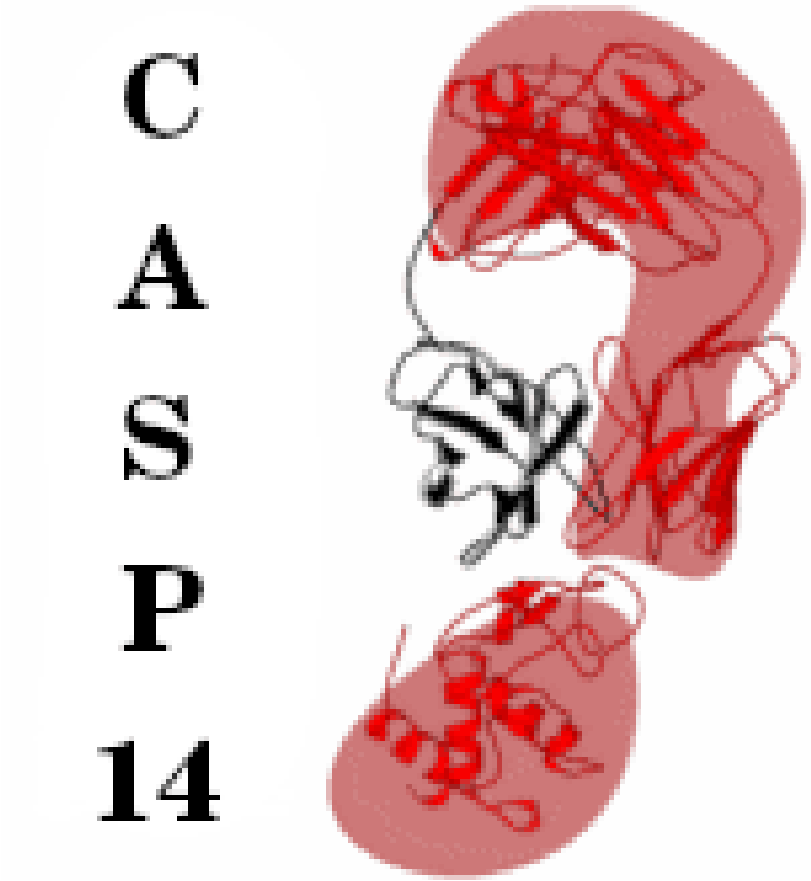

Critical Assessment of protein Structure Prediction (CASP) – established 1994

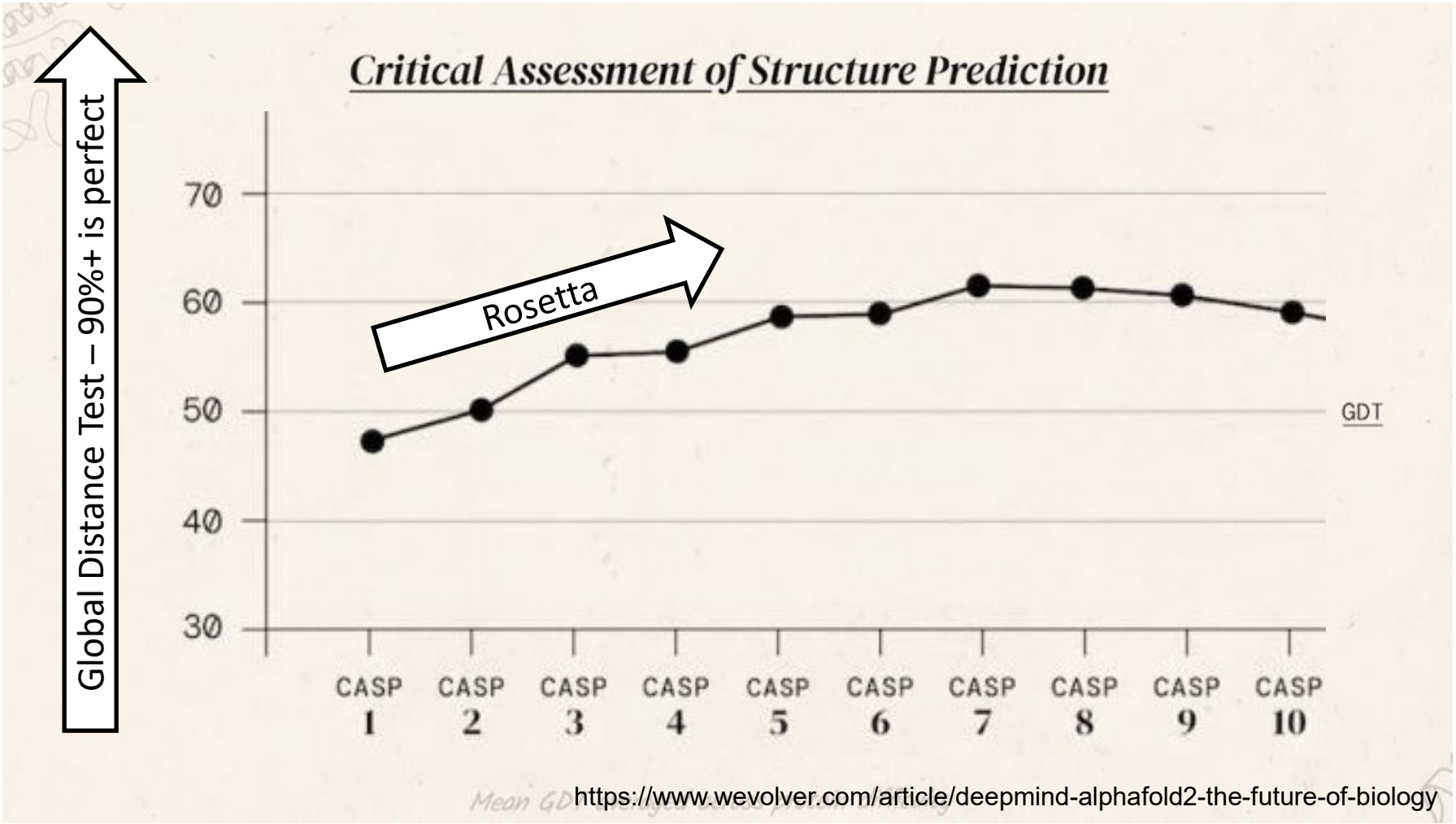

https://www.wevolver.com/article/deepmind-alphafold2-the-future-of-biology

Critical Assessment of protein Structure Prediction (CASP) – established 1994

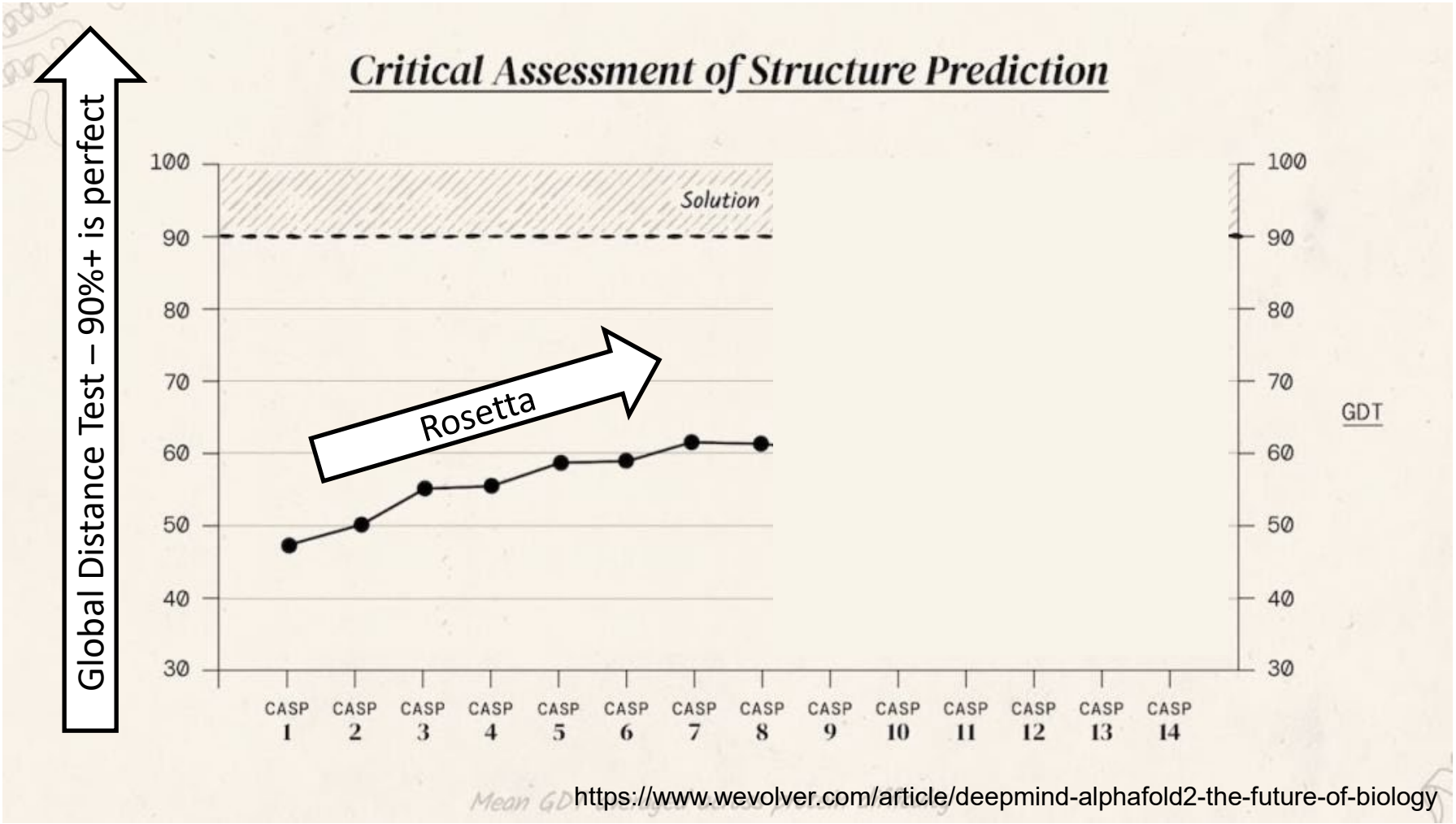

https://www.wevolver.com/article/deepmind-alphafold2-the-future-of-biology

Critical Assessment of protein Structure Prediction (CASP) – established 1994

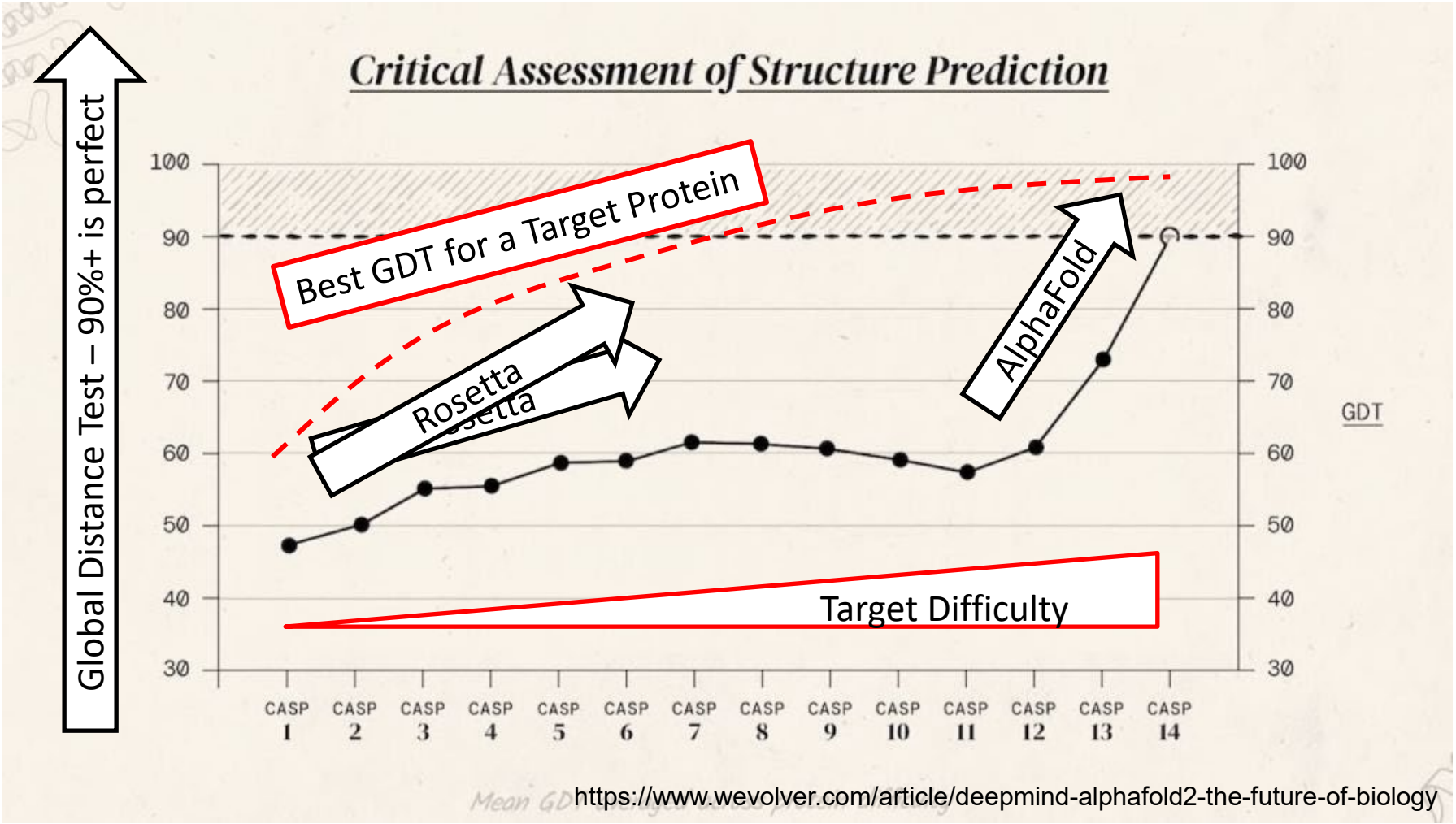

https://www.wevolver.com/article/deepmind-alphafold2-the-future-of-biology

Highly accurate protein structure prediction with AlphaFold

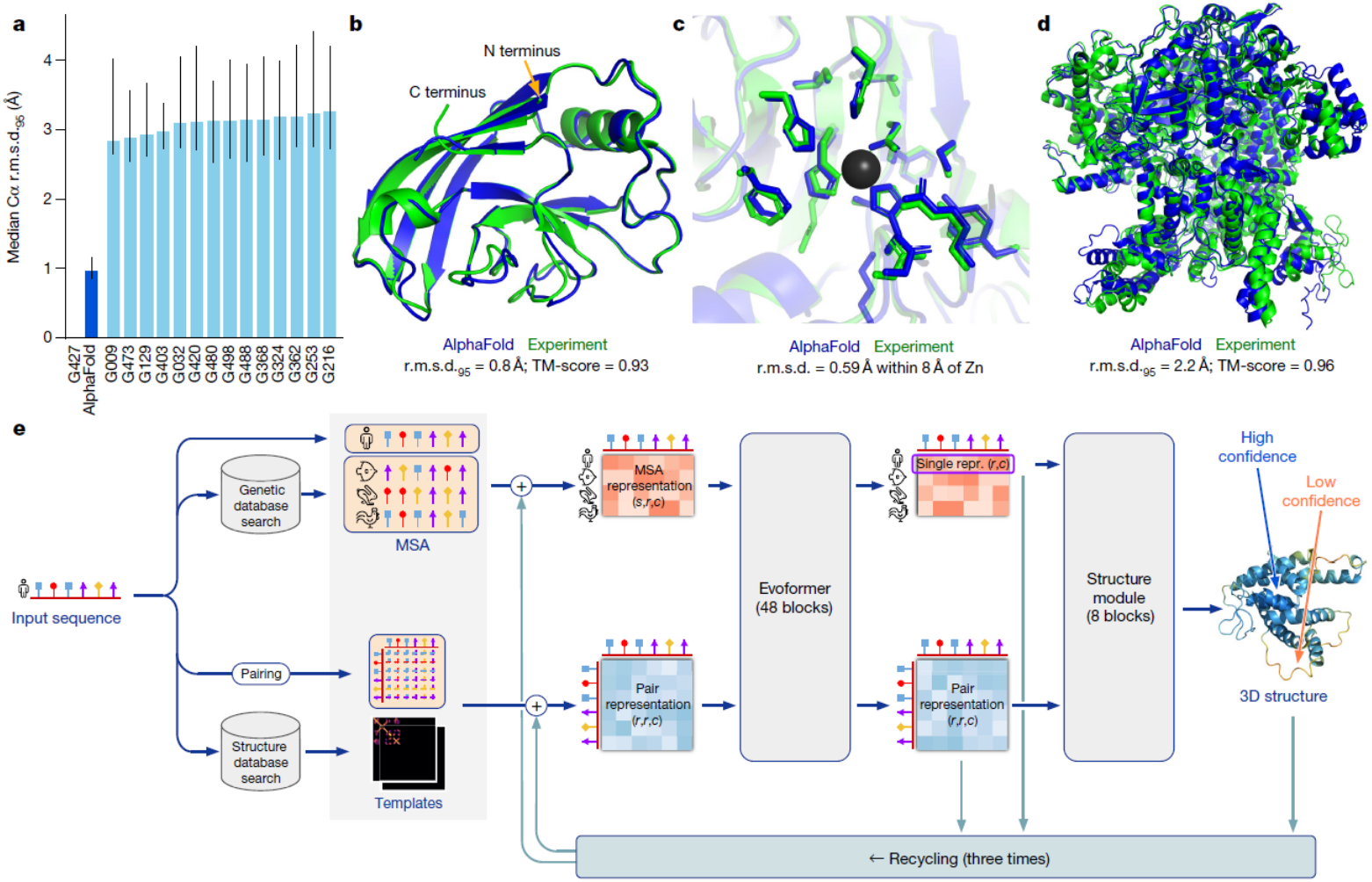

J. Jumper, et al.; "Highly accurate protein structure prediction with AlphaFold"; *Nature*; **2021**; Vol. 596 (7873): p. 583-589.

AlphaFoldMania – The number of research papers and preprints

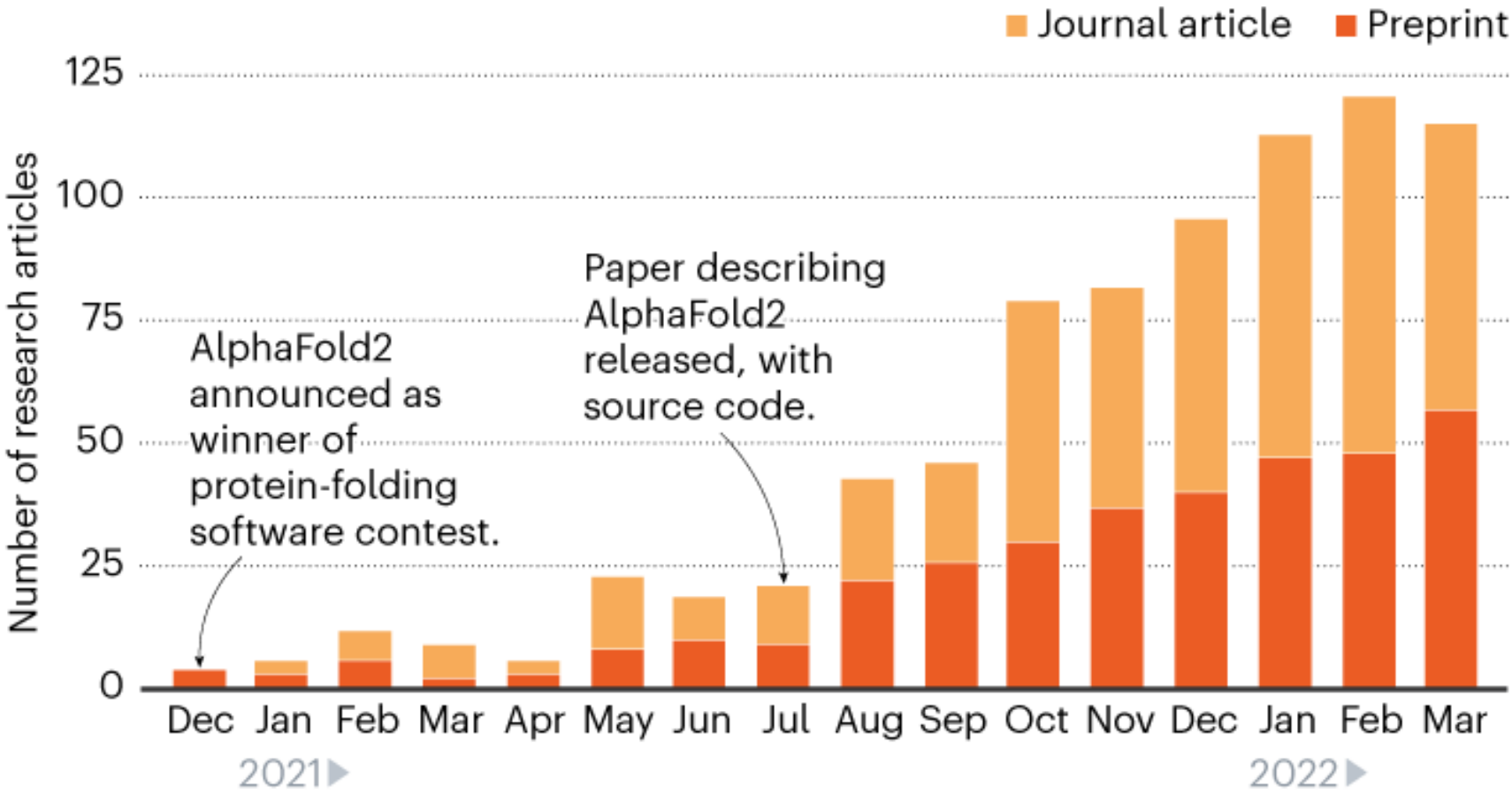

Nature, News Feature, 13 April 2022

Molecular Architecture of the Human Caveolin-1 Complex with AlphaFold2

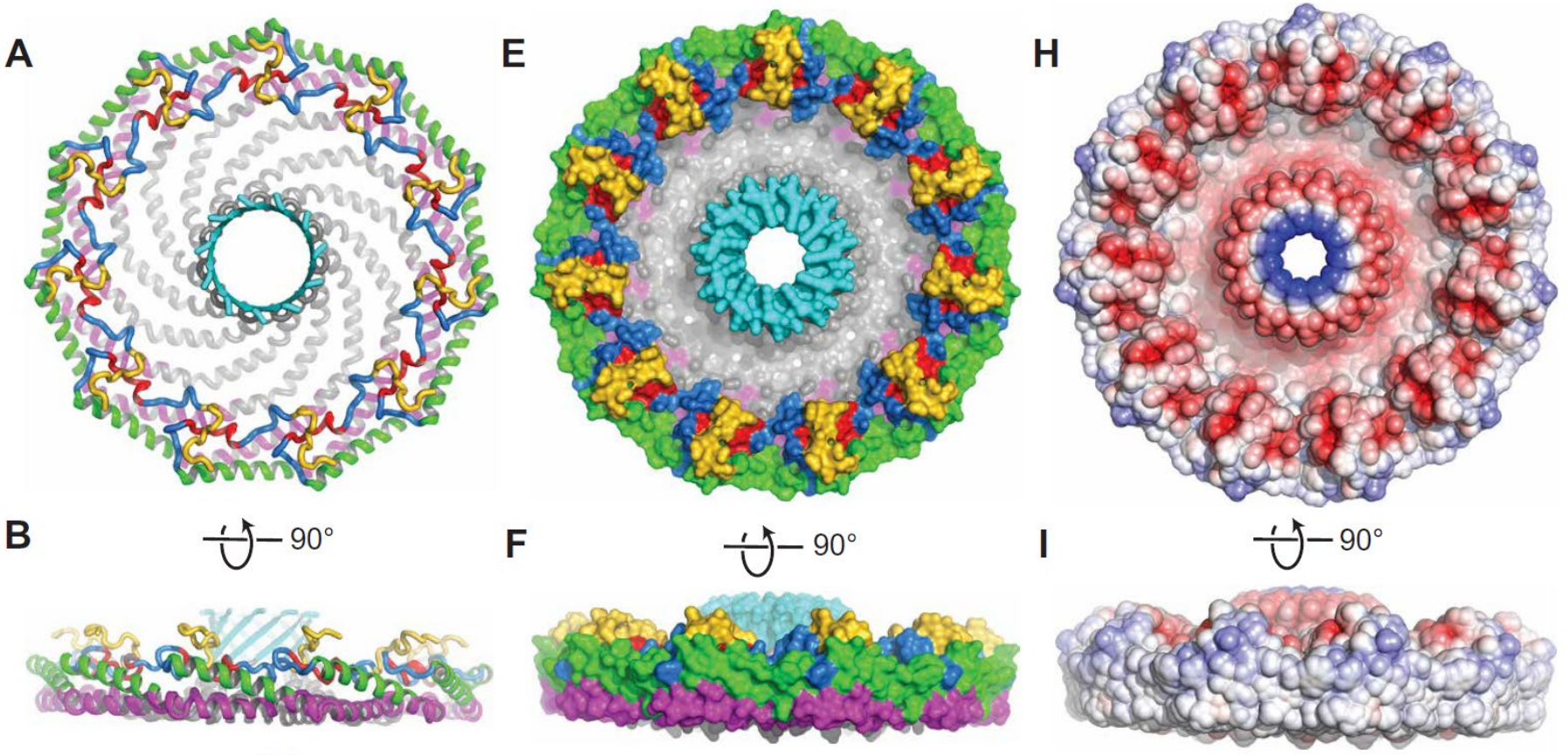

J. C. Porta, B. Han, A. Gulsevin, J. Chung, Y. Peskova, S. Connolly, H. S. Mchaourab, J. Meiler, E. Karakas, A. K. Kenworthy and M. D. Ohi; "Molecular architecture of the human caveolin-1 complex"; *Science Advances*; **2022**; Vol. p.

Molecular Architecture of the Human Caveolin-1 Complex with AlphaFold2

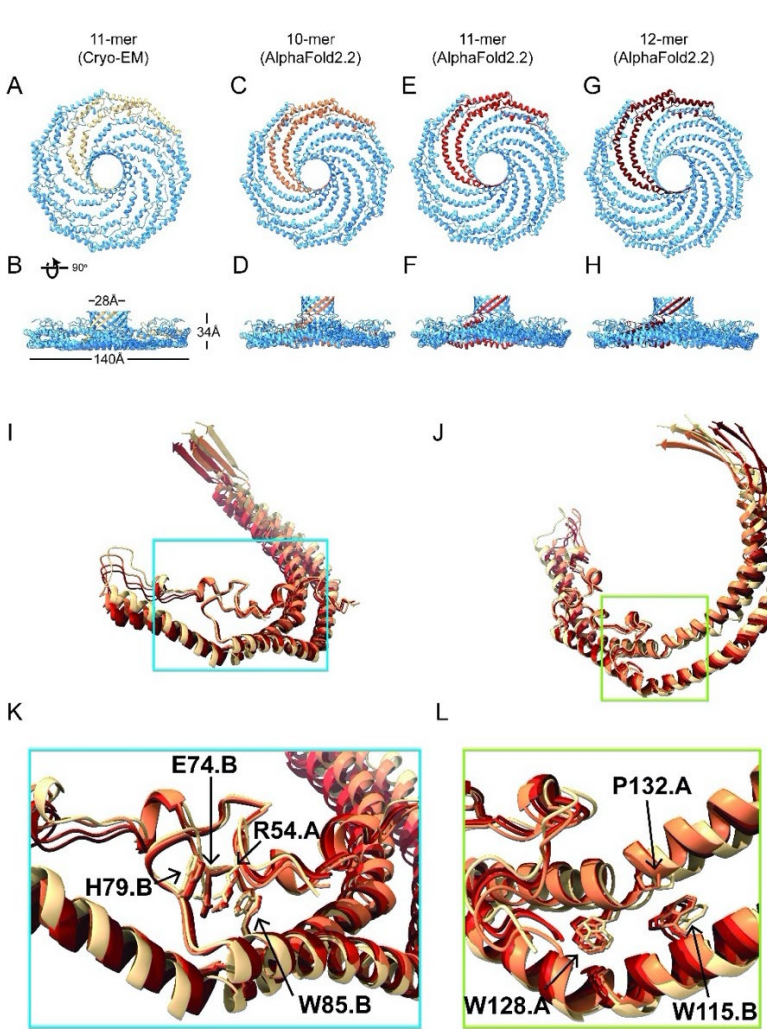

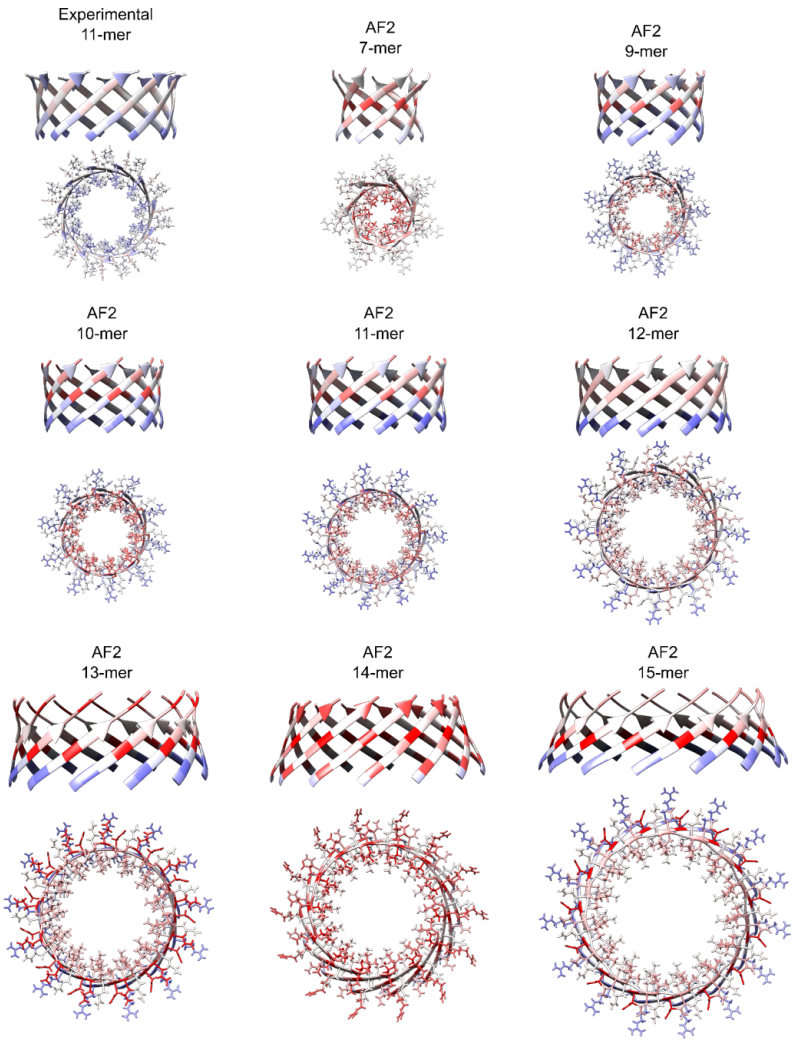

A. Gulsevin, B. Han, J. C. Porta, H. S. McHaourab, J. Meiler and A. K. Kenworthy; "Template-free prediction of a new monotopic membrane protein fold and assembly by AlphaFold2"; *Biophys J;* ***2022; Vol. p.***

J. C. Porta, B. et al. "Molecular architecture of the human caveolin-1 complex"; *Science Advances*; **2022**; Vol. p.

Molecular Architecture of the Human Caveolin-1 Complex with AlphaFold2

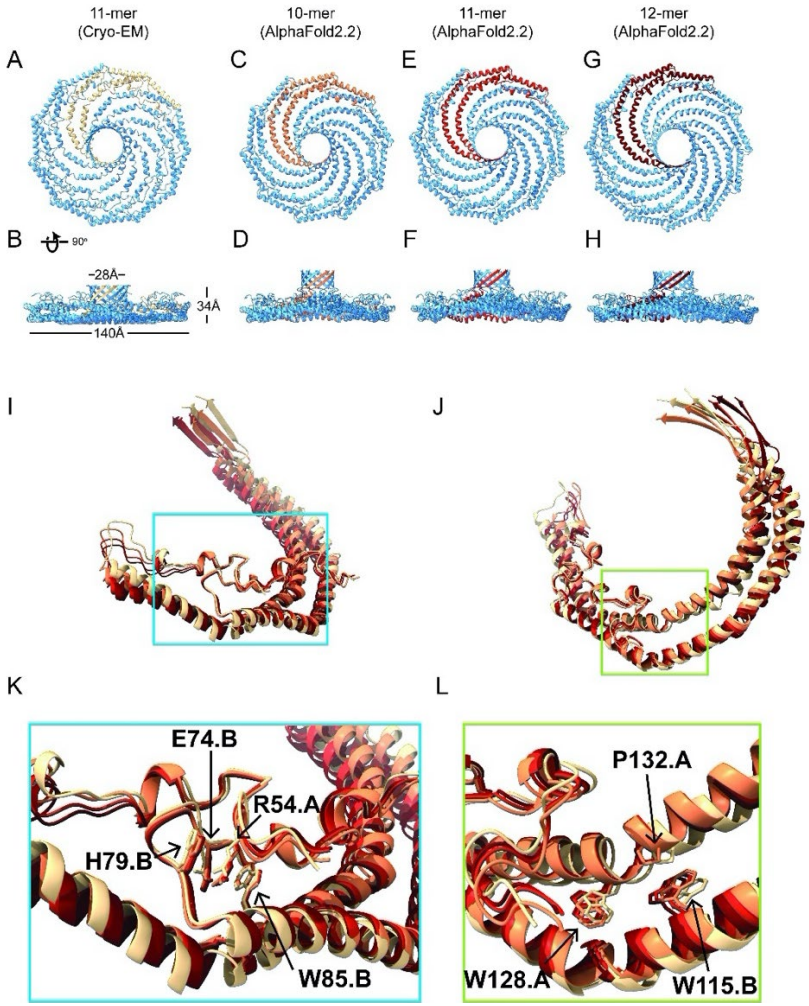

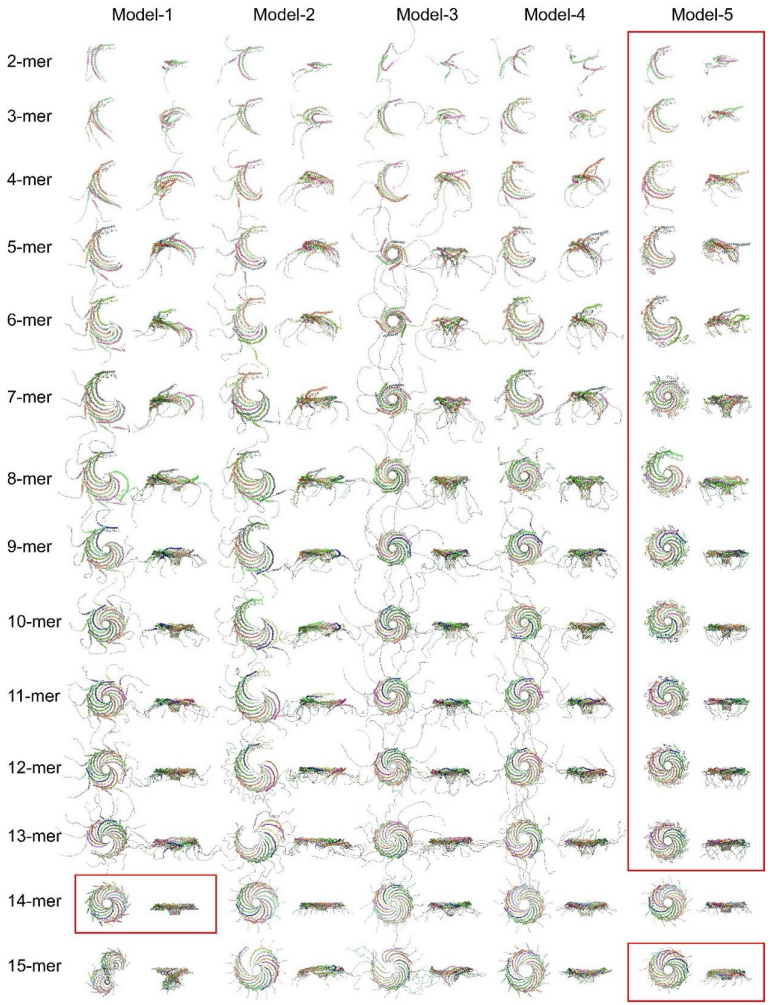

A. Gulsevin, B. Han, J. C. Porta, H. S. McHaourab, J. Meiler and A. K. Kenworthy; "Template-free prediction of a new monotopic membrane protein fold and assembly by AlphaFold2"; *Biophys J;* ***2022; Vol. p.***

J. C. Porta, B. et al. "Molecular architecture of the human caveolin-1 complex"; *Science Advances*; **2022**; Vol. p.

Sampling Alternative Conformational States with AlphaFold2

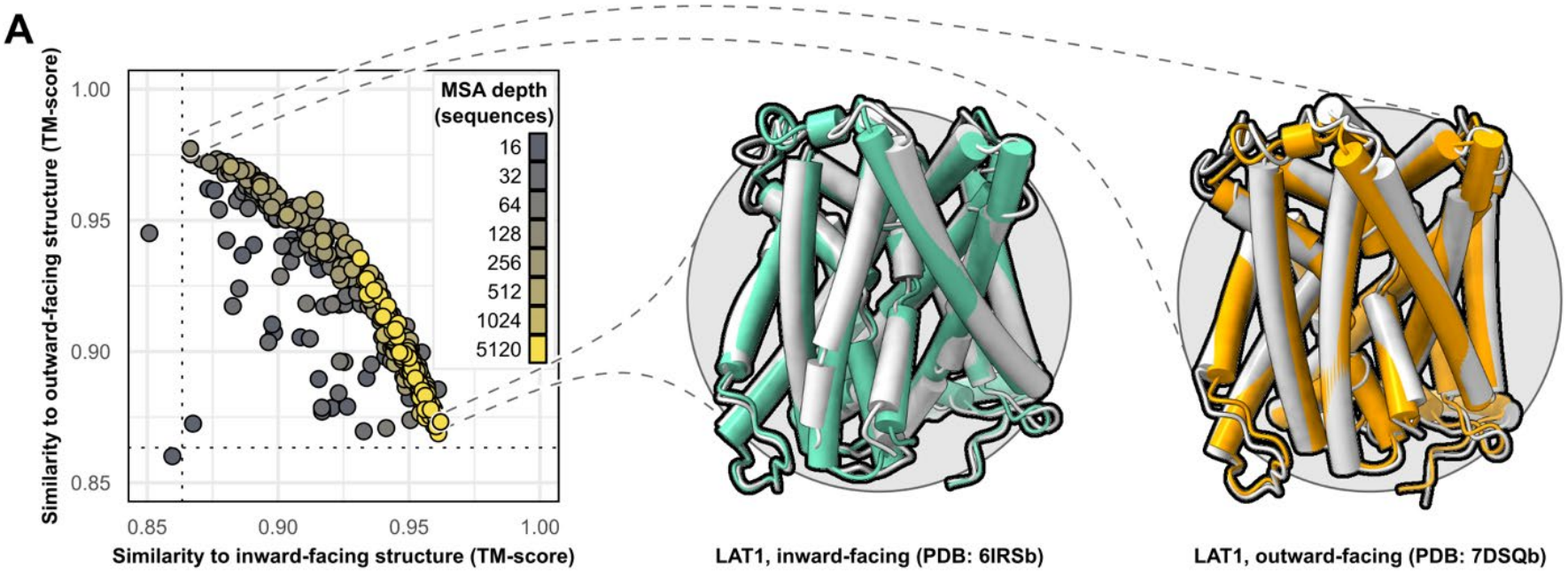

Figure 1. Alternative conformations of transporters and GPCRs can be predicted by AF2. (A) Representative models of the transporter LAT1 in IF and OF conformations. Experimental structures shown in gray and models shown in teal and orange.

D. Del Alamo, D. Sala, H. S. McHaourab and J. Meiler; "Sampling alternative conformational states of transporters and receptors with AlphaFold2"; *Elife*; **2022**; Vol. 11 p.

AF2 Predicted Conformations for the Adhesion GPCR ADGRG5/GPR114

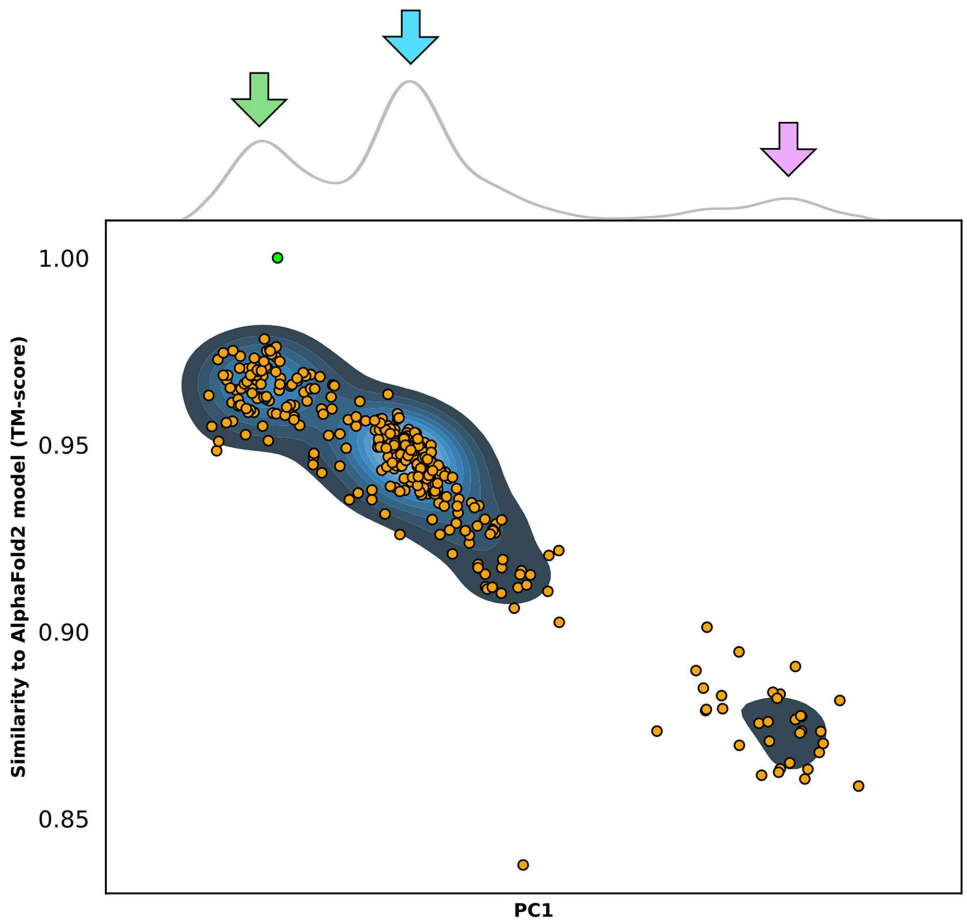

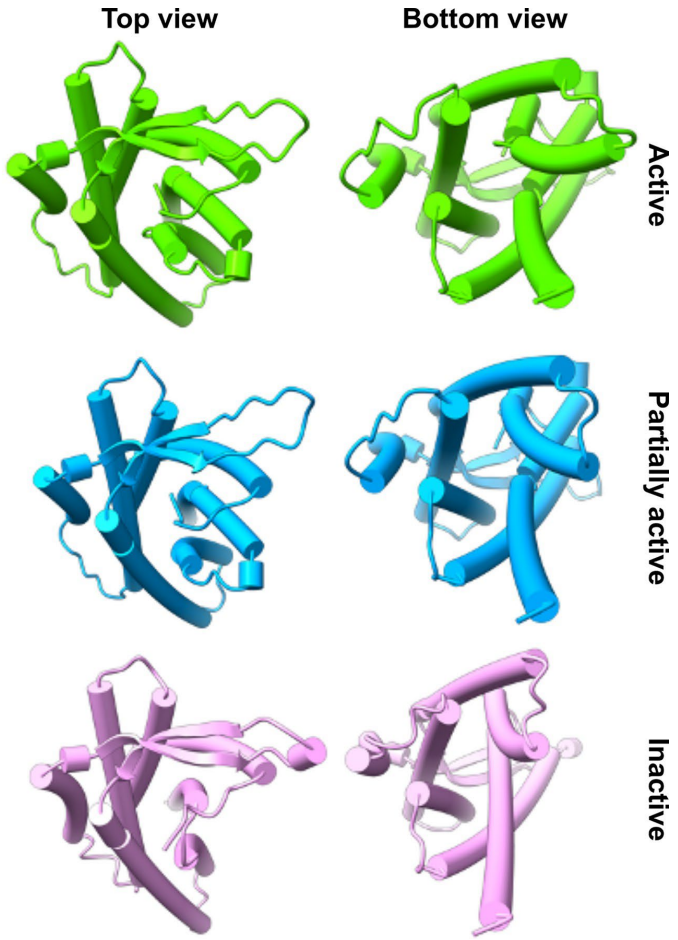

D. Del Alamo, D. Sala, H. S. McHaourab and J. Meiler; "Sampling alternative conformational states of transporters and receptors with AlphaFold2"; *Elife*; **2022**; Vol. 11 p.

Integrating Limited Experimental Data: NMR, EPR, MassSpec, cryo-EM, …

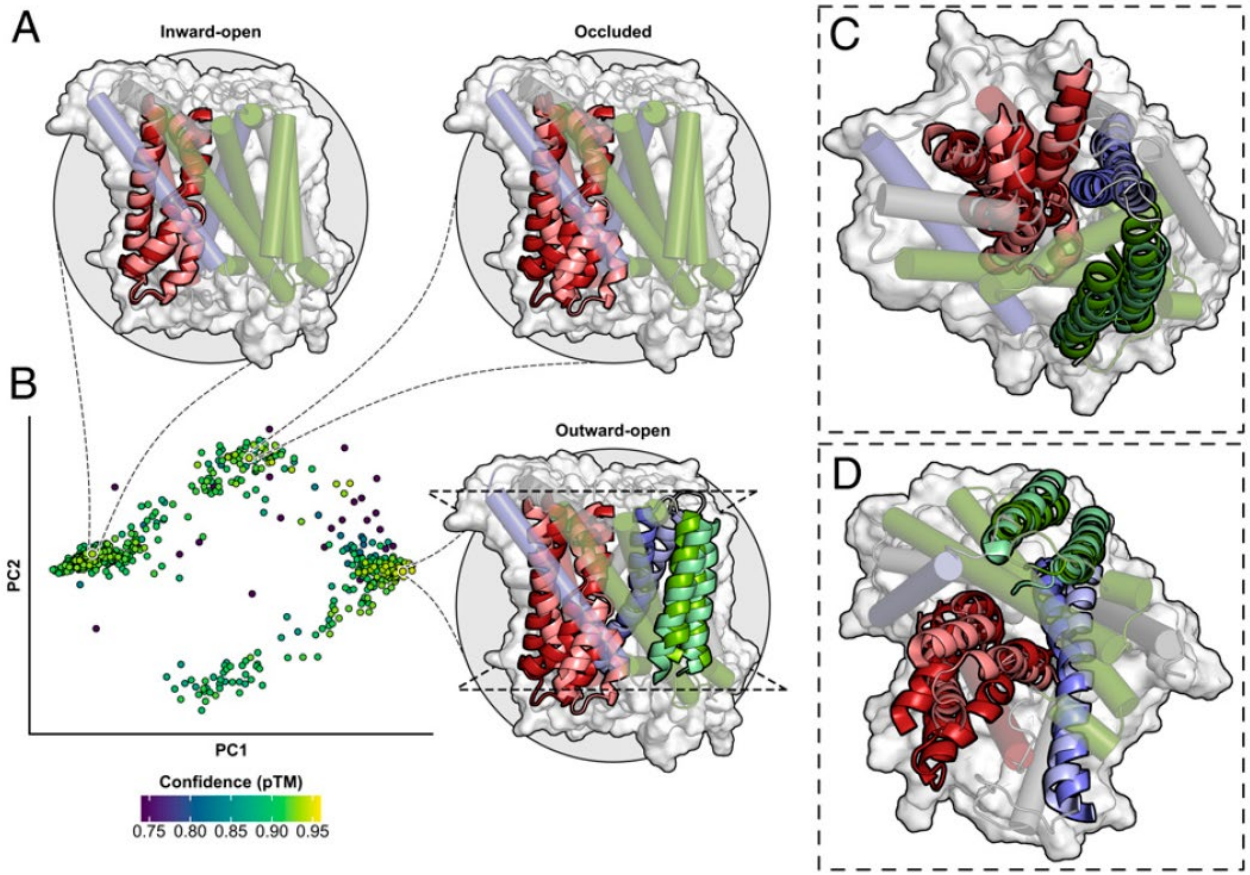

D. Del Alamo, L. DeSousa, R. M. Nair, S. Rahman, J. Meiler and H. S. Mchaourab; "Integrated AlphaFold2 and DEER investigation of the conformational dynamics of a pH-dependent APC antiporter"; *Proc Natl Acad Sci U S A;* ***2022; Vol. 119 (34): p. e2206129119***

AlphaFold Protein Structure Database 200 Million Predicted Protein Structures

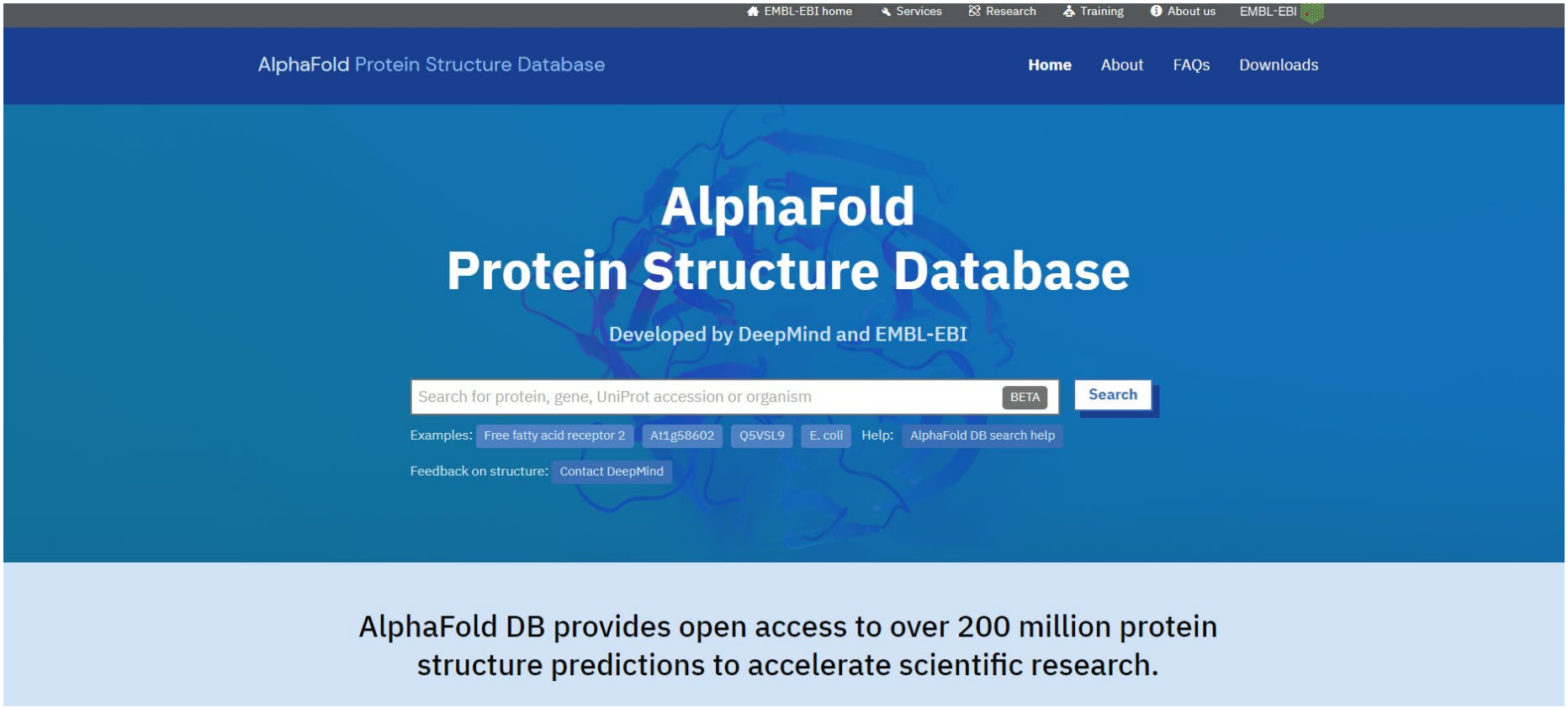

Since 1993(!) – Neural Networks for Chemists

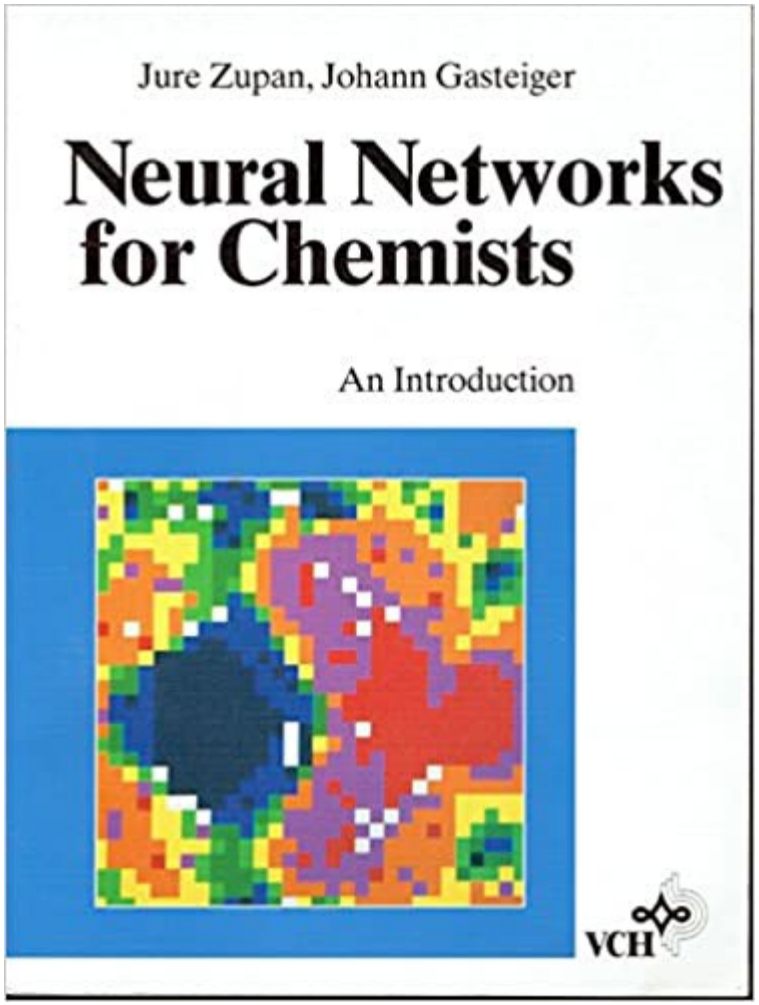

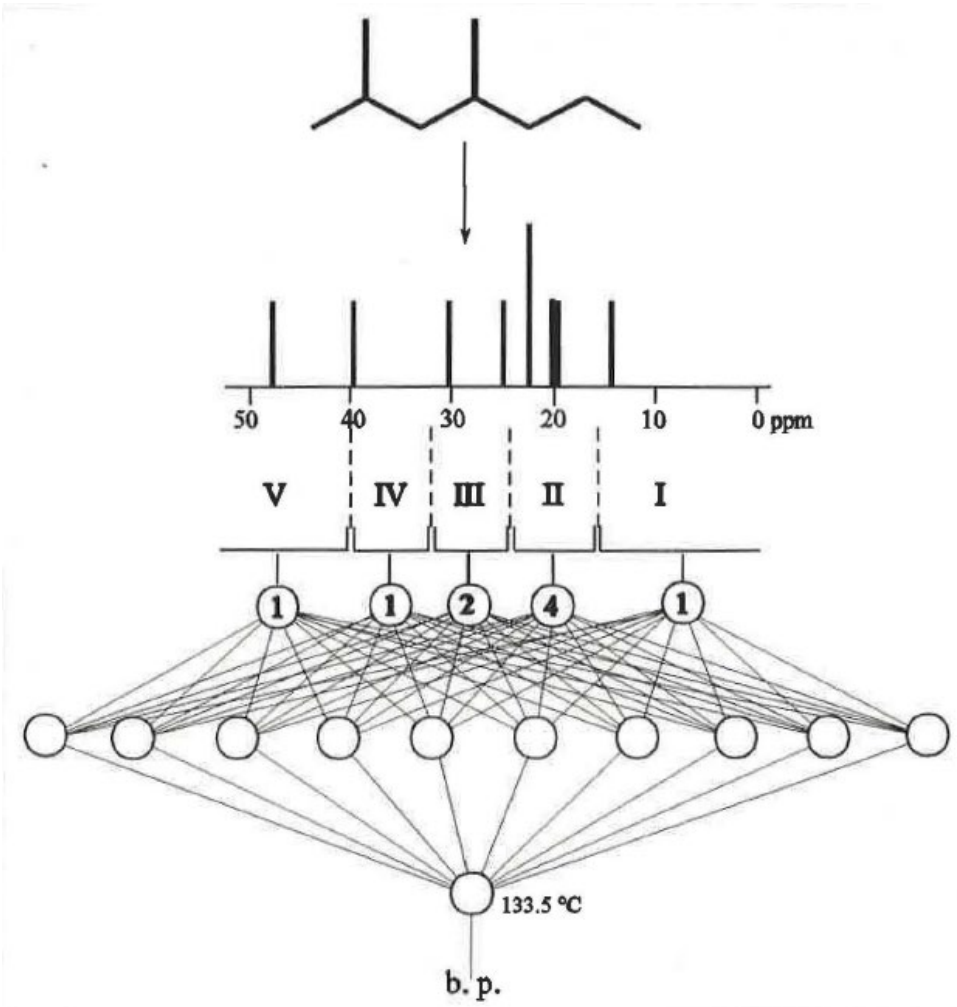

J. Meiler and R. Meusinger "Use of Neural Networks to Determine Properties of Alkanes from their 13C-NMR Spectra" in *Software - Entwicklung in der Chemie*; Gasteiger, J., Ed. Gesellschaft Deutscher Chemiker: Frankfurt am Main; **1995**; Vol. 10: p. 259-263.

Back Propagation of Errors is the most popular Training Algorithm

- Teaching process of multi-layer neural network employing *backpropagation* algorithm. To illustrate this process, consider the three layer neural network with two inputs and one output:

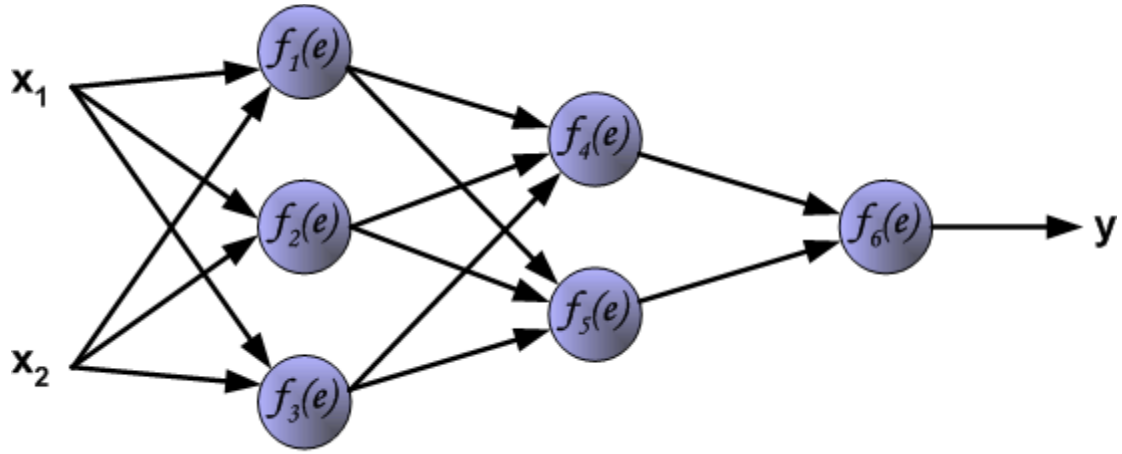

http://galaxy.agh.edu.pl/~vlsi/AI/backp_t_en/backprop.html

Back Propagation of Errors is the most popular Training Algorithm

- Each neuron is composed of two units. First unit adds products of weights coefficients and input signals. The second unit realizes nonlinear function, called neuron activation function. Signal *e* is summed weighted input signal, and *y = f(e)* is output signal of nonlinear element. Signal *y* is also output signal of neuron:

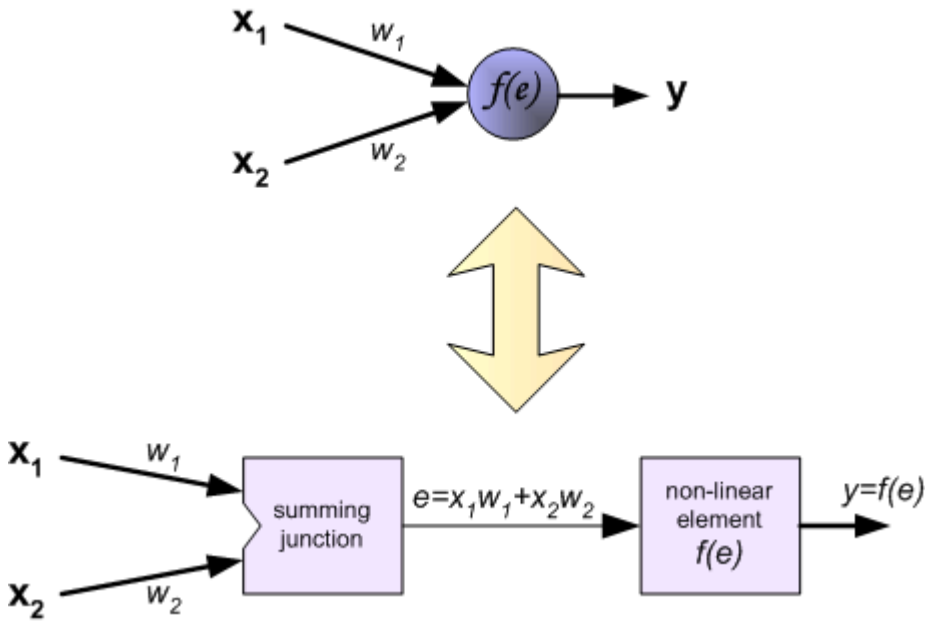

http://galaxy.agh.edu.pl/~vlsi/AI/backp_t_en/backprop.html

Back Propagation of Errors is the most popular Training Algorithm

- To teach the neural network we need training data set. The training data set consists of input signals (x_1 and x_2) assigned with corresponding target (desired output) z. The network training is an iterative process. In each iteration weights coefficients of nodes are modified using new data from training data set. Modification is calculated using algorithm described below: Each teaching step starts with forcing both input signals from training set. After this stage we can determine output signals values for each neuron in each network layer. Pictures below illustrate how signal is propagating through the network, Symbols $w_{(xm)n}$ represent weights of connections between network input x_m and neuron n in input layer. Symbols y_n represents output signal of neuron n.

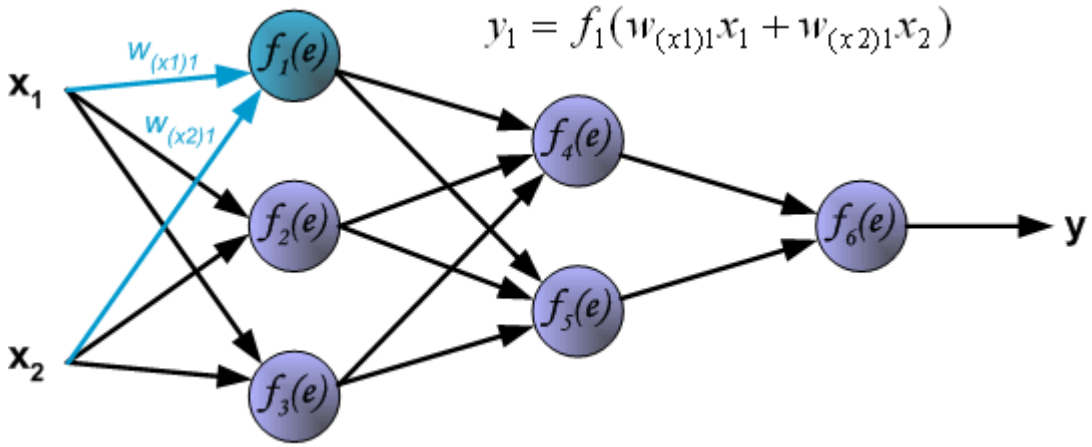

http://galaxy.agh.edu.pl/~vlsi/AI/backp_t_en/backprop.html

Back Propagation of Errors is the most popular Training Algorithm

- To teach the neural network we need training data set. The training data set consists of input signals (x_1 and x_2) assigned with corresponding target (desired output) z. The network training is an iterative process. In each iteration weights coefficients of nodes are modified using new data from training data set. Modification is calculated using algorithm described below: Each teaching step starts with forcing both input signals from training set. After this stage we can determine output signals values for each neuron in each network layer. Pictures below illustrate how signal is propagating through the network, Symbols $w_{(xm)n}$ represent weights of connections between network input x_m and neuron n in input layer. Symbols y_n represents output signal of neuron n.

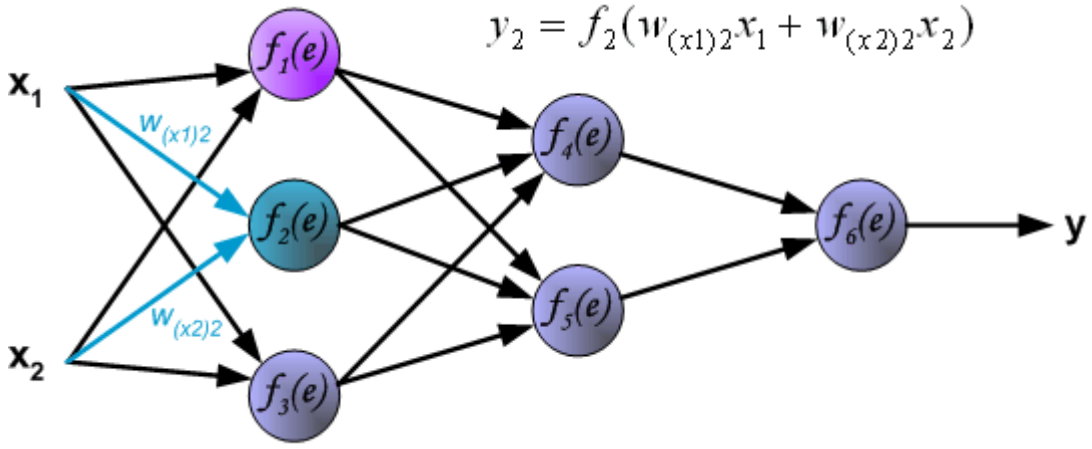

http://galaxy.agh.edu.pl/~vlsi/AI/backp_t_en/backprop.html

Back Propagation of Errors is the most popular Training Algorithm

- To teach the neural network we need training data set. The training data set consists of input signals (x_1 and x_2) assigned with corresponding target (desired output) z. The network training is an iterative process. In each iteration weights coefficients of nodes are modified using new data from training data set. Modification is calculated using algorithm described below: Each teaching step starts with forcing both input signals from training set. After this stage we can determine output signals values for each neuron in each network layer. Pictures below illustrate how signal is propagating through the network, Symbols $w_{(xm)n}$ represent weights of connections between network input x_m and neuron n in input layer. Symbols y_n represents output signal of neuron n.

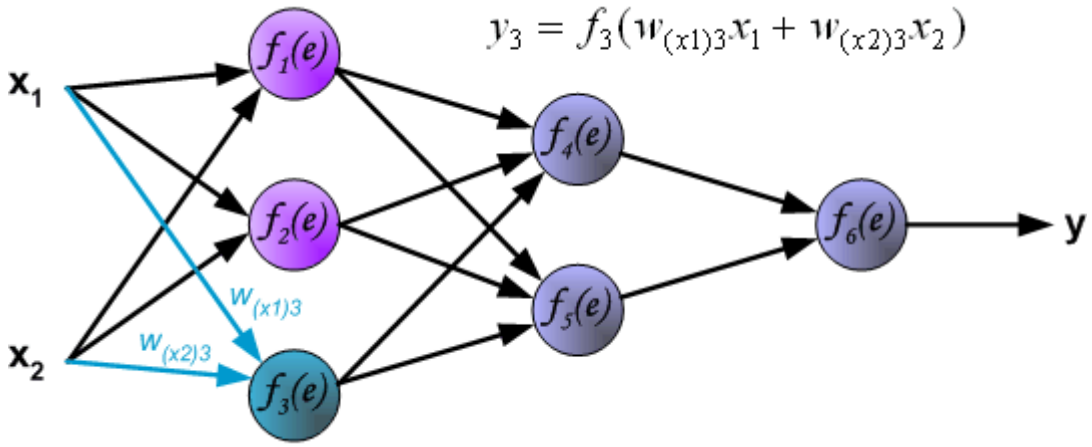

http://galaxy.agh.edu.pl/~vlsi/AI/backp_t_en/backprop.html

Back Propagation of Errors is the most popular Training Algorithm

- Propagation of signals through the hidden layer. Symbols w_{mn} represent weights of connections between output of neuron m and input of neuron n in the next layer.

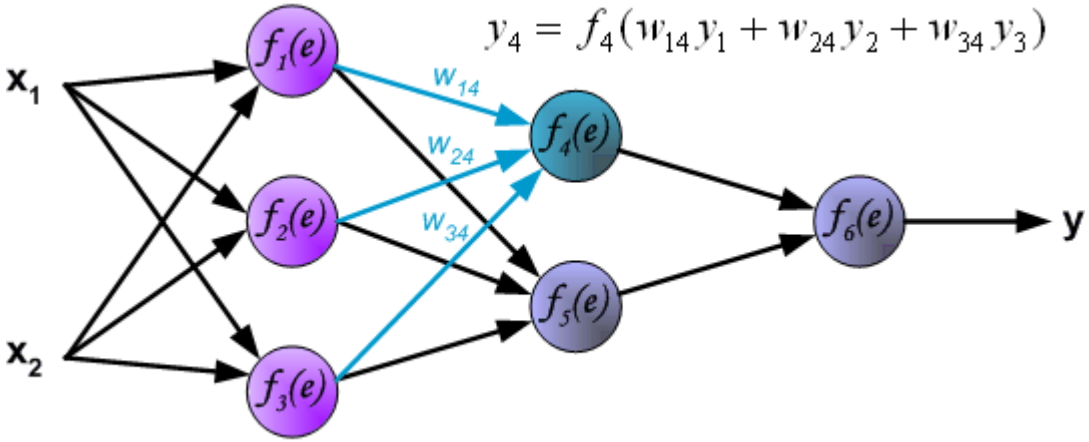

http://galaxy.agh.edu.pl/~vlsi/AI/backp_t_en/backprop.html

Back Propagation of Errors is the most popular Training Algorithm

- Propagation of signals through the hidden layer. Symbols w_{mn} represent weights of connections between output of neuron m and input of neuron n in the next layer.

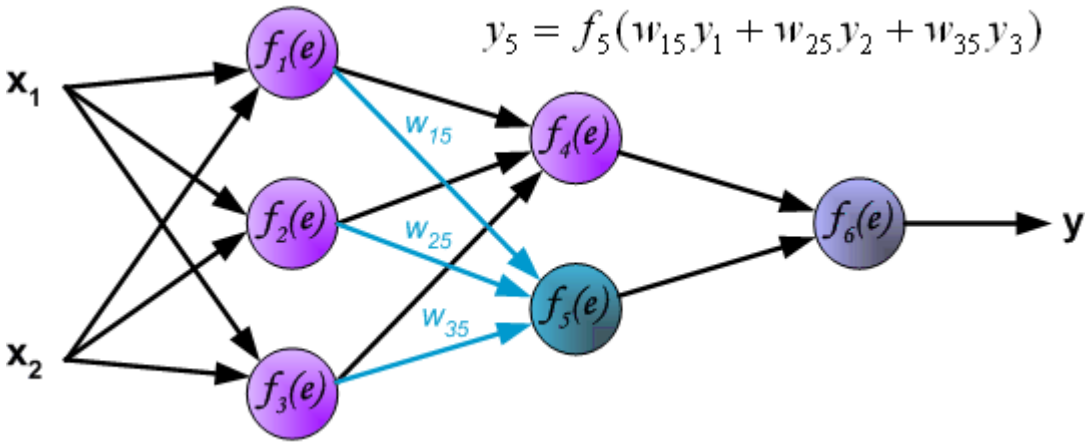

http://galaxy.agh.edu.pl/~vlsi/AI/backp_t_en/backprop.html

Back Propagation of Errors is the most popular Training Algorithm

- Propagation of signals through the output layer.

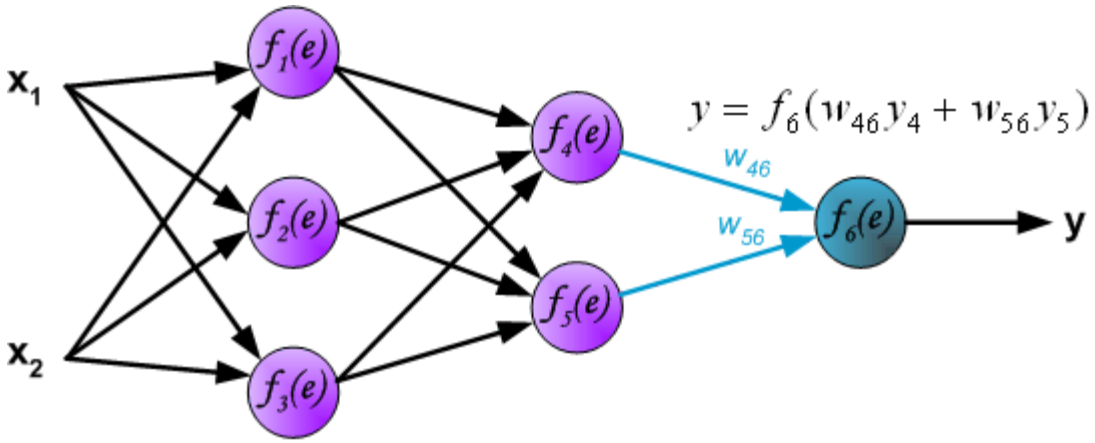

http://galaxy.agh.edu.pl/~vlsi/AI/backp_t_en/backprop.html

Back Propagation of Errors is the most popular Training Algorithm

- In the next algorithm step the output signal of the network *y* is compared with the desired output value (the target), which is found in training data set. The difference is called error signal *d* of output layer neuron.

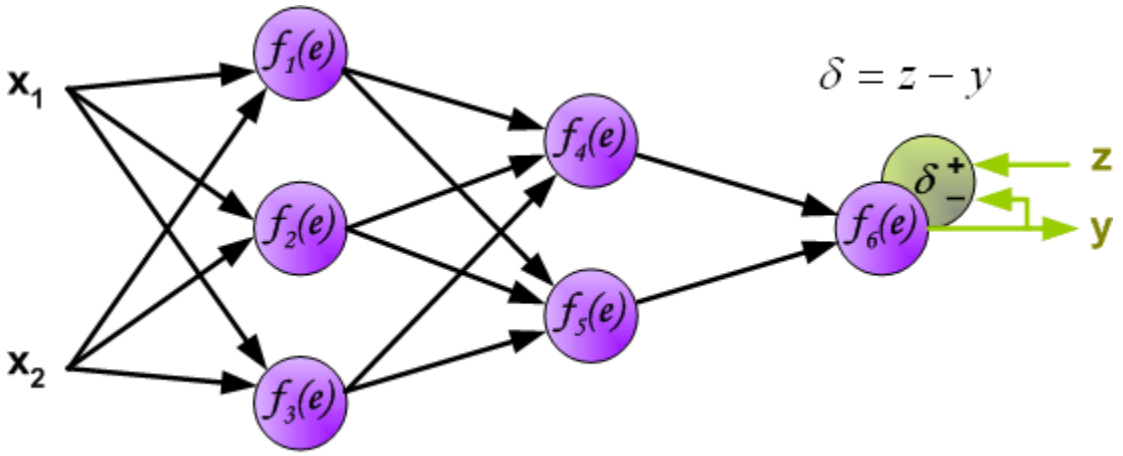

http://galaxy.agh.edu.pl/~vlsi/AI/backp_t_en/backprop.html

Back Propagation of Errors is the most popular Training Algorithm

- It is impossible to compute error signal for internal neurons directly, because output values of these neurons are unknown. The idea is to propagate error signal *d* (computed in single teaching step) back to all neurons, which output signals were input for discussed neuron.

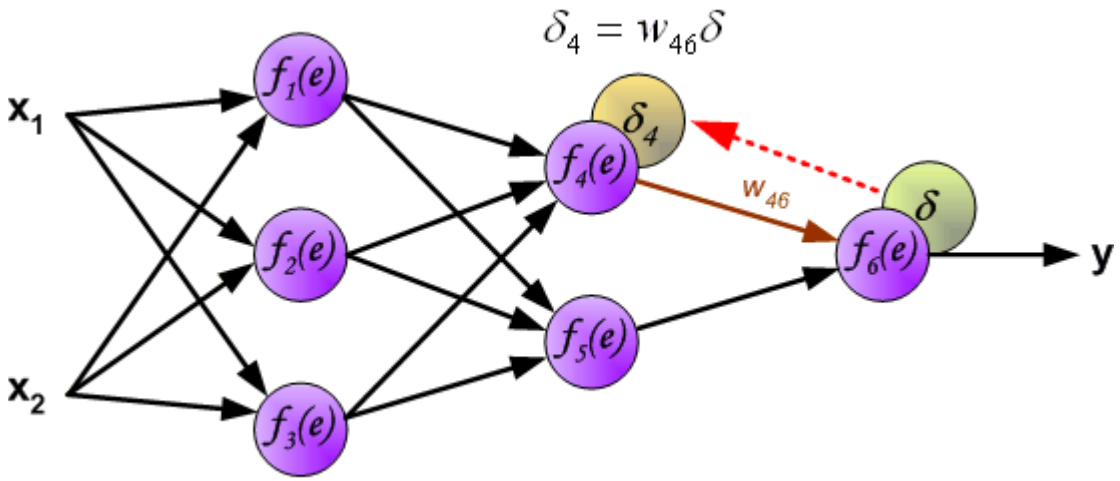

http://galaxy.agh.edu.pl/~vlsi/AI/backp_t_en/backprop.html

Back Propagation of Errors is the most popular Training Algorithm

- It is impossible to compute error signal for internal neurons directly, because output values of these neurons are unknown. The idea is to propagate error signal *d* (computed in single teaching step) back to all neurons, which output signals were input for discussed neuron.

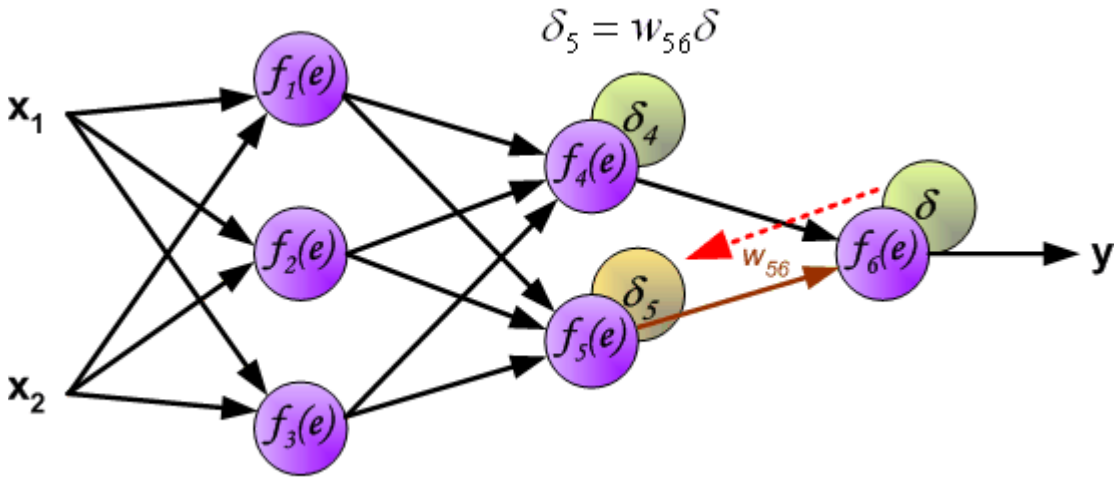

http://galaxy.agh.edu.pl/~vlsi/AI/backp_t_en/backprop.html

Back Propagation of Errors is the most popular Training Algorithm

- The weights' coefficients w_{mn} used to propagate errors back are equal to this used during computing output value. Only the direction of data flow is changed - signals are propagated from output to inputs one after the other. This technique is used for all network layers. If propagated errors came from few neurons they are added. The illustration is below:

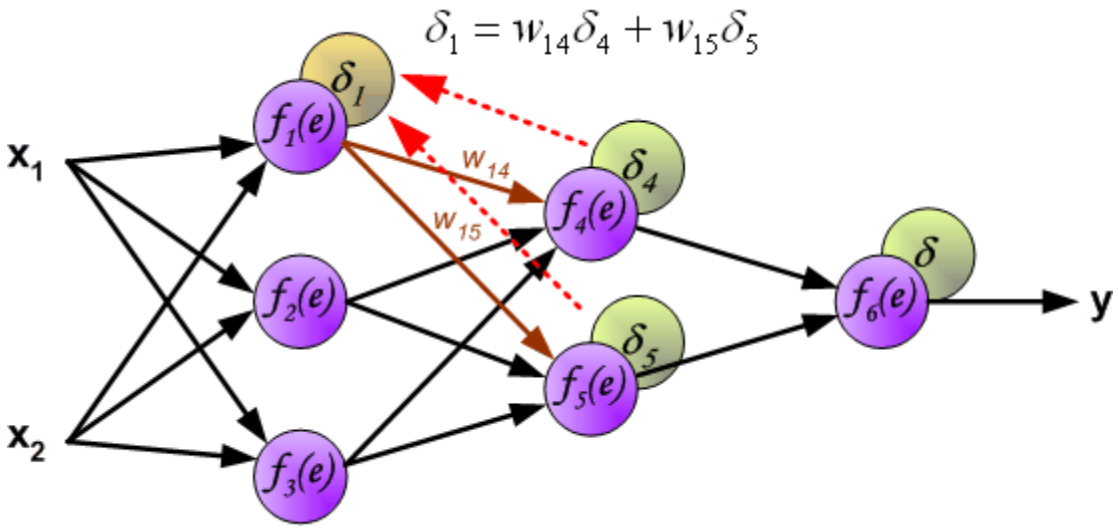

http://galaxy.agh.edu.pl/~vlsi/AI/backp_t_en/backprop.html

Back Propagation of Errors is the most popular Training Algorithm

- The weights' coefficients w_{mn} used to propagate errors back are equal to this used during computing output value. Only the direction of data flow is changed - signals are propagated from output to inputs one after the other. This technique is used for all network layers. If propagated errors came from few neurons they are added. The illustration is below:

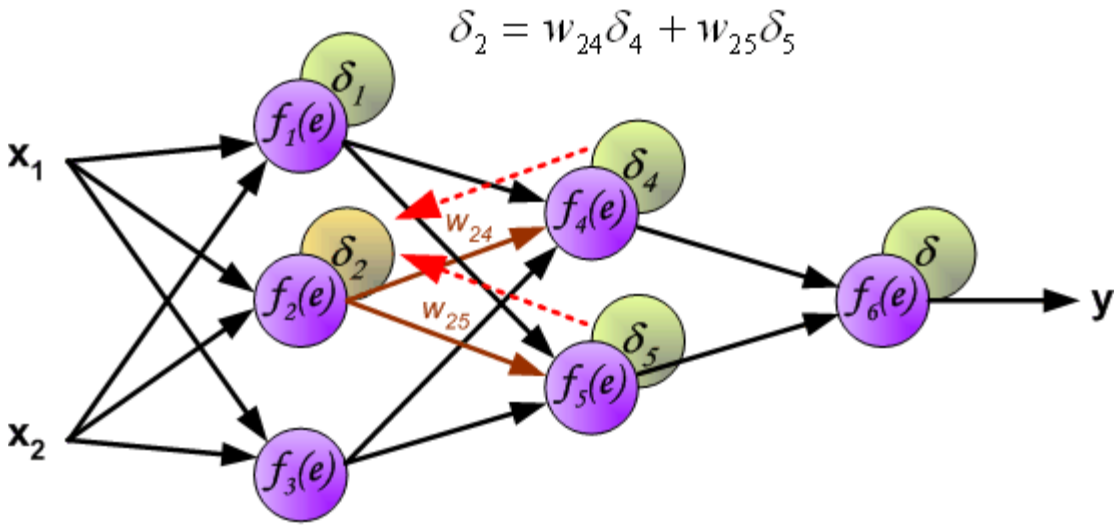

http://galaxy.agh.edu.pl/~vlsi/AI/backp_t_en/backprop.html

Back Propagation of Errors is the most popular Training Algorithm

- The weights' coefficients w_{mn} used to propagate errors back are equal to this used during computing output value. Only the direction of data flow is changed - signals are propagated from output to inputs one after the other. This technique is used for all network layers. If propagated errors came from few neurons they are added. The illustration is below:

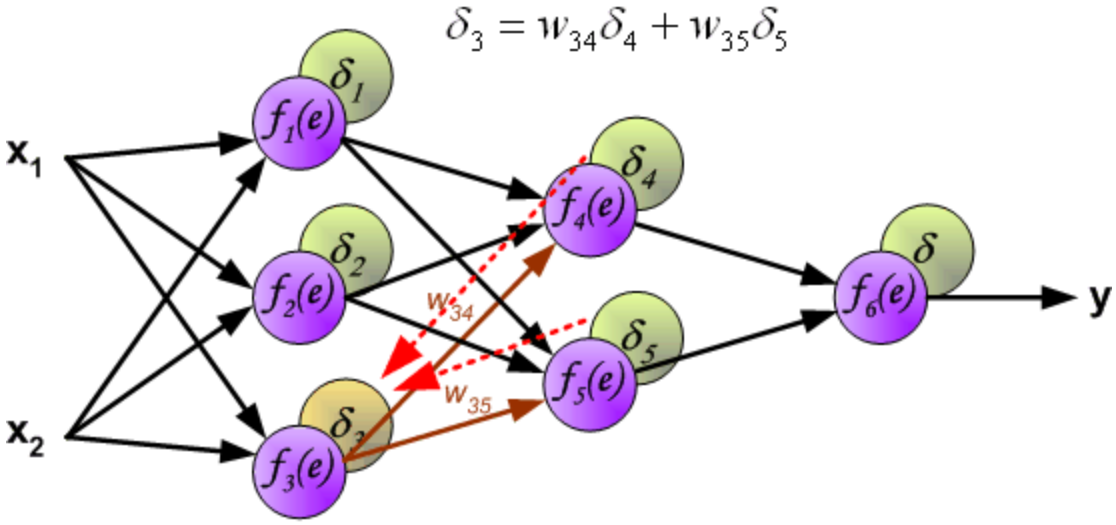

http://galaxy.agh.edu.pl/~vlsi/AI/backp_t_en/backprop.html

Back Propagation of Errors is the most popular Training Algorithm

- When the error signal for each neuron is computed, the weights coefficients of each neuron input node may be modified. In formulas below *df(e)/de* represents derivative of neuron activation function (which weights are modified).

$$w'_{(x1)1} = w_{(x1)1} + \eta \delta_1 \frac{df_1(e)}{de} x_1$$

$$w'_{(x2)1} = w_{(x2)1} + \eta \delta_1 \frac{df_1(e)}{de} x_2$$

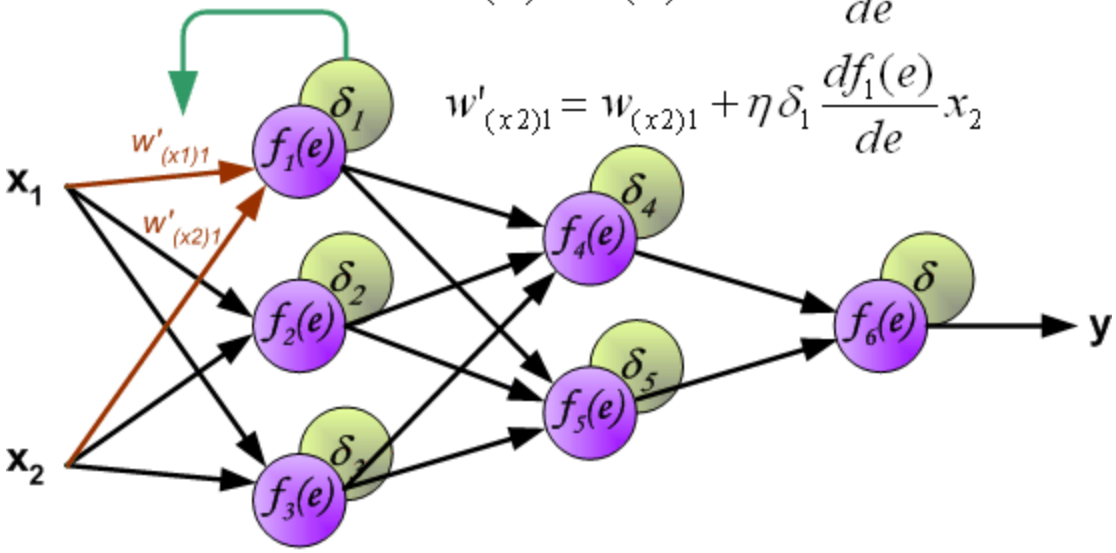

http://galaxy.agh.edu.pl/~vlsi/AI/backp_t_en/backprop.html

Back Propagation of Errors is the most popular Training Algorithm

- When the error signal for each neuron is computed, the weights coefficients of each neuron input node may be modified. In formulas below *df(e)/de* represents derivative of neuron activation function (which weights are modified).

$$w'_{(x1)2} = w_{(x1)2} + \eta \delta_2 \frac{df_2(e)}{de} x_1$$

$$w'_{(x2)2} = w_{(x2)2} + \eta \delta_2 \frac{df_2(e)}{de} x_2$$

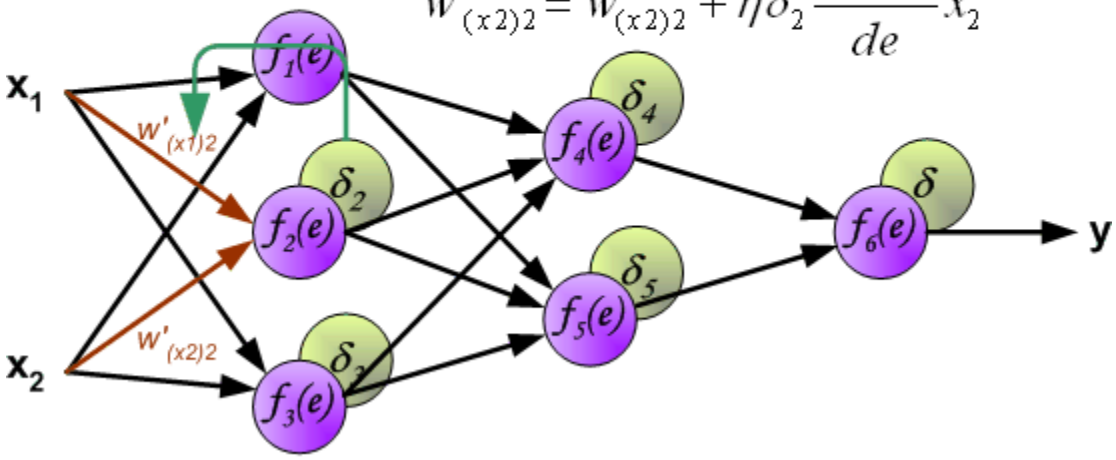

http://galaxy.agh.edu.pl/~vlsi/AI/backp_t_en/backprop.html

Back Propagation of Errors is the most popular Training Algorithm

- When the error signal for each neuron is computed, the weights coefficients of each neuron input node may be modified. In formulas below *df(e)/de* represents derivative of neuron activation function (which weights are modified).

$$w'_{(x1)3} = w_{(x1)3} + \eta \delta_3 \frac{df_3(e)}{de} x_1$$

$$w'_{(x2)3} = w_{(x2)3} + \eta \delta_3 \frac{df_3(e)}{de} x_2$$

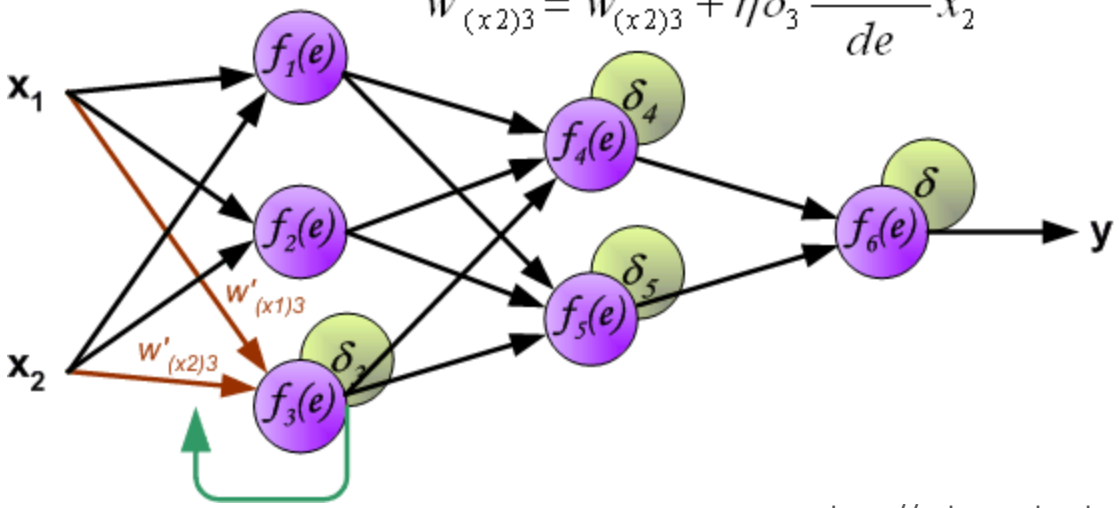

http://galaxy.agh.edu.pl/~vlsi/AI/backp_t_en/backprop.html

Back Propagation of Errors is the most popular Training Algorithm

- When the error signal for each neuron is computed, the weights coefficients of each neuron input node may be modified.

$$w'_{14} = w_{14} + \eta \delta_4 \frac{df_4(e)}{de} y_1$$

$$w'_{24} = w_{24} + \eta \delta_4 \frac{df_4(e)}{de} y_2$$

$$w'_{34} = w_{34} + \eta \delta_4 \frac{df_4(e)}{de} y_3$$

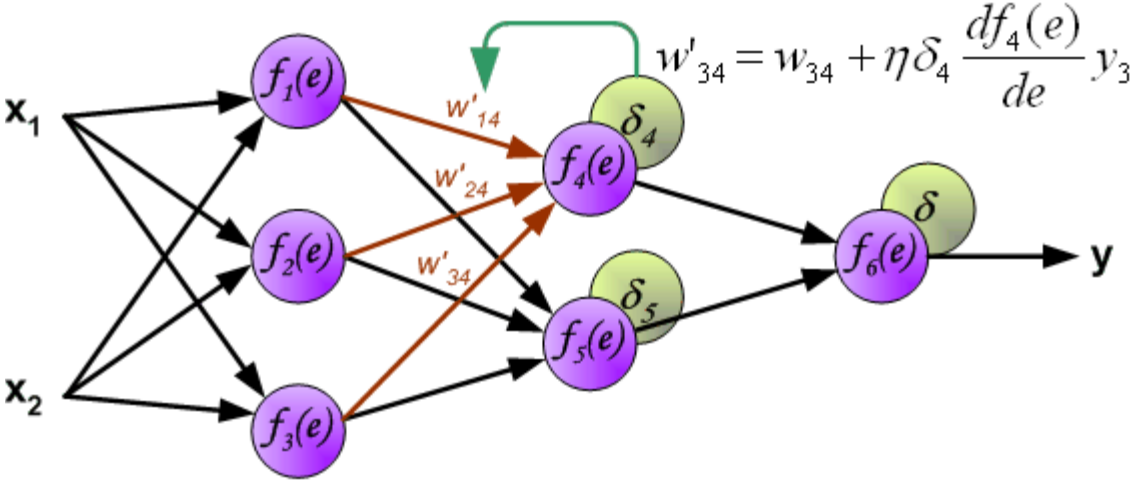

http://galaxy.agh.edu.pl/~vlsi/AI/backp_t_en/backprop.html

Back Propagation of Errors is the most popular Training Algorithm

- When the error signal for each neuron is computed, the weights coefficients of each neuron input node may be modified.

$$w'_{15} = w_{15} + \eta \delta_5 \frac{df_5(e)}{de} y_1$$

$$w'_{25} = w_{25} + \eta \delta_5 \frac{df_5(e)}{de} y_2$$

$$w'_{35} = w_{35} + \eta \delta_5 \frac{df_5(e)}{de} y_3$$

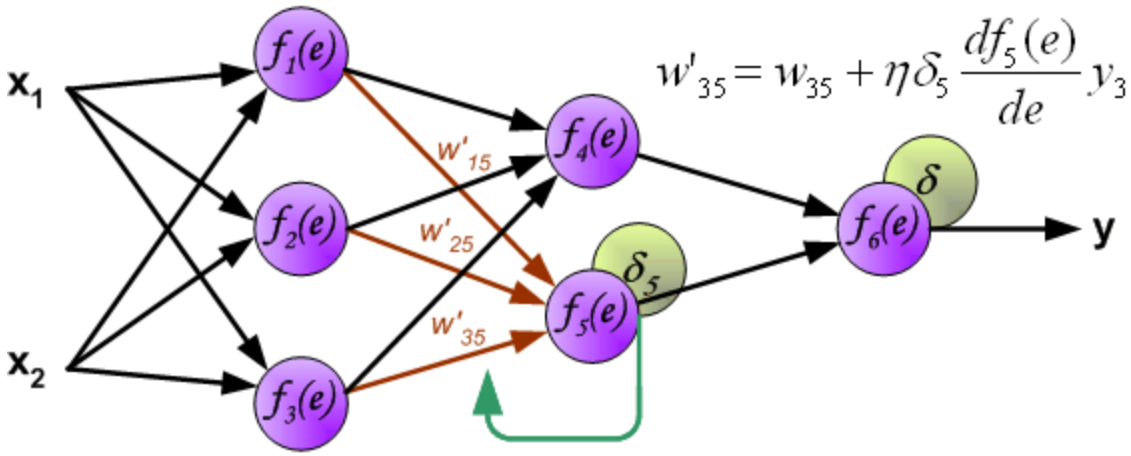

http://galaxy.agh.edu.pl/~vlsi/AI/backp_t_en/backprop.html

Back Propagation of Errors is the most popular Training Algorithm

- When the error signal for each neuron is computed, the weights coefficients of each neuron input node may be modified. In formulas below *df(e)/de* represents derivative of neuron activation function (which weights are modified).

$$w'_{46} = w_{46} + \eta \delta \frac{df_6(e)}{de} y_4$$

$$w'_{56} = w_{56} + \eta \delta \frac{df_6(e)}{de} y_5$$

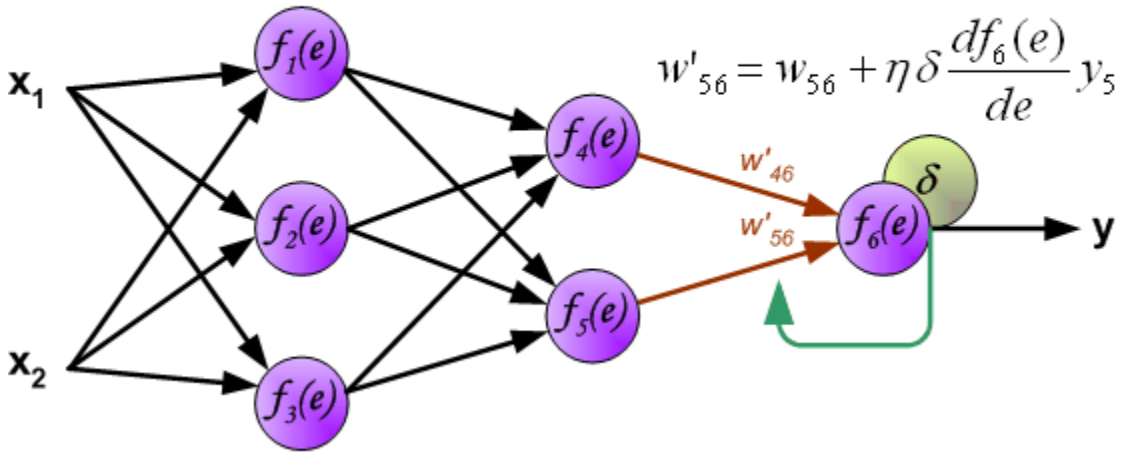

http://galaxy.agh.edu.pl/~vlsi/AI/backp_t_en/backprop.html

The (Inverse) Protein Folding Problem
Holy Grail of Comp. Structural Biology

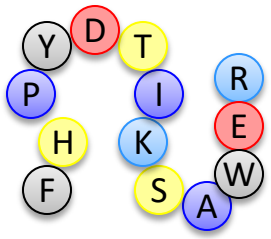

Protein Folding Problem

Sequence ⇌ Structure

Inverse Folding Problem

- Given a protein's AA sequence, what is its 3-dimensional fold , and how does it get there?
- Assume 100 conformations for each amino acid in a 100 amino acid protein ⇨ 10^{200} possible conformations!
- Exhaustive sampling is impossible – e.g. earth is less than 10^{10} years old.
- Cyrus Levinthal's paradox of protein folding,1968.

Protein Folding using Lattice Models and Grid Searches

- Arrange amino acids randomly on three-dimensional grid
- Define a simplified energy function that measures exposure (red=buried, blue exposed), etc.
- Search arrangements using Monte Carlo or Genetic algorithms
- Works only for very small proteins (<50AA)
- Popular in earlier days of protein structure prediction (1990-2000) for reduced computational requirements

R. Unger and J. Moult; "Genetic algorithms for protein folding simulations"; *J Mol Biol*; **1993**; Vol. 231 (1): p. 75-81.

A. Kolinski and J. Skolnick; "Monte Carlo simulations of protein folding. I. Lattice model and interaction scheme"; *Proteins*; **1994**; Vol. 18 (4): p. 338-52.

A. Sali, E. Shakhnovich and M. Karplus; "Kinetics of protein folding. A lattice model study of the requirements for folding to the native state"; *J Mol Biol*; **1994**; Vol. 235 (5): p. 1614-36.

K. A. Dill, S. Bromberg, K. Yue, K. M. Fiebig, D. P. Yee, P. D. Thomas and H. S. Chan; "Principles of protein folding--a perspective from simple exact models"; *Protein Sci*; **1995**; Vol. 4 (4): p. 561-602.

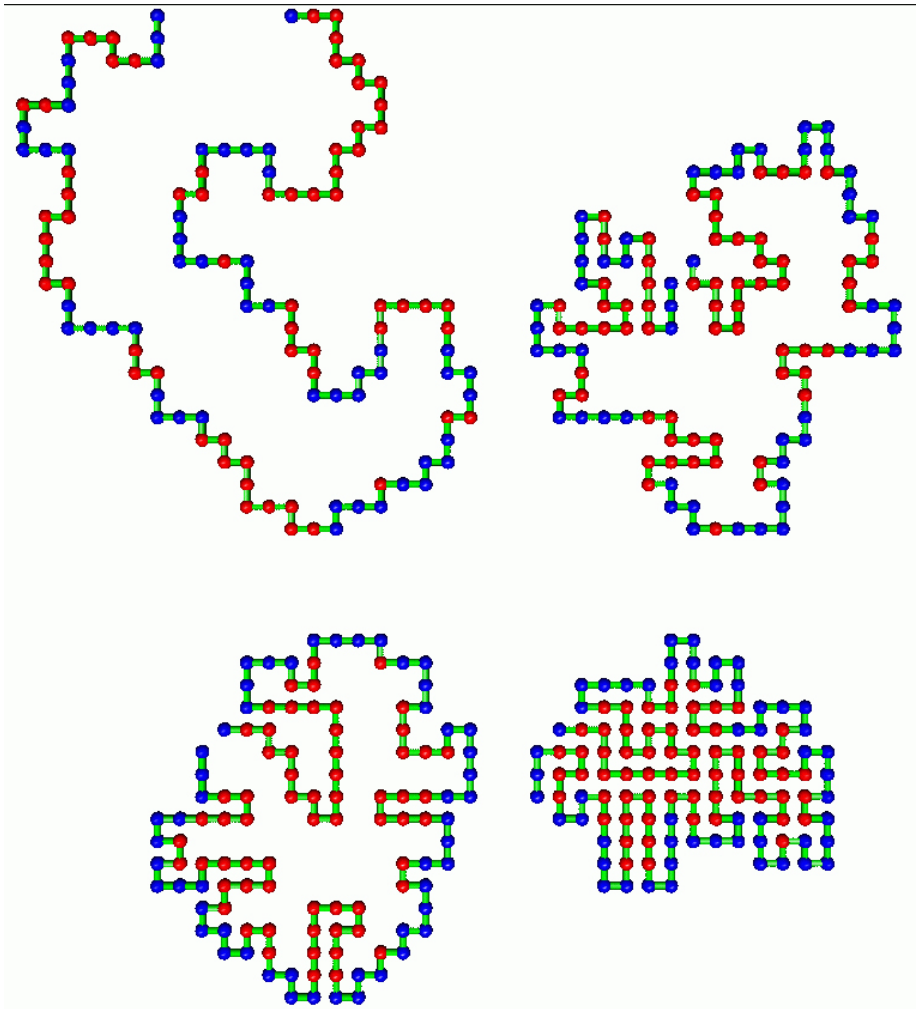

General Scheme of Protein Structure Prediction

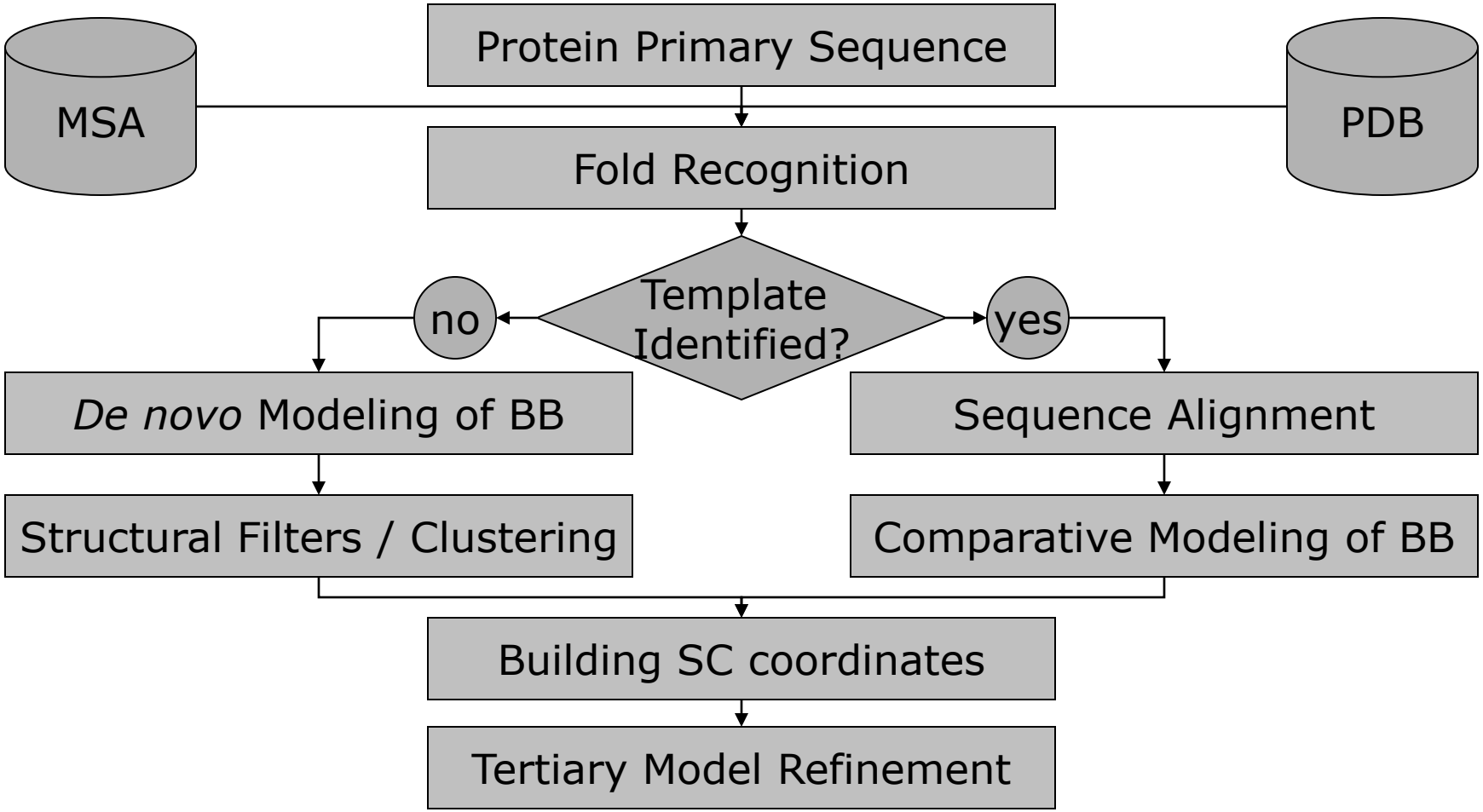

PhD - Prediction of protein secondary structure at better than 70% accuracy

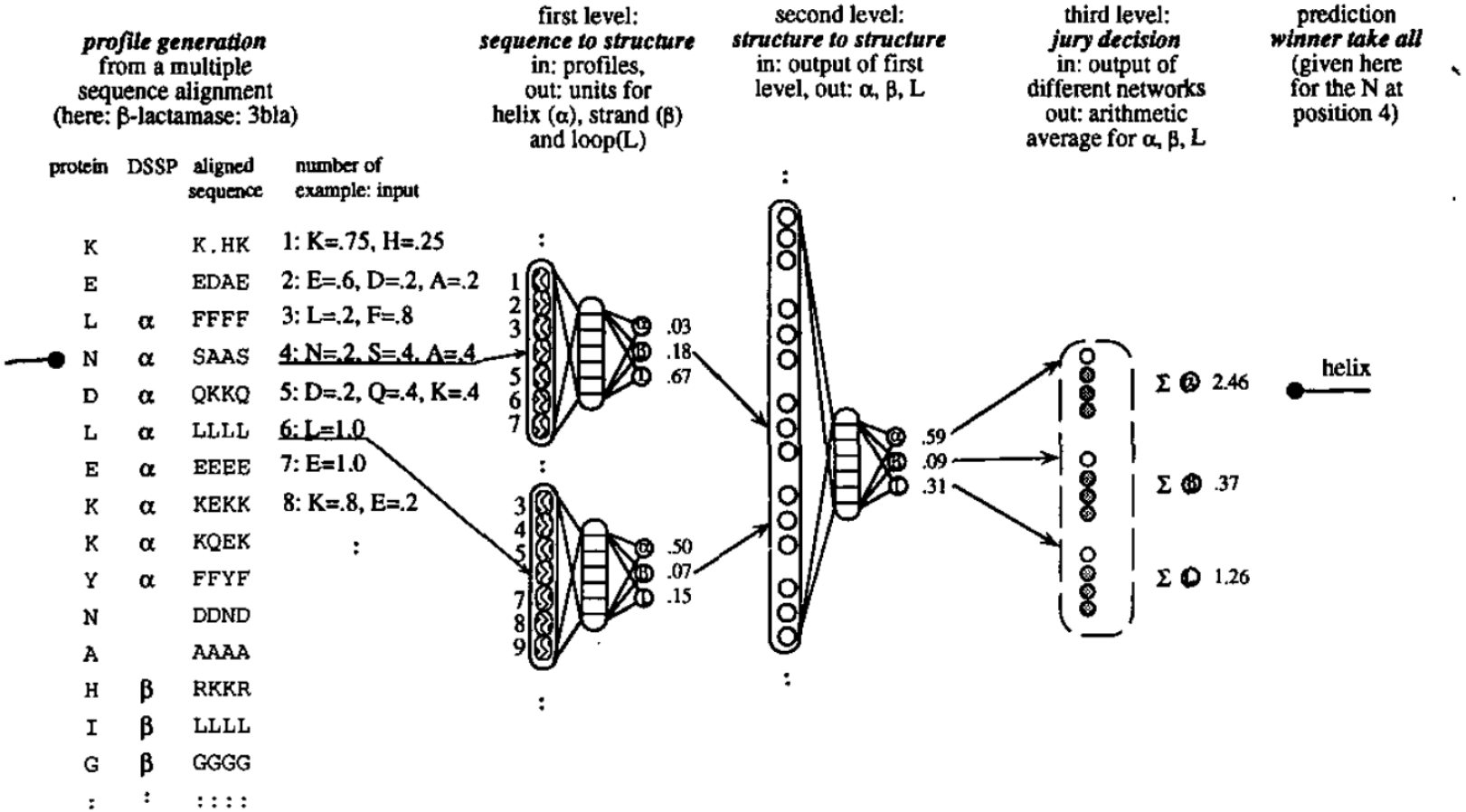

B. Rost and C. Sander; "Prediction of protein secondary structure at better than 70% accuracy"; *J. Mol. Biol.*; **1993**; Vol. 232 (2): p. 584-99; J. Meiler, A. Zeidler, F. Schmaschke and M. Muller; "Generation and evaluation of dimension-reduced amino acid parameter representations by artificial neural networks"; *Journal of Molecular Modeling*; **2001**; Vol. 7 (9): p. 360-369.

BCL::Jufo9D >70% correct 9-state prediction, >80% SS, >90% TM

REAL STATE \ PREDICTION	tm_C	tr_C	sol_C	tm_S	tr_S	sol_S	tm_H	tr_H	sol_H
tm_C	63.7	13.3	1.9	4.8	2.0	1.1	6.0	6.9	0.5
tr_C	4.8	64.7	3.4	1.9	7.8	0.5	0.9	15.3	0.8
sol_C	3.8	23.0	43.9	2.4	2.5	8.7	2.1	2.4	11.2
tm_S	6.2	0.9	0.9	78.6	7.5	5.1	0.0	0.3	0.4
tr_S	3.0	12.0	1.7	14.2	66.5	1.8	0.6	0.1	0.0
sol_S	3.7	6.2	11.1	7.0	4.9	55.9	4.0	4.2	3.1
tm_H	2.0	3.8	0.1	0.4	0.1	0.1	80.1	13.2	0.4
tr_H	2.0	16.9	0.2	0.2	1.1	0.1	12.0	66.0	1.6
sol_H	1.4	6.0	9.0	0.8	0.7	2.9	2.0	8.8	68.5

TM trans-membrane
TR transition
SOL solution

H helix
S strand
C coil

J. K. Leman, R. Mueller, M. Karakas, N. Woetzel and J. Meiler; "Simultaneous prediction of protein secondary structure and transmembrane spans"; *Proteins*; **2013**; Vol. 81 (7): p. 1127-40.

Example 1: Succinate dehydrogenase (1NEK)

- Secondary structure prediction

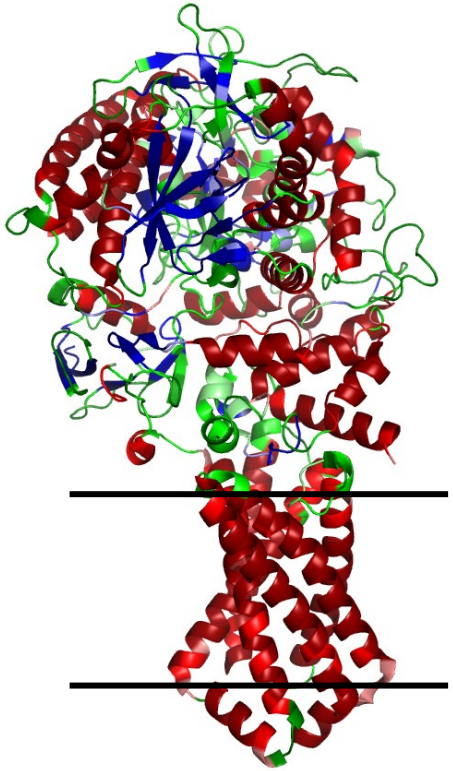

helix
strand
coil

membrane
transition
solution

92% **81%**
residues correct

- Trans-membrane span identification

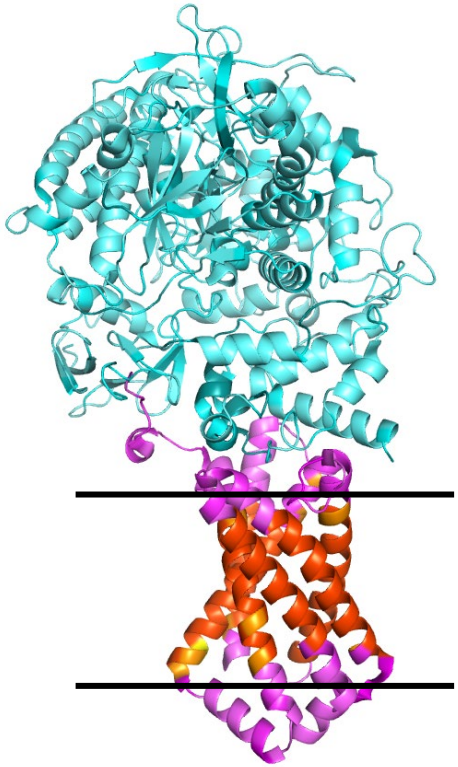

Example 2: EspP autotransporter beta-domain (2QOM)

- Secondary structure prediction

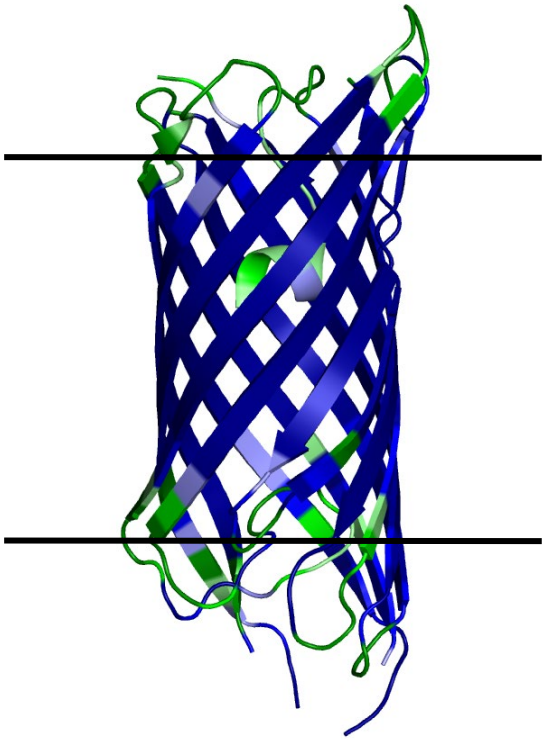

helix
strand
coil

membrane
transition
solution

- Trans-membrane span identification

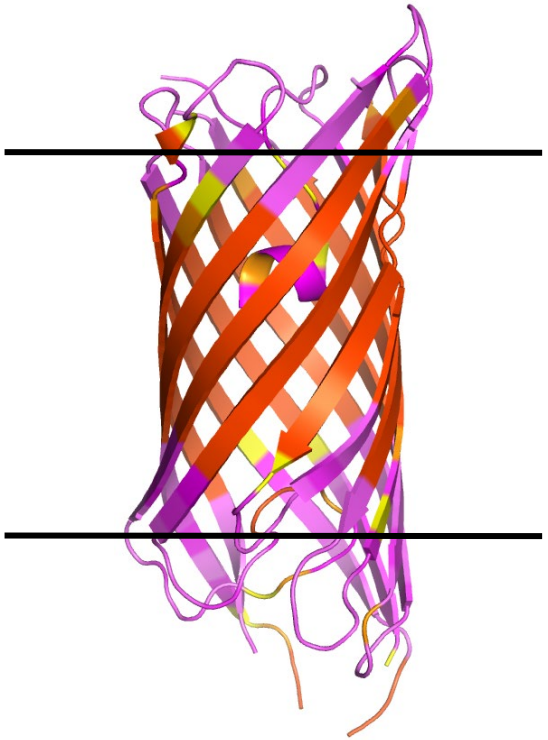

80% **74%**
residues correct

A NN–based Consensus Predictor that Improves Fold Recognition

During recent years many protein fold recognition methods have been developed, based on different algorithms and using various kinds of information. To examine the performance of these methods several evaluation experiments have been conducted. These include blind tests in CASP/CAFASP, large scale benchmarks, and long-term, continuous assessment with newly solved protein structures. These studies confirm the expectation that for different targets different methods produce the best predictions, and the final prediction accuracy could be improved if the available methods were combined in a perfect manner. In this article a neural-network-based consensus predictor, Pcons, is presented that attempts this task. Pcons attempts to select the best model out of those produced by six prediction servers, each using different methods. Pcons translates the confidence scores reported by each server into uniformly scaled values corresponding to the expected accuracy of each model. The translated scores as well as the similarity between models produced by different servers is used in the final selection. According to the analysis based on two unrelated sets of newly solved proteins, Pcons outperforms any single server by generating ~8%–10% more correct predictions. Furthermore, the specificity of Pcons is significantly higher than for any individual server. From analyzing different input data to Pcons it can be shown that the improvement is mainly attributable to measurement of the similarity between the different models. Pcons is freely accessible for the academic community through the protein structure-prediction metaserver at http://bioinfo.pl/meta/.

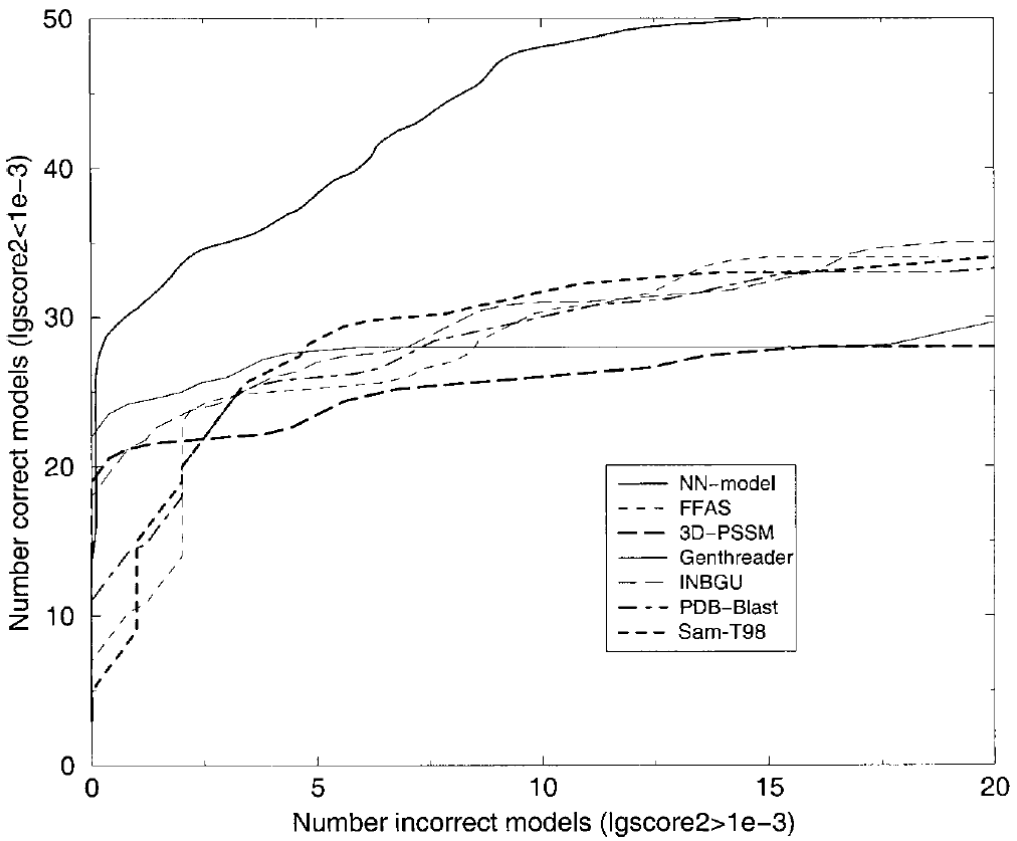

- Lundstroem, J.; Rychlewski, L.; Bujnicki, J.; Elofsson, A., Pcons: A neural-network –based consensus predictor that improves fold recognition. Protein Sci. 2001, 10, 2354-2362.


Hidden Markov Models Identify Local Structural Motives from Sequence

Type I β-hairpin

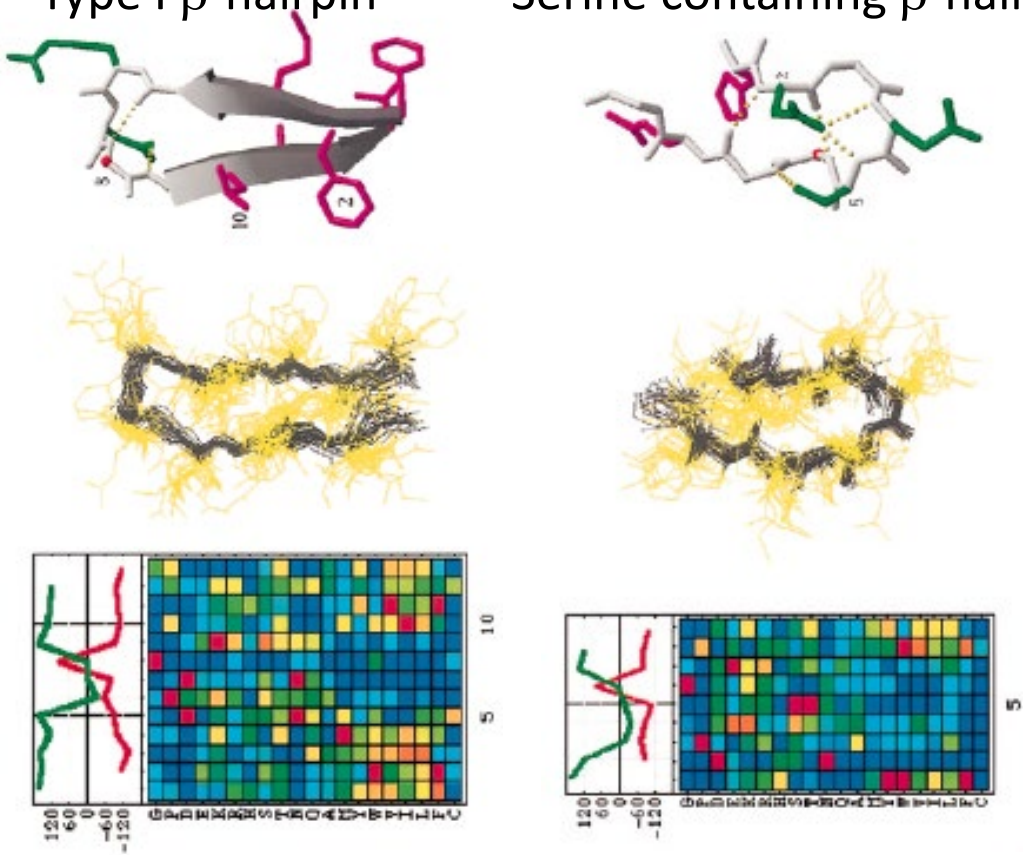

Serine containing β-hairpin

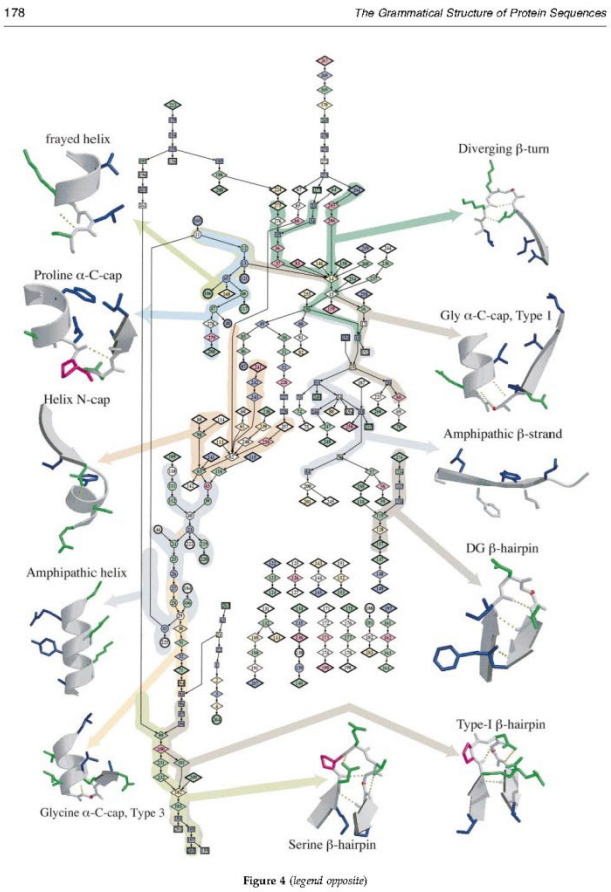

Figure 4 (*legend opposite*)

1. Bystroff, C.; Baker, D., Prediction of Local Structure in Proteins Using a Library of Sequence-Structure Motifs. *J. Mol. Biol.* **1998,** 281, 565-577. 2. Bystroff, C.; Thorsson, V.; Baker, D., HMMSTR: a Hidden Markov Model for Local Sequence-Structure Correlations in Proteins. *J. Mol. Biol.* **2000,** 301, 173-190.

ANN – Derived Contact Numbers Improve Membrane Protein Structure Prediction

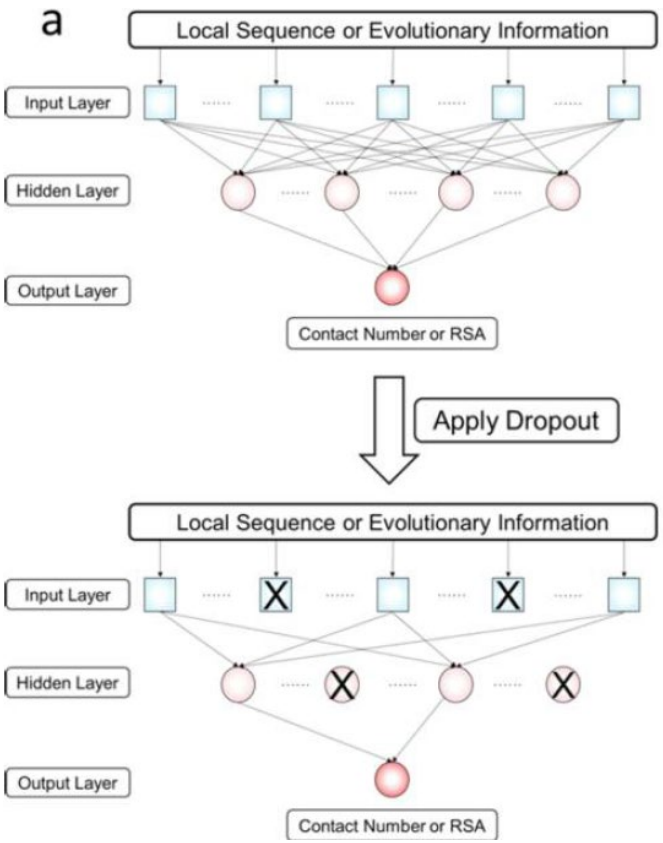

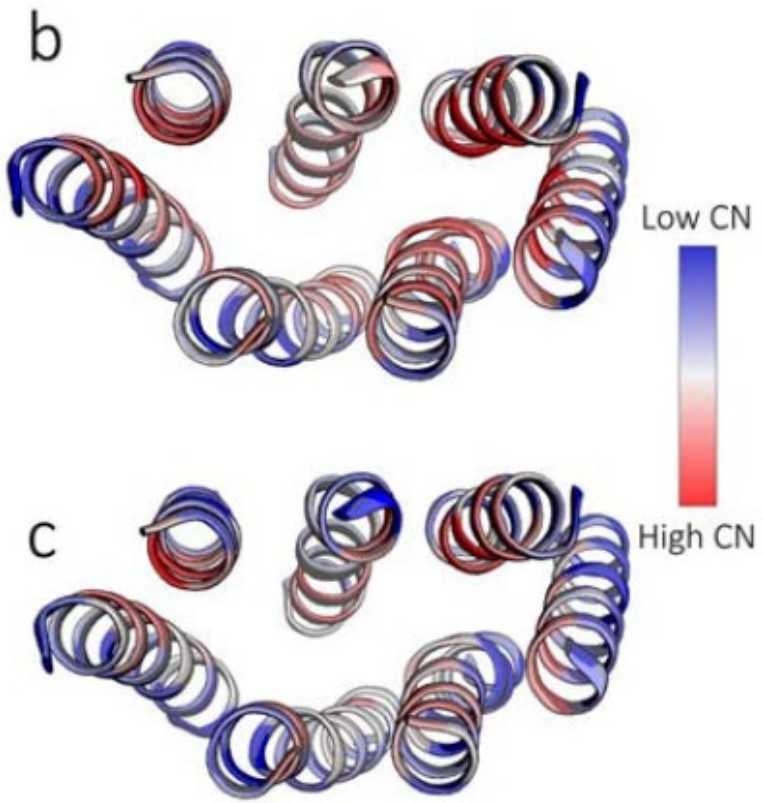

B. Li, J. Mendenhall, E. D. Nguyen, B. E. Weiner, A. W. Fischer and J. Meiler; "Accurate Prediction of Contact Numbers for Multi-Spanning Helical Membrane Proteins"; *J Chem Inf Model*; **2016**; Vol. 56 (2): p. 423-34.
B. Li, J. Mendenhall, E. D. Nguyen, B. E. Weiner, A. W. Fischer and J. Meiler; "Improving prediction of helix-helix packing in membrane proteins using predicted contact numbers as restraints"; *Proteins*; **2017**; Vol. 85 (7): p. 1212-1221.

Convolutional Neural Networks (CNN) can understand Different Levels of Resolution

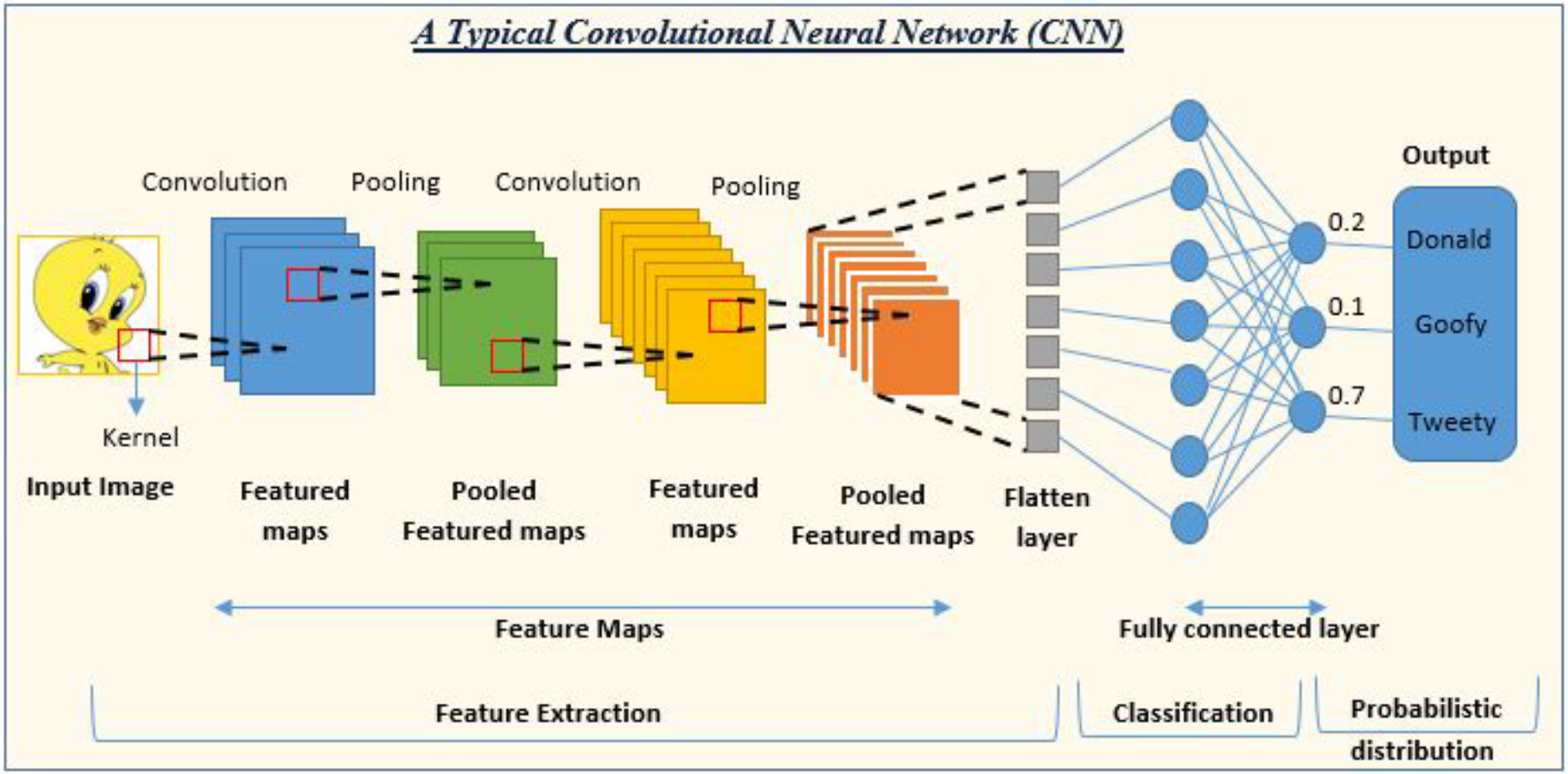

Paying Attention

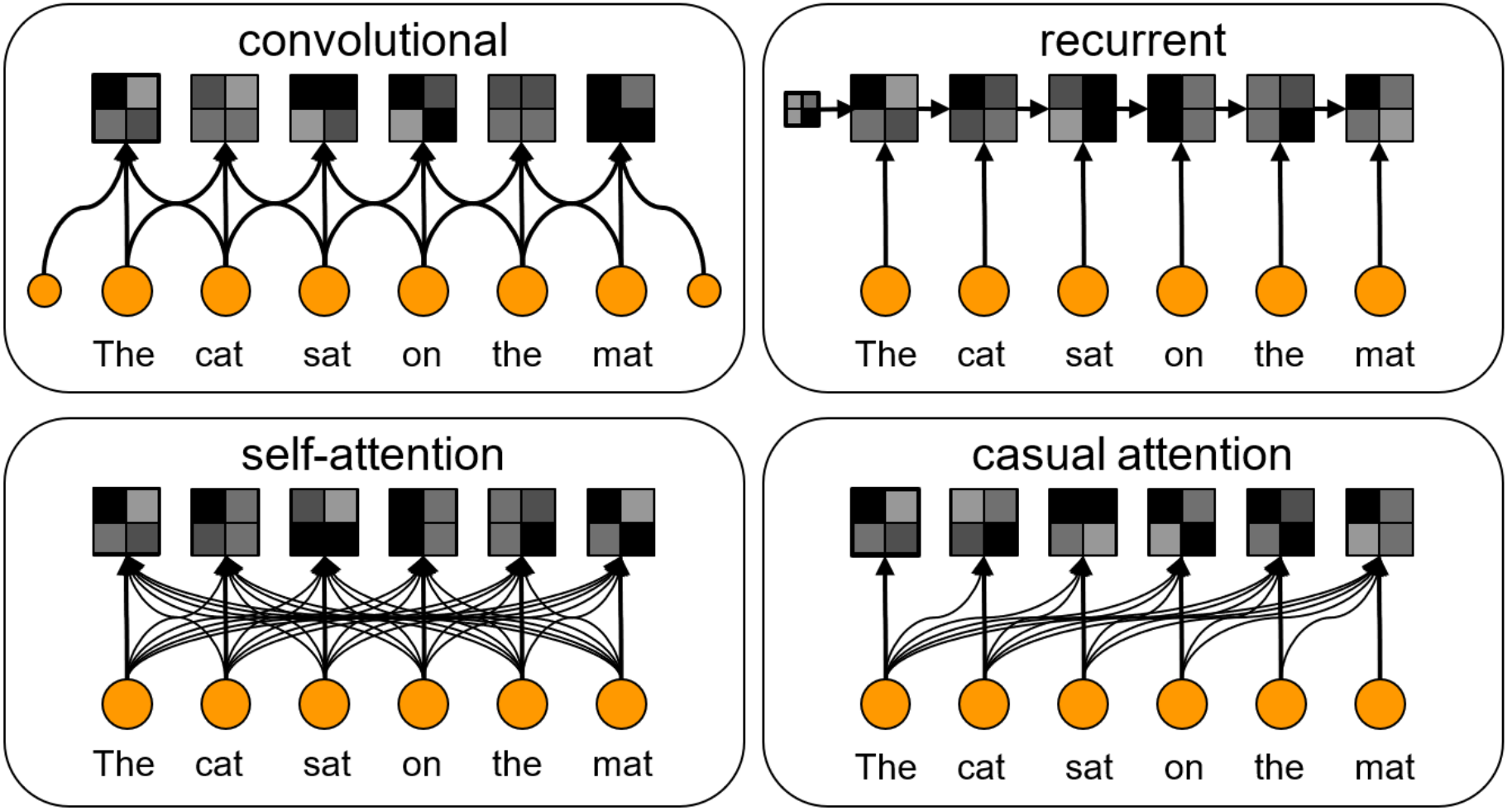

Transformers and Attention – let the Neural Network figure out Importance

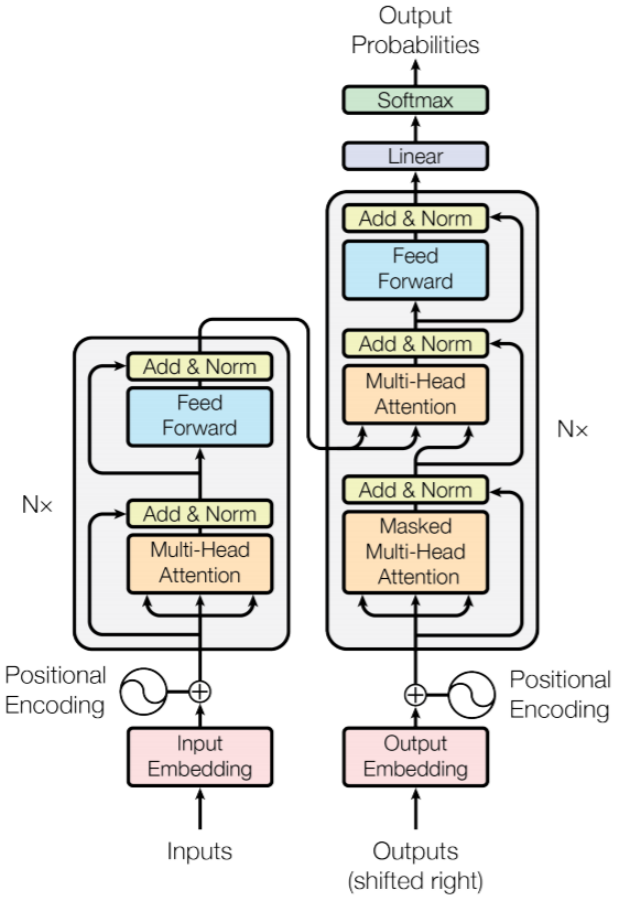

Figure 1: The Transformer - model architecture.

Transformers and Attention – let the Neural Network figure out Importance

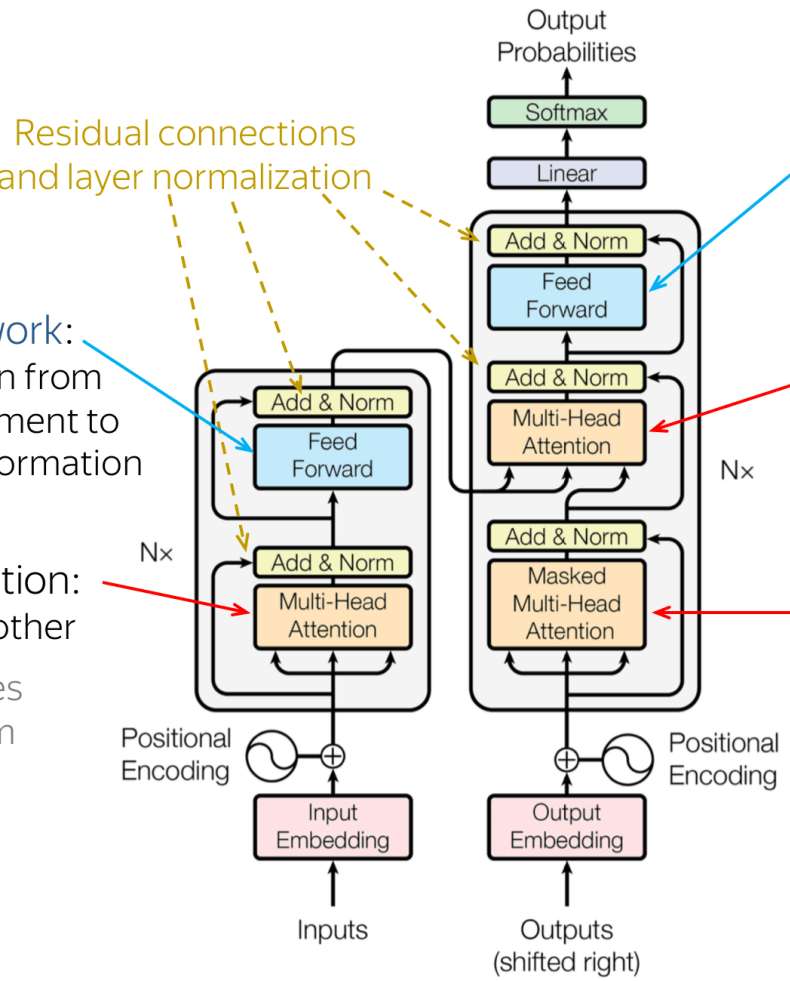

Residual connections and layer normalization

Feed-forward network: after taking information from other tokens, take a moment to think and process this information

Encoder self-attention: tokens look at each other

queries, keys, values are computed from encoder states

Feed-forward network: after taking information from other tokens, take a moment to think and process this information

Decoder-encoder attention: target token looks at the source

queries – from decoder states; keys and values from encoder states

Decoder self-attention (masked): tokens look at the previous tokens

queries, keys, values are computed from decoder states

The Future of Artificial Neural Networks in Biomedical Research – Some Thesis

1. All problems that have infinite/near infinite data available for training will be smashed (think language processing, sequence problems in biochemistry, protein structure)
2. New architectures and structures of ANNs will emerge that will be parallel in size to or larger then the human brain (10^{14} connections) with substructures matching in complexity
3. The biggest challenge for biomedical research will emerge with limited datasets that forbid training of super-large ANNs; Expert Knowledge will Design the Optimal ANN
4. For the next Decade (at least), you need to be an expert in machine learning and structural/chemical biology to contribute to progress in a meaningful way
5. We will start an honest discussion on ethics of artificial intelligence as these systems will start to act human-like on many levels all the way to having self-awareness


Highly accurate protein structure prediction with AlphaFold

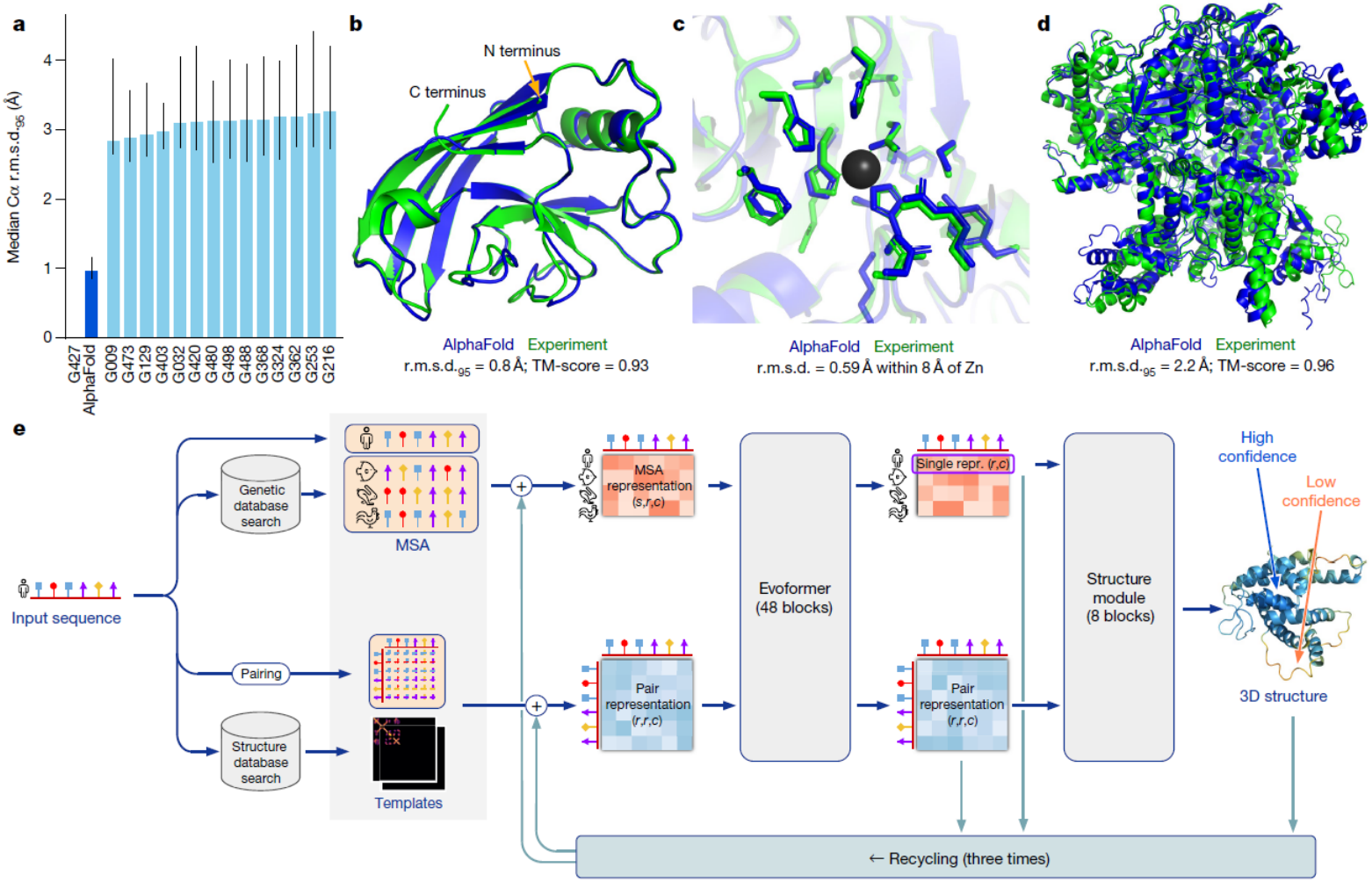

J. Jumper, et al.; "Highly accurate protein structure prediction with AlphaFold"; *Nature*; **2021**; Vol. 596 (7873): p. 583-589.

Highly accurate protein structure prediction with AlphaFold – Evoformer

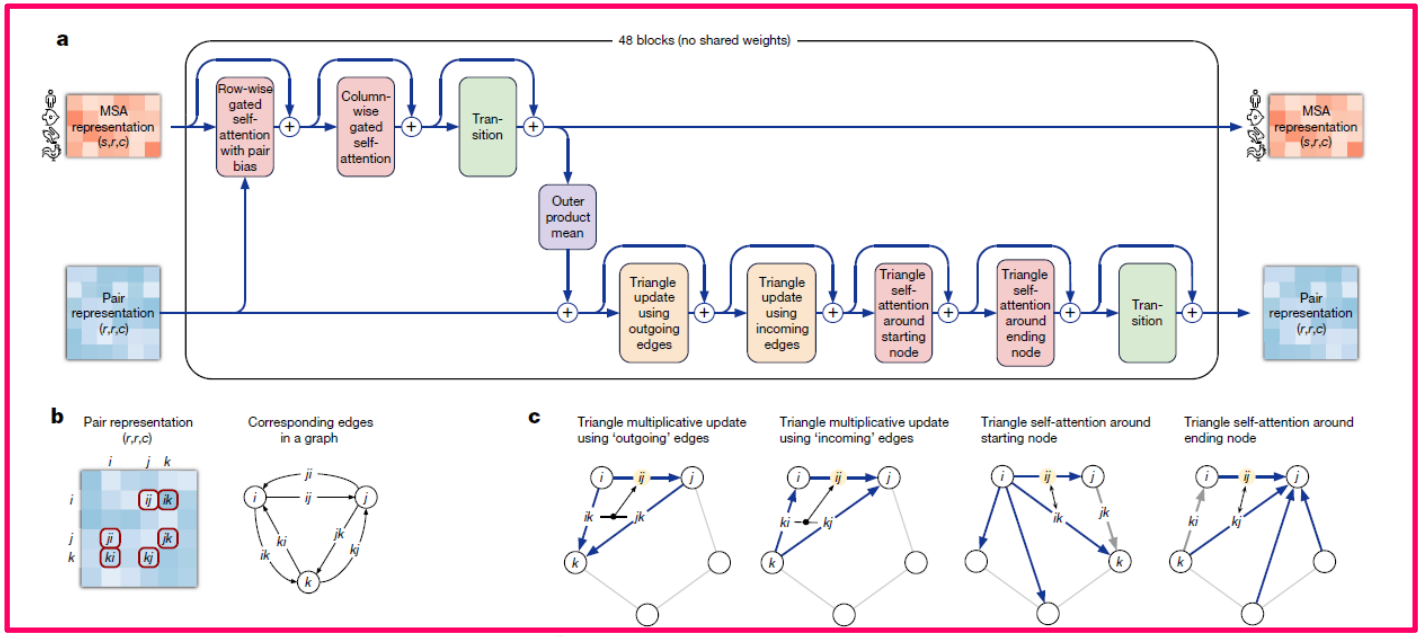

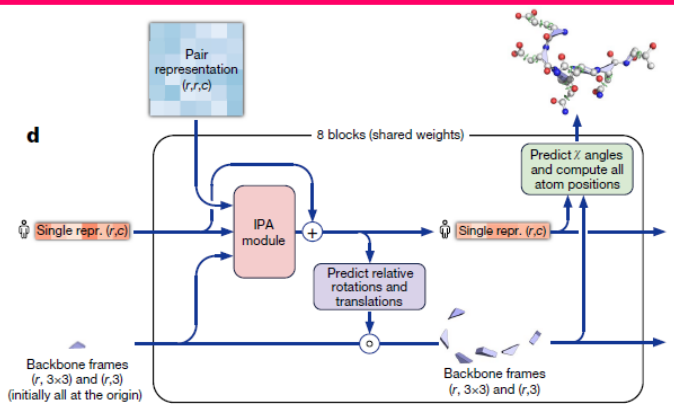

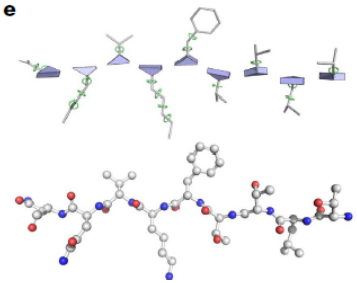

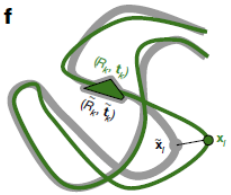

J. Jumper, et al.; "Highly accurate protein structure prediction with AlphaFold"; *Nature*; **2021**; Vol. 596 (7873): p. 583-589.

Highly accurate protein structure prediction with AlphaFold – Structure

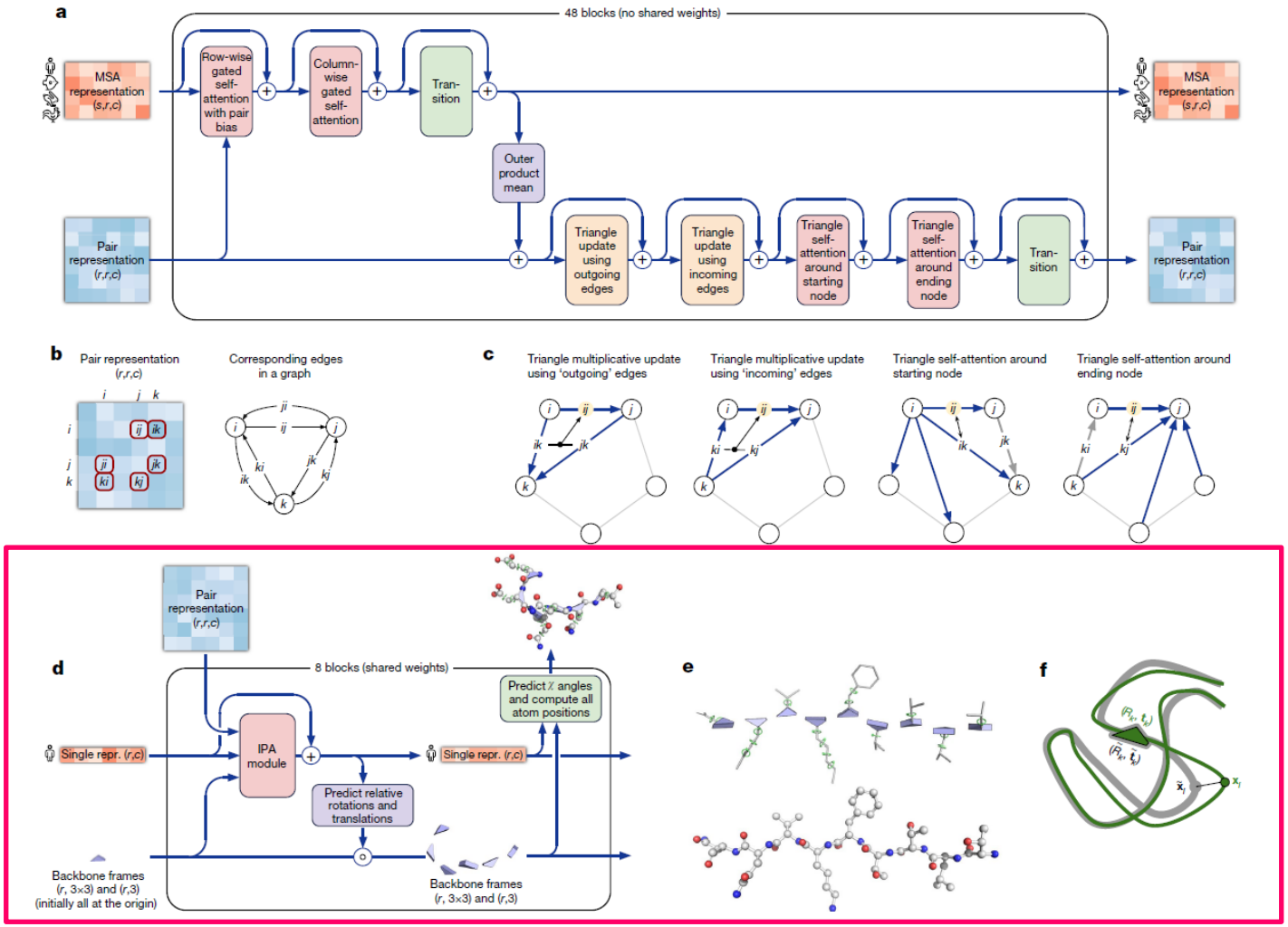

J. Jumper, et al.; "Highly accurate protein structure prediction with AlphaFold"; *Nature*; **2021**; Vol. 596 (7873): p. 583-589.

Sampling Alternative Conformational States with AlphaFold2

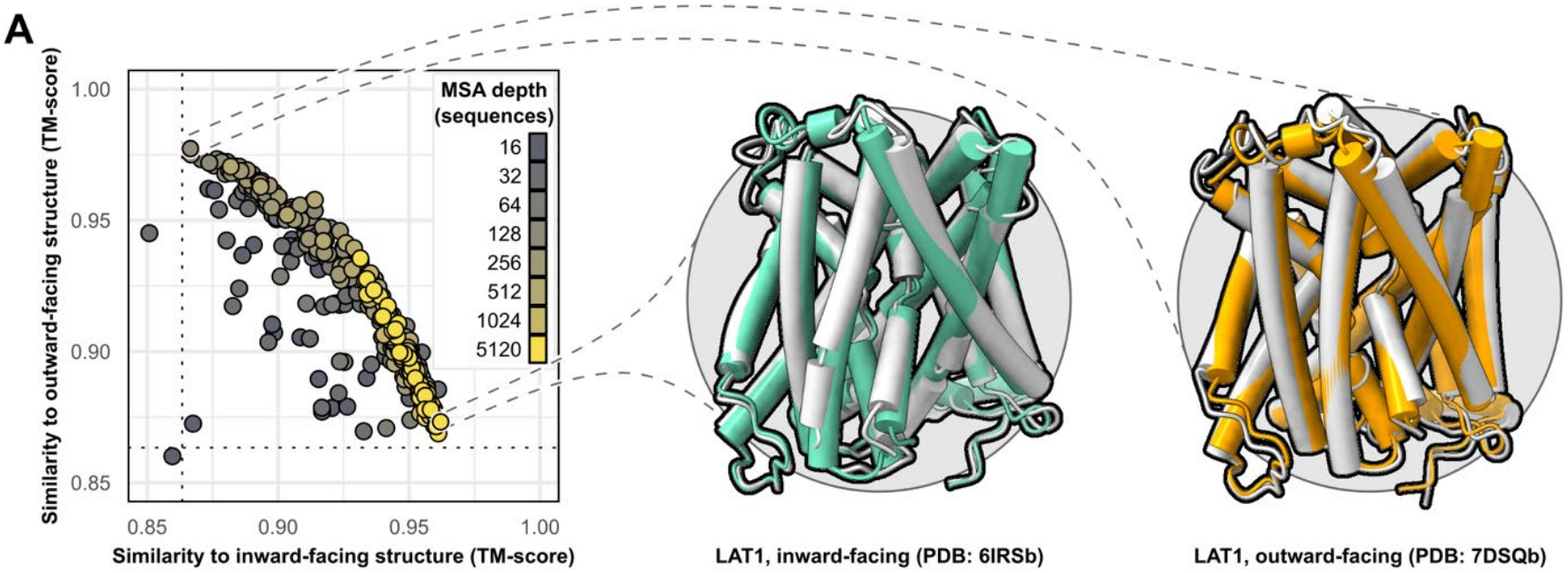

Figure 1. Alternative conformations of transporters and GPCRs can be predicted by AF2. (A) Representative models of the transporter LAT1 in IF and OF conformations. Experimental structures shown in gray and models shown in teal and orange.

D. Del Alamo, D. Sala, H. S. McHaourab and J. Meiler; "Sampling alternative conformational states of transporters and receptors with AlphaFold2"; *Elife*; **2022**; Vol. 11 p.

Molecular Architecture of the Human Caveolin-1 Complex with AlphaFold2

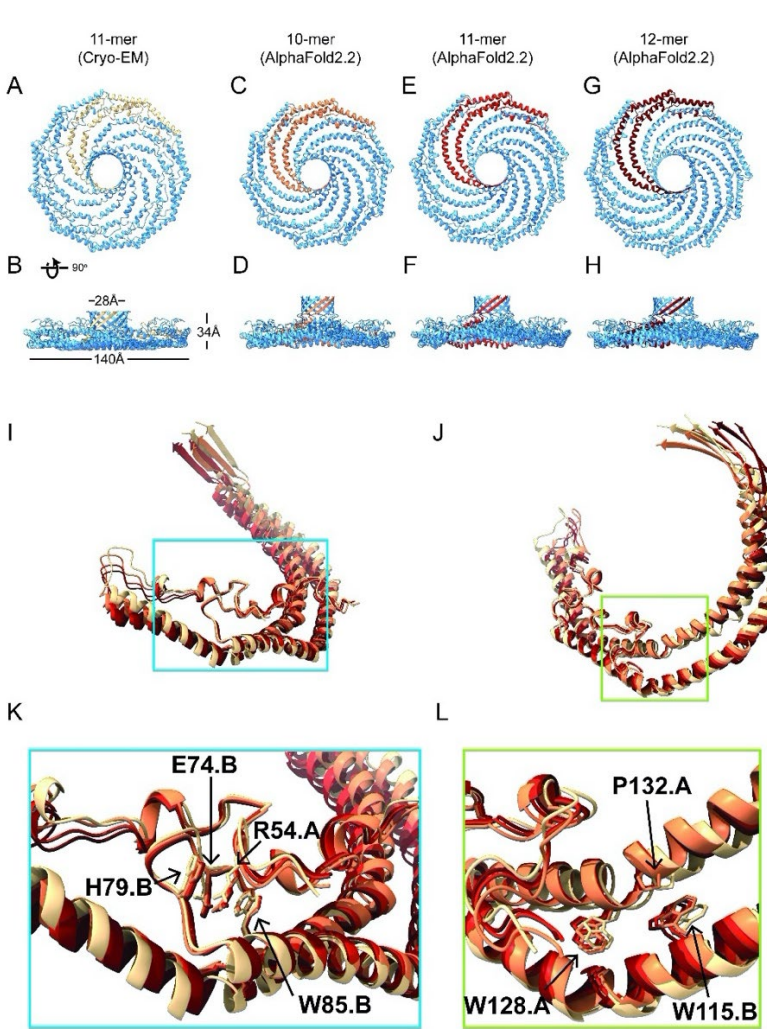

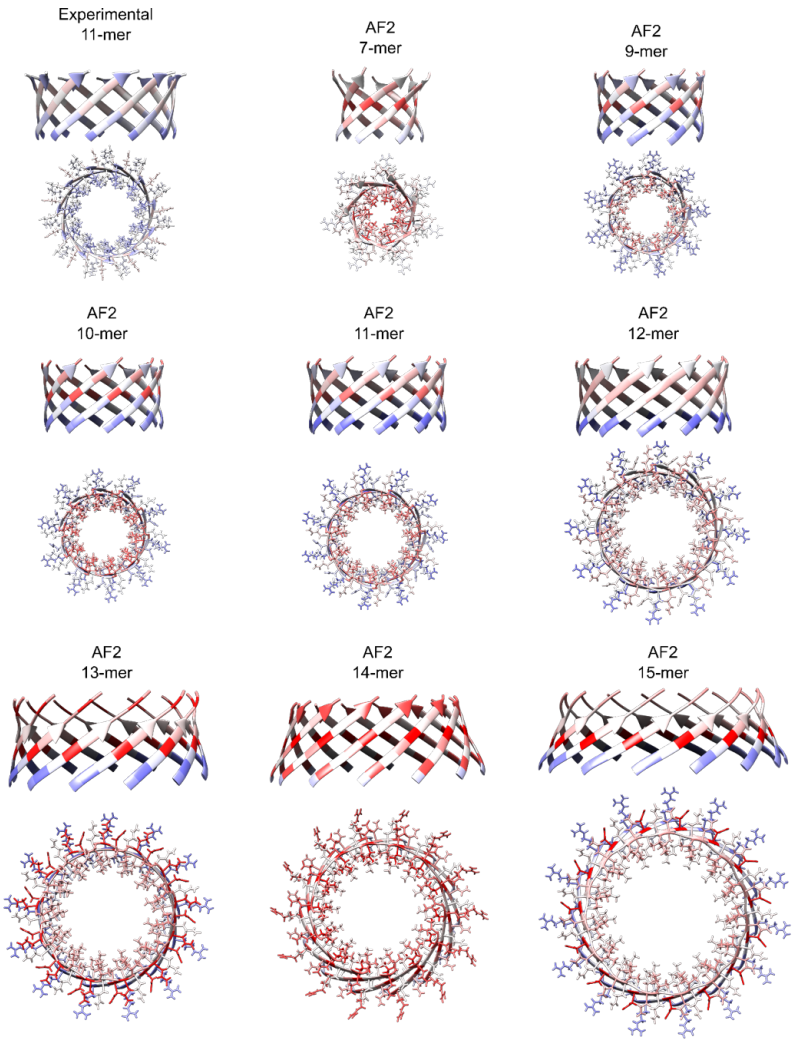

J. C. Porta, B. Han, A. Gulsevin, J. Chung, Y. Peskova, S. Connolly, H. S. Mchaourab, J. Meiler, E. Karakas, A. K. Kenworthy and M. D. Ohi; "Molecular architecture of the human caveolin-1 complex"; *Science Advances*; **2022**; Vol. p.

Molecular Architecture of the Human Caveolin-1 Complex with AlphaFold2

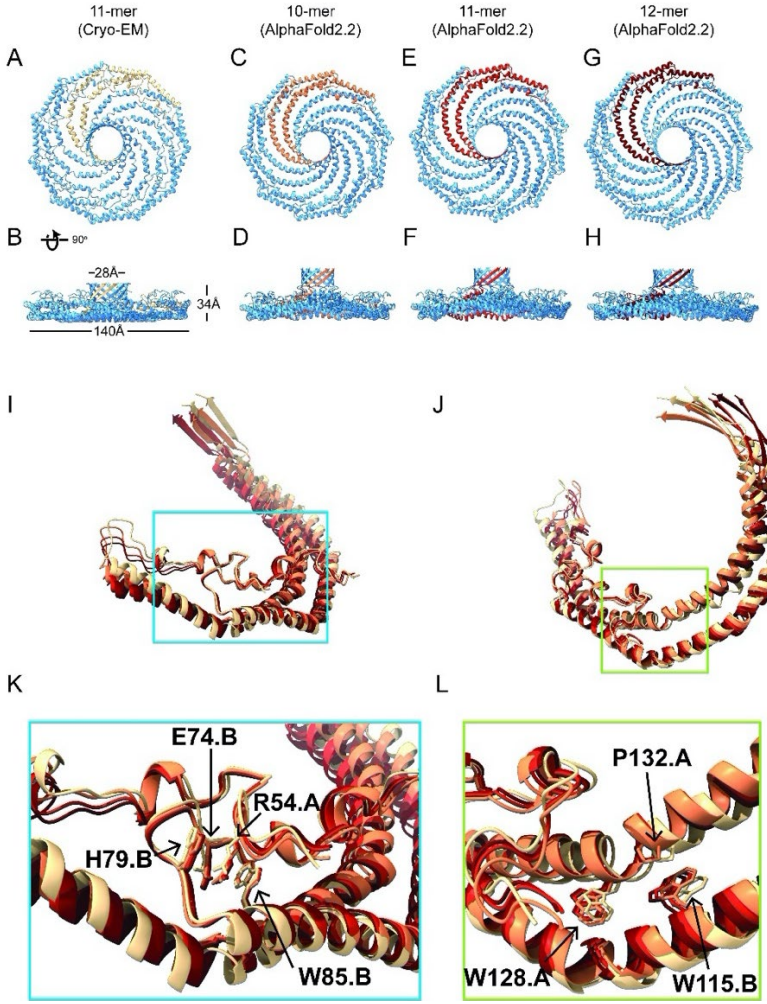

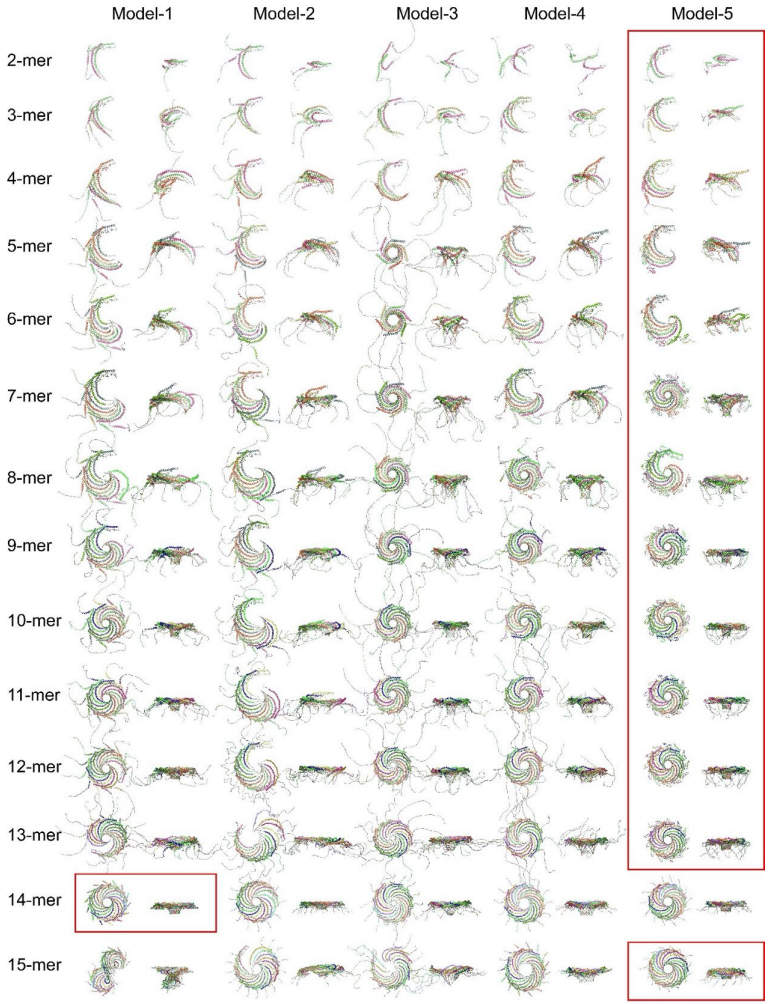

J. C. Porta, B. Han, A. Gulsevin, J. Chung, Y. Peskova, S. Connolly, H. S. Mchaourab, J. Meiler, E. Karakas, A. K. Kenworthy and M. D. Ohi; "Molecular architecture of the human caveolin-1 complex"; *Science Advances*; **2022**; Vol. p.

Antibody Diversity is Limited to 10^{11} Germline Antibodies

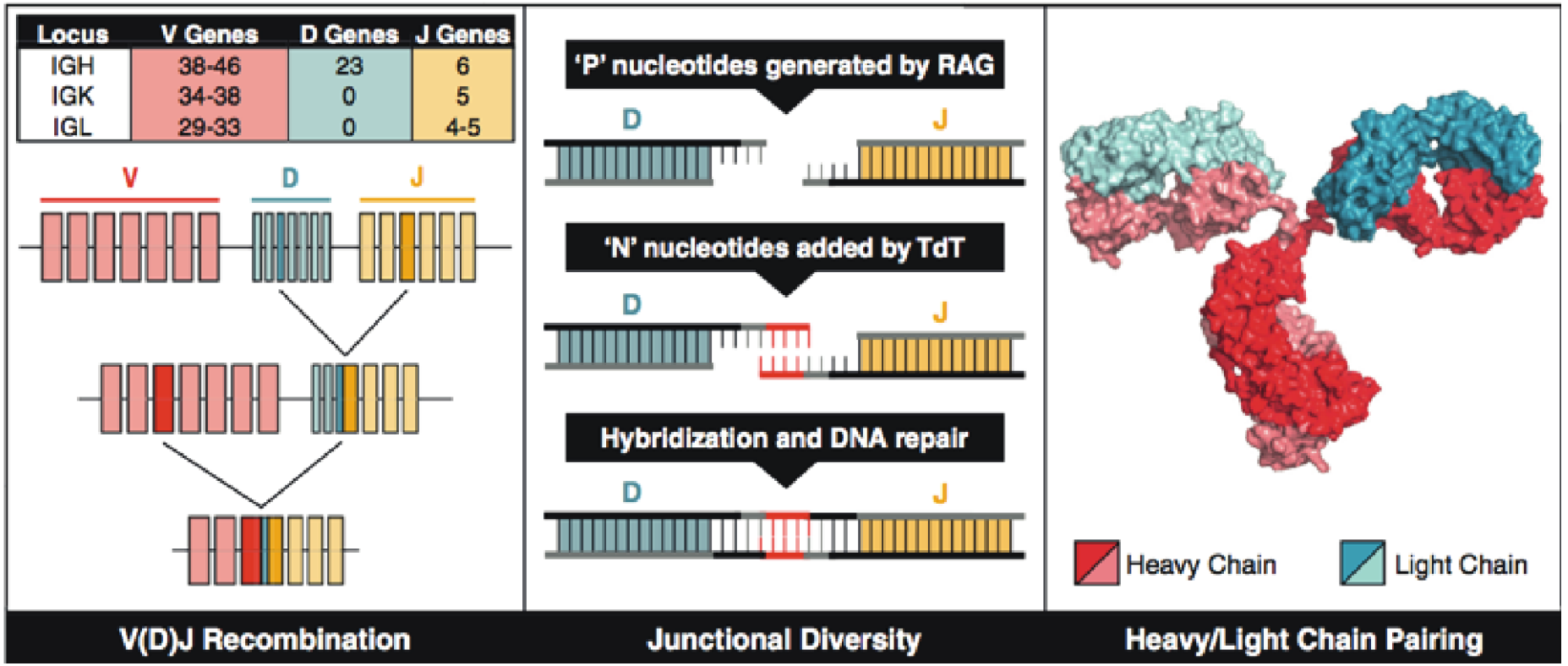

V-Gene || non-templated (N) Nucleotides || D-Gene || N-Nucleotides || J-Gene

Finn et al. ***Curr Opin. Immunol*** 2013

Complementarity Determining Regions (CDRs) recognize Antigens

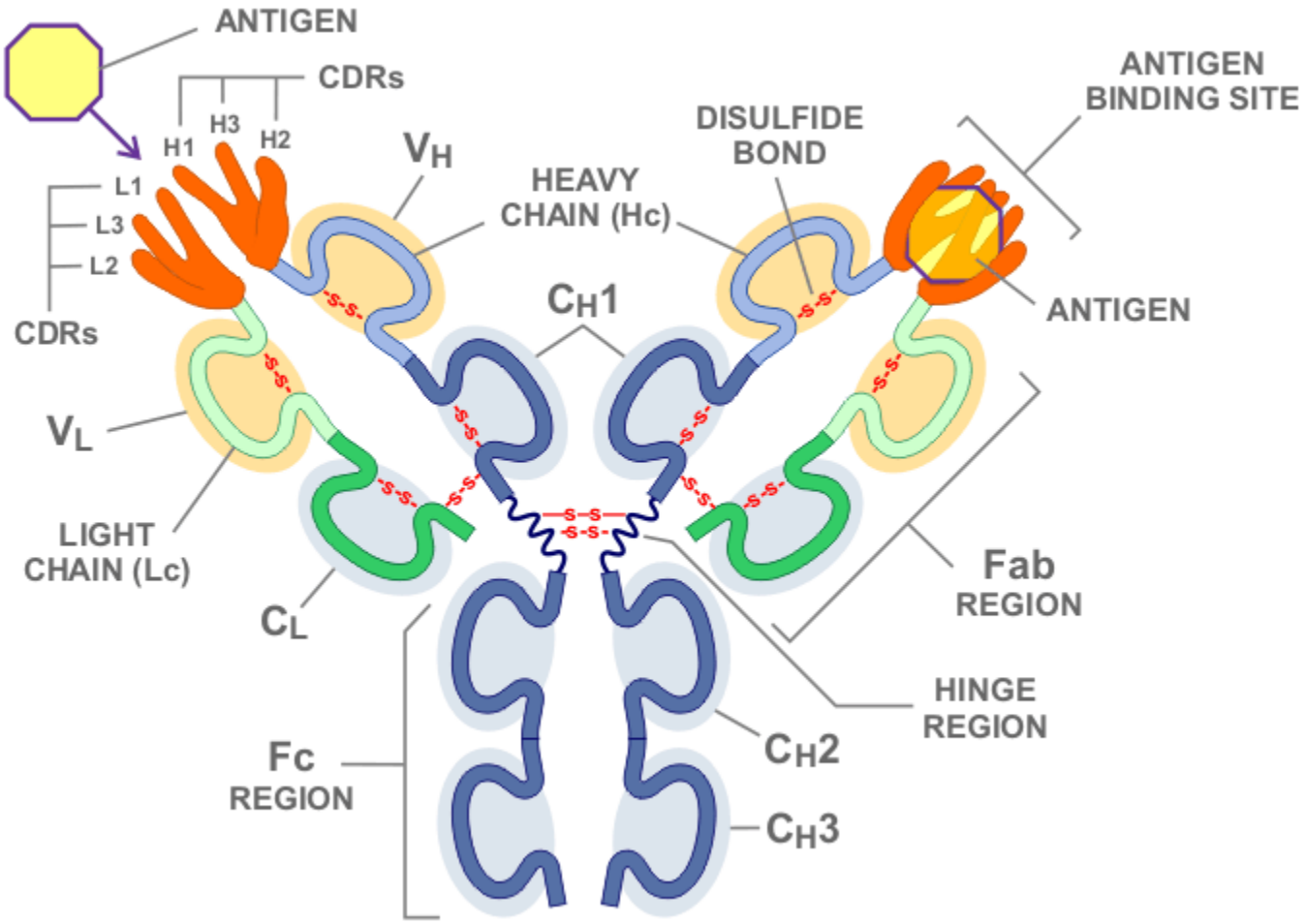

MSD of flexible proteins predicts sequences optimal for conformational change

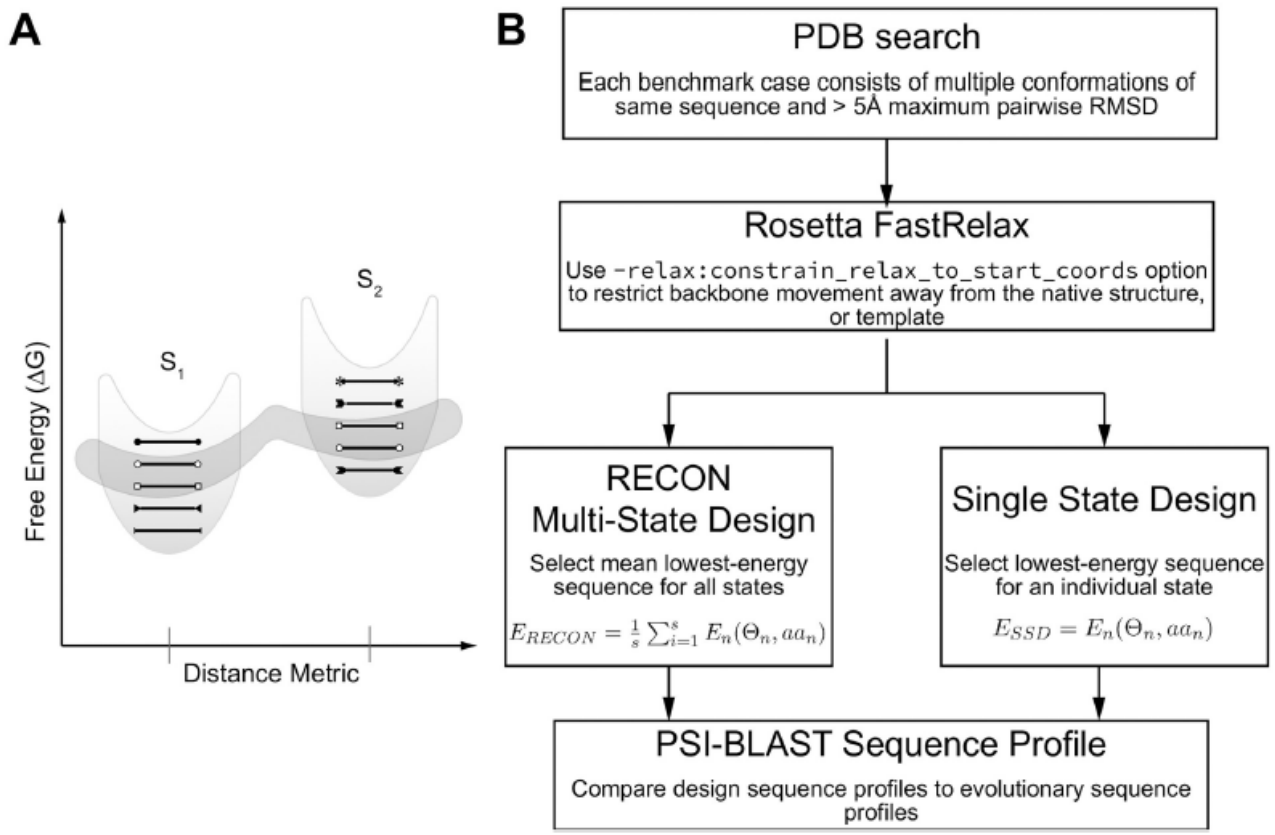

Fig 1. Graphical representation of hypothesis and experimental design. (A) Schematic of sequence space and the impact of flexibility on sequence tolerance. S_1 and S_2 represent two unique conformations of the same residue length separated by some RMSD that populate two local energy minima. Black lines with end caps represent unique sequences that are energetically most favorable for a single conformation. The dark shaded area encircles sequences that are energetically favorable for both conformations. Here we illustrate that by using multiple conformations during protein design, we identify sequences that are energetically suitable for conformational flexibility, yet are not necessarily the most stable sequence for any given conformation. Additionally, the requirement to adopt multiple conformations constrains the number of suitable sequences (B) Flow chart of benchmark design.

Sauer, M. F., Sevy, A. M., Crowe, J. E., Jr., & Meiler, J. (2020). Multi-state design of flexible proteins predicts sequences optimal for conformational change. *PLoS Comput Biol, 16(2), e1007339. https://doi.org/10.1371/journal.pcbi.1007339*

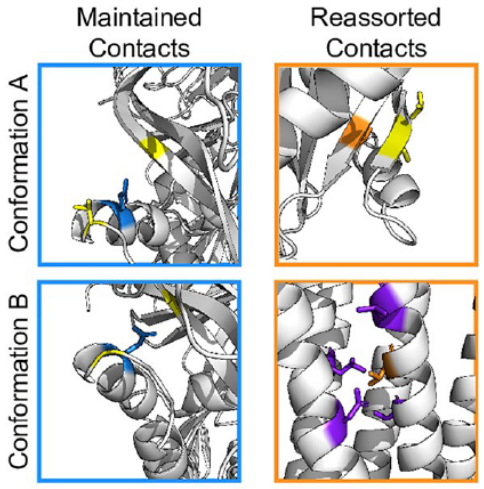

Local side chain environment changes based on global conformational rearrangements

Simulating Antibody Affinity Maturation in the Computer

- Rapid Multi-State Design Algorithm for Rosetta

Table 6. Comparison of design-generated sequences to evolutionary sequence profiles of input proteins.

	Evolutionary sequence similarity (%)[a]		
Benchmarkcase	RECON FBB	RECON BBM	MPI_MSD
CheY	56.3	70.5	57.5
Elastase	60.3	70.7	65.9
FYN	87.0	87.0	96.0
PAPD	61.7	65.3	52.4
Ran	76.6	79.3	82.5
V_H1-69	90.6	91.7	32.0
V_H3-23	50.7	50.7	36.4
V_H5-51	69.0	67.0	30.4
Average	**69.0**	**72.8**	**56.6**

Designs produced by MPI_MSD or fixed backbone (FBB) or backbone minimized (BBM) RECON algorithms were compared to sequence profiles of evolutionarily related proteins at designed positions.
[a]Sequence similarity is computed as the Sandelin-Wasserman similarity, normalized as a percentage. See methods for details.

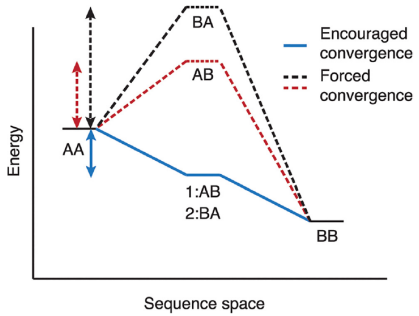

A. M. Sevy, T. M. Jacobs, J. E. Crowe, Jr. and J. Meiler; "Design of Protein Multi-specificity Using an Independent Sequence Search Reduces the Barrier to Low Energy Sequences"; *PLoS Comput Biol*; **2015**; Vol. 11 (7): p. e1004300.

- SSD for Affinity Maturation
- MSD for Broad Neutralization

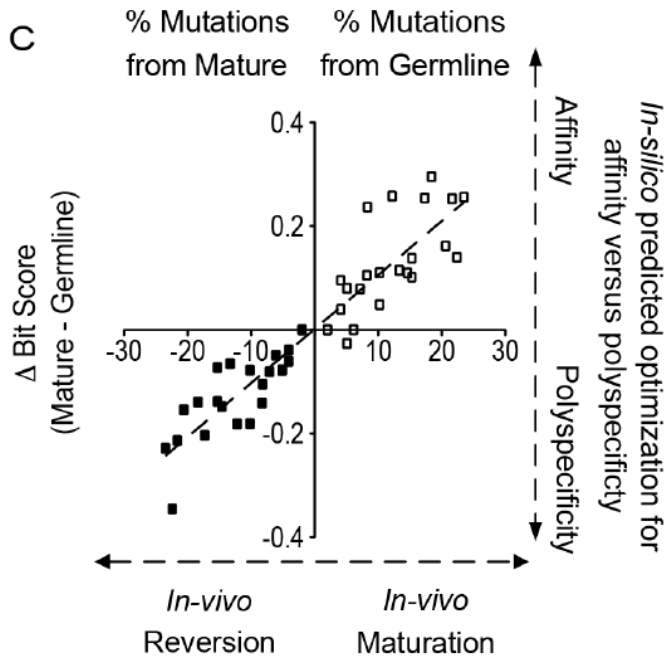

J. R. Willis, B. S. Briney, S. L. DeLuca, J. E. Crowe, Jr. and J. Meiler; "Human germline antibody gene segments encode polyspecific antibodies"; *PLoS Comput Biol*; **2013**; Vol. 9 (4): p. e1003045.

Redesign of PG9 Enhances Binding Potency and Breadth of Neutralization

- 30 Amino Acid HCDR3 but few somatic mutations
- N109Y Mutant is Predicted to Stabilize HCDR3 in Active Conformation

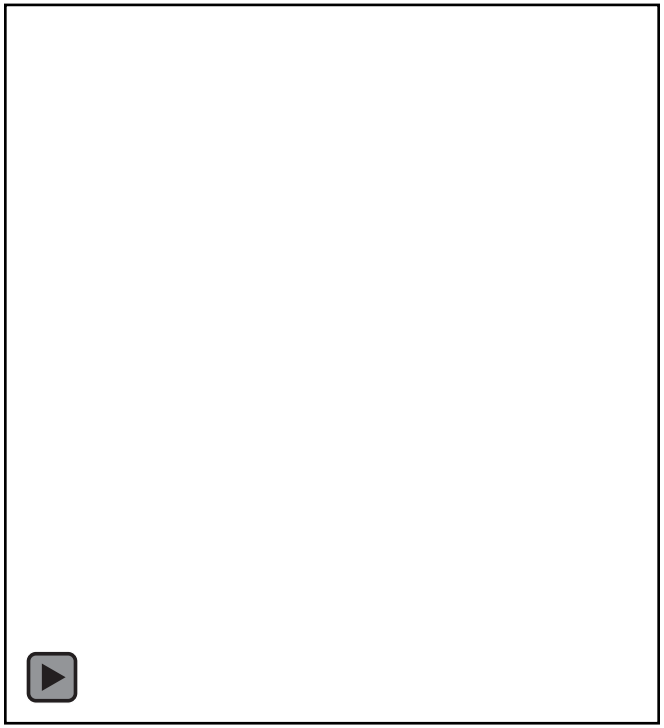

		EC_{50} (μg/mL)					IC_{50} (μg/mL)				
Virus	N160	PG9wt	LEU100F	ASN100L	TYR100F	4MUT	PG9wt	EU100F	ASN10	TYR100F	4MUT
6535.3	N	0.26	0.10	0.49	0.09	7.74	ND	ND	ND	ND	ND
7165.18	N	>100	>100	>100	>100	>100	ND	ND	ND	ND	ND
0260.v5.c36	N	ND	ND	ND	ND	ND	1.69	0.50	2.10	0.30	ND
1054_07_TC4_1499	N	ND	ND	ND	ND	ND	>33	>33	>33	>33	ND
1056_10_TA11_1826	N	ND	ND	ND	ND	ND	6.34	1.10	13.60	0.70	ND
246F C1G	**S**	**ND**	**ND**	**ND**	**ND**	**ND**	>33	>33	>33	**2.70**	**ND**
3016.v5.c45	N	ND	ND	ND	ND	ND	2.46	1.60	9.00	0.20	ND
398_F1_F5_20	N	ND	ND	ND	ND	ND	>33	>33	>33	10.80	>33
7030102001E5(Rev-)	S	ND	ND	ND	ND	ND	>33	>33	>33	12.90	ND
703357.c02	N	ND	ND	ND	ND	ND	1.16	0.28	19.40	0.23	ND
AC10.0.29	N	>100	>100	>100	>100	>100	ND	ND	ND	ND	ND
BaL.26	N	0.54	0.04	>100	0.05	>100	0.07	0.03	0.52	0.01	>33.3
BG505.N332	N	1.48	0.42	3.63	0.25	2.86	0.04	0.02	0.11	0.02	0.28
BJOX009000.02.4	N	ND	ND	ND	ND	ND	1.73	1.20	>33	1.50	ND
CAAN5342.A2	N	1.20	0.47	1.06	0.44	2.33	4.60	7.60	>33	1.80	ND
CAP45.2.00.G3	N	0.03	0.01	0.13	0.01	9.45	<0.01	<0.01	0.01	<0.01	<0.01
Ce1086_B2	**K**	**ND**	**ND**	**ND**	**ND**	**ND**	>33	>33	>33	**15.40**	**ND**
Ce1086_B2.K160N.LucR.T2A.ecto	N	ND	ND	ND	ND	ND	ND	0.03	0.10	0.04	ND
Ce1086_B2.LucR.T2A.ecto	**K**	**ND**	**ND**	**ND**	**ND**	**ND**	ND	>33	>33	**10.20**	**ND**
Ce2010_F5	N	ND	ND	ND	ND	ND	>33	>33	>33	15.40	ND
Ce703010217-_B6	N	ND	ND	ND	ND	ND	0.02	0.01	0.03	0.01	0.04
CNE55	N	ND	ND	ND	ND	ND	1.13	1.80	8.60	0.65	25.20
Du422.1	N	ND	ND	ND	ND	ND	1.90	0.15	2.80	0.44	5.00
HIV-16845-2.22	N	ND	ND	ND	ND	ND	4.40	1.90	17.40	0.80	ND
HxBC2P3.2	N	2.41	0.25	0.74	0.49	7.78	>3.3	0.59	>33	0.09	>33
PVO.4	N	>100	>100	>100	>100	>100	ND	ND	ND	ND	ND
Q461.e2	N	ND	ND	ND	ND	ND	1.48	0.80	9.60	0.40	ND
QH0692.42	**S**	>100	>100	>100	>100	>100	>33	>33	>33	>33	**ND**
R2184.c04	N	ND	ND	ND	ND	ND	0.28	0.49	17.20	0.11	>33
REJO4541.67	N	>100	>100	>100	>100	>100	ND	ND	ND	ND	ND
RHPA.LucR.T2A.ecto	N	ND	ND	ND	ND	ND	>10	5.60	>33	2.30	ND
RHPA/N160A.5.LucR.T2A.ecto	**A**	**ND**	**ND**	**ND**	**ND**	**ND**	**ND**	>33	>33	**8.40**	**ND**
RHPA4259.7	N	0.66	0.13	1.32	0.16	15.70	ND	ND	ND	ND	ND
SC22.3C2.LucR.T2A.ecto	N	ND	ND	ND	ND	ND	>33	>33	>33	12.90	>33
SC422661.8	N	2.48	0.25	1.89	0.31	24.87	1.80	0.30	13.70	0.20	>33
TH023.6	N	ND	ND	ND	ND	ND	0.11	0.04	1.40	0.05	11.10
TH023.6/N160A.5	**A**	**ND**	**ND**	**ND**	**ND**	**ND**	>33	>33	>33	**3.72**	>33
THRO4156.18	N	>100	>100	>100	>100	>100	ND	ND	ND	ND	ND
TRJO4551.58	N	0.17	0.05	0.39	0.07	>100	ND	ND	ND	ND	ND
TRO.11	N	>100	>100	>100	>100	>100	>33	11.03	>33	3.10	>33
WEAU_d15_410_5017	N	ND	ND	ND	ND	ND	4.08	0.06	>33	0.05	ND
WITO4160.33	N	ND	ND	ND	ND	ND	0.03	0.01	0.05	0.01	0.07
X1632_S2_B10	N	ND	ND	ND	ND	ND	0.47	0.24	4.20	0.13	19.20
X2088_c9	N	ND	ND	ND	ND	ND	>33	>33	>33	20.70	ND
X2278_C2_B6	N	ND	ND	ND	ND	ND	0.07	0.01	0.35	0.02	2.70
YU2	N	>100	>100	>100	>100	>100	3.09	1.27	3.88	0.66	>33
ZM109F.B	N	0.02	0.01	0.04	< 0.01	2.27	0.38	0.24	1.57	0.14	>33
ZM214M.PL15	**K**	**ND**	**ND**	**ND**	**ND**	**ND**	>33	>33	>33	**13.00**	**ND**

J. R. Willis, G. Sapparapu, S. Murrell, J. P. Julien, V. Singh, H. G. King, Y. Xia, J. A. Pickens, C. C. LaBranche, J. C. Slaughter, D. C. Montefiori, I. A. Wilson, J. Meiler and J. E. Crowe, Jr.; "Redesigned HIV antibodies exhibit enhanced neutralizing potency and breadth"; *J Clin Invest*; **2015**; Vol. 125 (6): p. 2523-31.

Position Specific Scoring Matrix for Screening of Candidate Antibodies

- Do HIV-Naïve Humans have PG9-like Antibodies?
- Screening of 25,000 HCDR3s using Rosetta-Inspired PSSMs

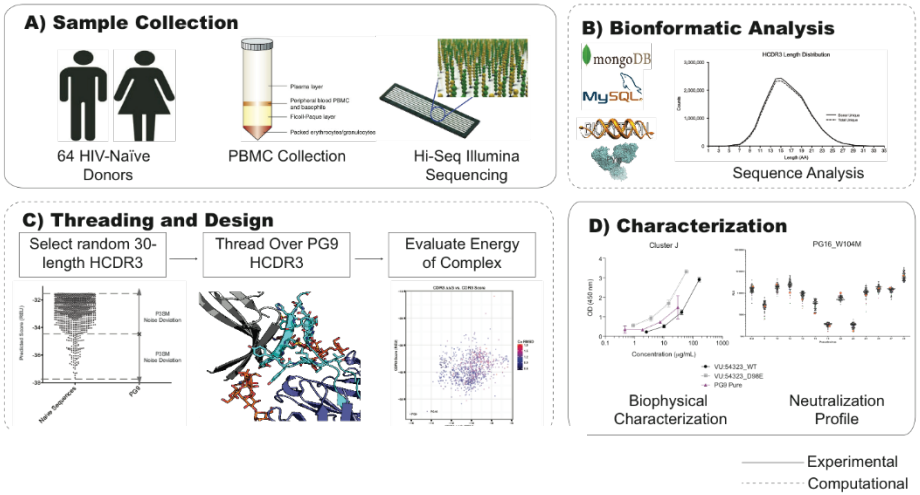

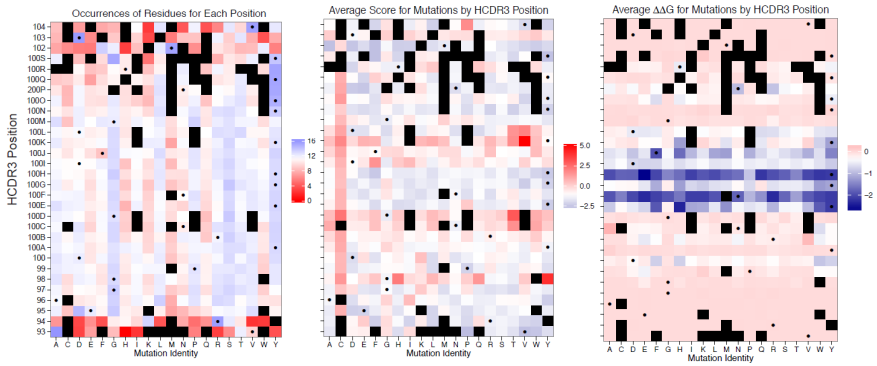

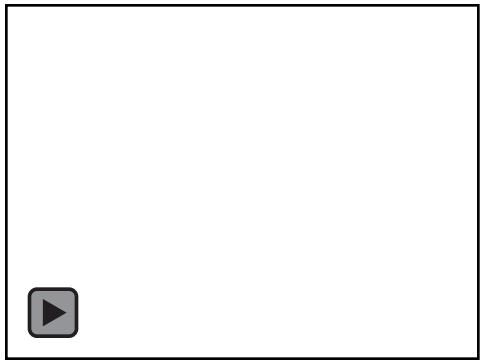

Finn, J. A., Dong, J., Sevy, A. M., Parrish, E., Gilchuk, I., Nargi, R., Scarlett-Jones, M., Reichard, W., Bombardi, R., Voss, T. G., Meiler, J., & Crowe, J. E., Jr. (2020). Identification of Structurally Related Antibodies in Antibody Sequence Databases Using Rosetta-Derived Position-Specific Scoring. *Structure, 28(10), 1124-1130 e1125. https://doi.org/10.1016/j.str.2020.07.012*

In silico Affinity Maturation of Candidate Antibody HCDR3s

- Rosetta Design

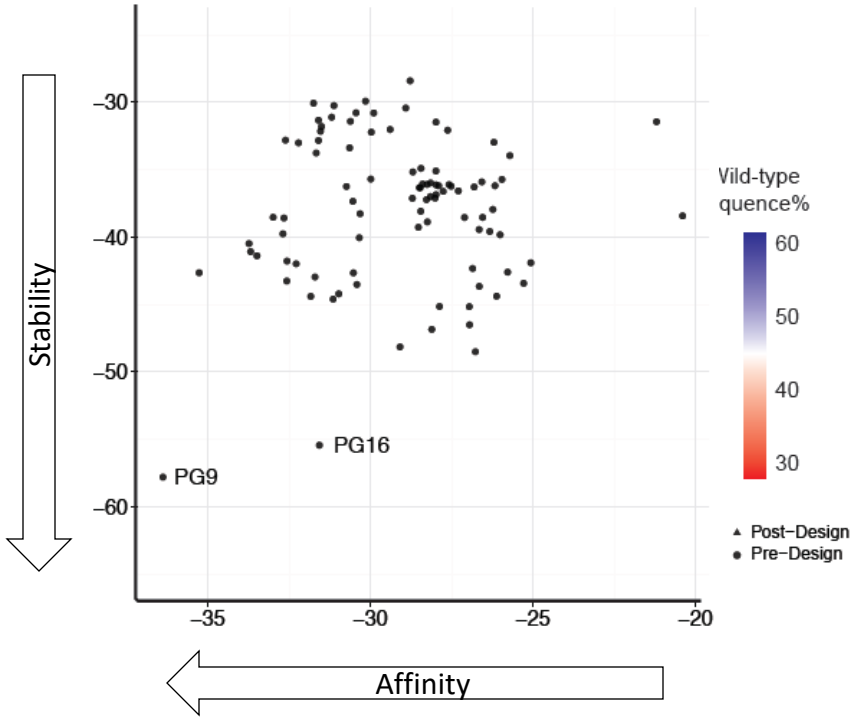

- Experimental Verification

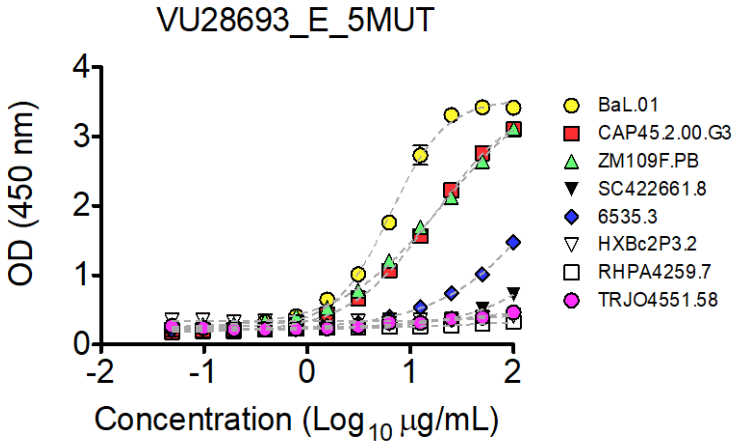

J. R. Willis, …, J. Meiler and J. E. Crowe, Jr.; "Long antibody HCDR3s from HIV-naive donors presented on a PG9 neutralizing antibody background mediate HIV neutralization"; Proc Natl Acad Sci U S A; 2016; Vol. 113 (16): p. 4446-51.

CDRH3-based cyclic peptides targeting influenza

A. Influenza antibody with long CDRH3 loop

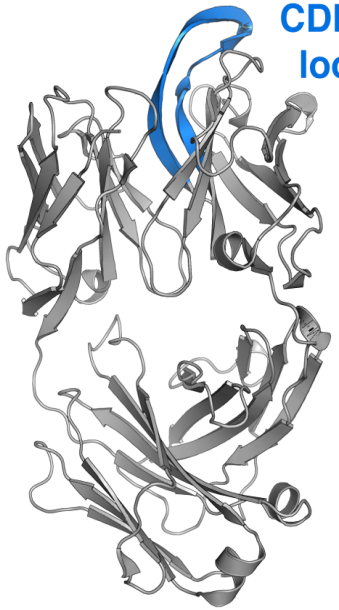

Remove CDRH3 loop
Add disulfide bond

B. Folding simulations with ROSETTA

Wild-type (WT)

Redesign

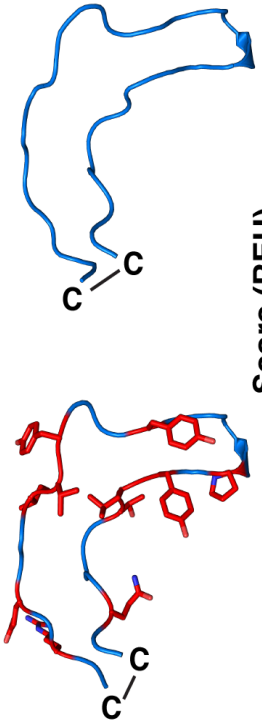

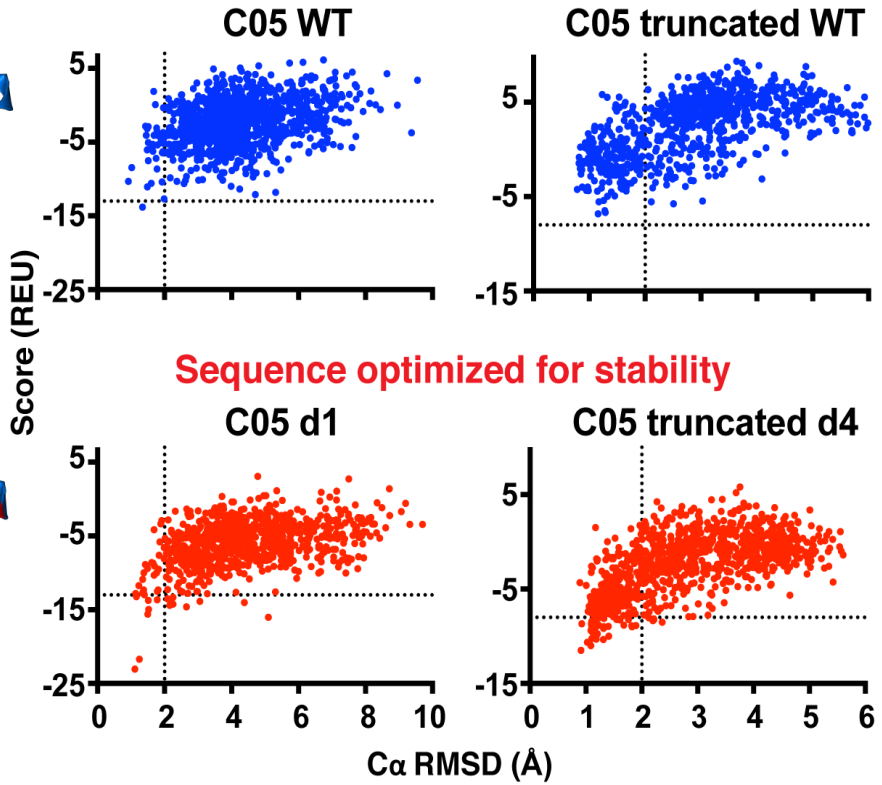

Alexander M Sevy, Iuliia M. Gilchuk, Rachel Nargi, Mattie Jensen, Jens Meiler, James E. Crowe; "Computationally designed cyclic peptides derived from an antibody loop increase breadth of binding for influenza variants; submitted

C05-based cyclic peptides have increased breadth of HA recognition

Group	Subtype	Strain	C05 d1	C05 d4	C05 IgG
1	H1N1	A/Solomon Islands/03/2006	+++	+++	++++
		A/Solomon Islands/03/2006 head domain	++	++	+++
		A/Brevig Mission/1/1918	-	-	-
		A/Tottori/YK012/2011	-	-	-
		A/mallard/Alberta/35/1976	-	-	++
		A/Puerto Rico/8/1934	+++	+++	-
		A/Texas/36/1991	-	-	-
		A/New Caledonia/20/1999	+++	+++	++
		A/California/04/2009	-	++++	-
	H2N2	A/Japan/305/1957	+++	++	++++
		A/Singapore/1/1957	+++	+++	++++
	H5N1	A/Vietnam/1203/2005	-	-	-
		A/Indonesia/5/2005	-	-	-
	H9N2	A/turkey/Wisconsin/1/1966	++++	+++	++
	H16N3	A/black-headed gull/Sweden/4/1999	-	-	-
2	H3N2	A/Hong Kong/1/68	+++	+++	++++
		A/Brisbane/10/2007	+++	+++	++++
		A/Perth/16/2009	+++	-	++++
		A/Panama/2007/1999	-	-	++++
		A/Bangkok/1/1979	-	-	-
	H4N6	A/duck/Czechoslovakia/1956	+++	+++	-
	H7N9	A/Shanghai/02/2013	+++	+++	-
		A/Netherlands/219/2003	-	-	-
	H15N8	A/shearwater/Western Australia/2576/1979	-	-	-

Legend

++++	<10 nM	Gray: No change in breadth compared to IgG
+++	10-100 nM	Green: Gain of breadth compared to IgG
++	100-1,000 nM	Orange: Loss of breadth compared to IgG
+	>1,000 nM	
-	Binding not detected	
NT	Not tested	


Proof of principle for epitope-focused vaccine design: respiratory syncytial virus

Vaccines prevent infectious disease largely by inducing protective neutralizing antibodies against vulnerable epitopes. Several major pathogens have resisted traditional vaccine development, although vulnerable epitopes targeted by neutralizing antibodies have been identified for several such cases. Hence, new vaccine design methods to induce epitope-specific neutralizing antibodies are needed. Here we show, with a neutralization epitope from respiratory syncytial virus, that computational protein design can generate small, thermally and conformationally stable protein scaffolds that accurately mimic the viral epitope structure and induce potent neutralizing antibodies. These scaffolds represent promising leads for the research and development of a human respiratory syncytial virus vaccine needed to protect infants, young children and the elderly. More generally, the results provide proof of principle for epitope-focused and scaffold-based vaccine design, and encourage the evaluation and further development of these strategies for a variety of other vaccine targets, including antigenically highly variable pathogens such as human immunodeficiency virus and influenza.

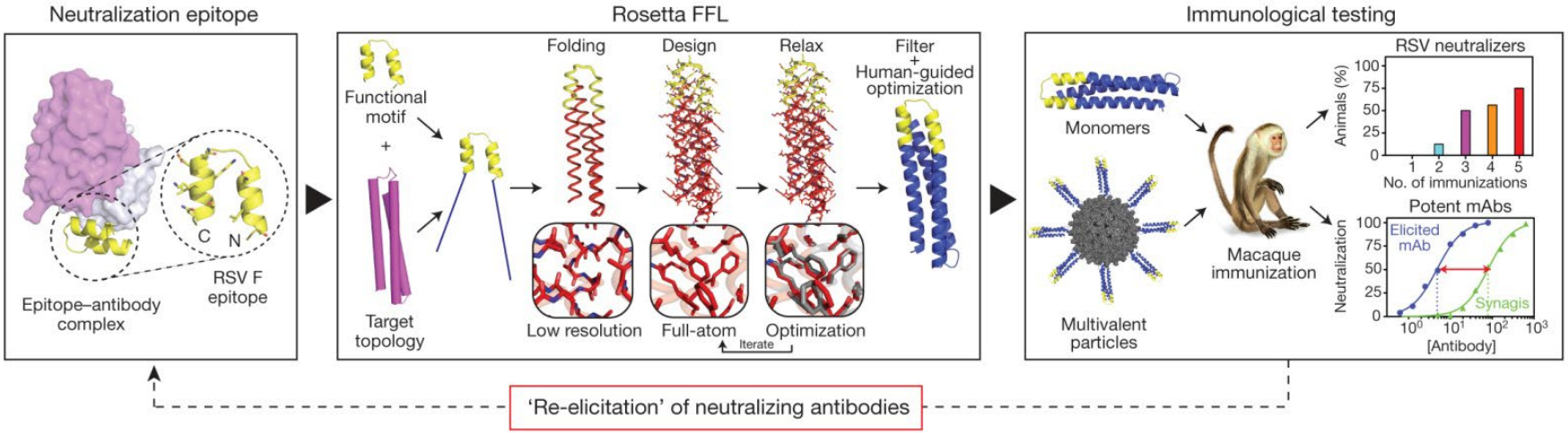

B. E. Correia, J. T. Bates, R. J. Loomis, G. Baneyx, C. Carrico, J. G. Jardine, P. Rupert, C. Correnti, O. Kalyuzhniy, V. Vittal, M. J. Connell, E. Stevens, A. Schroeter, M. Chen, S. Macpherson, A. M. Serra, Y. Adachi, M. A. Holmes, Y. Li, R. E. Klevit, B. S. Graham, R. T. Wyatt, D. Baker, R. K. Strong, J. E. Crowe, Jr., P. R. Johnson and W. R. Schief; "Proof of principle for epitope-focused vaccine design"; *Nature*; **2014**; Vol. 507 (7491): p. 201-6.

Epitope-focused vaccine design to elicit HR2/MPER antibodies

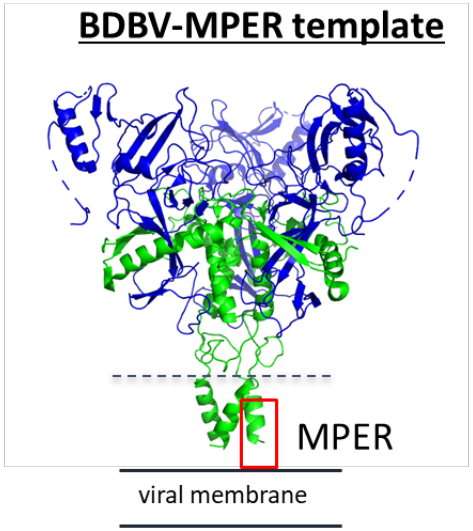

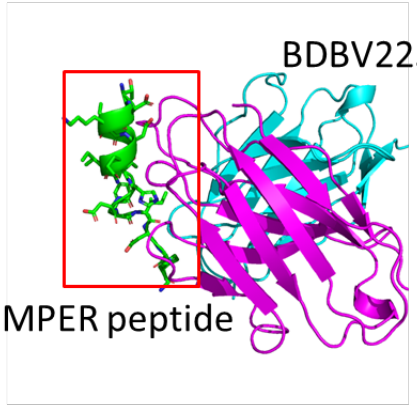

Epitope-focused vaccine design to elicit HR2/MPER antibodies

BDBV-MPER template

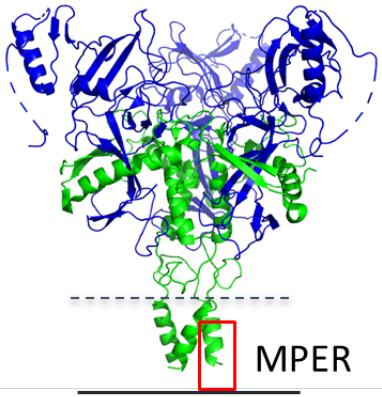

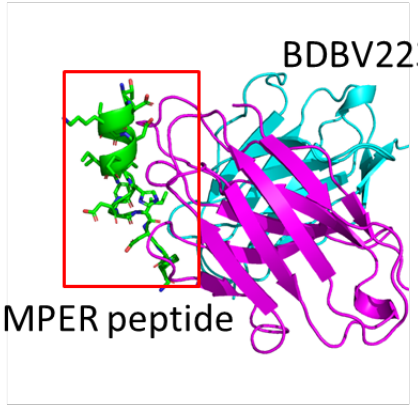

Rosetta immunogen design

Rosetta Commons

Sidechain Grafting
Backbone Grafting
FoldFromLoops
(1. Gen.)

PDB crystal structures
< 2.5 A resolution
E. coli expressed

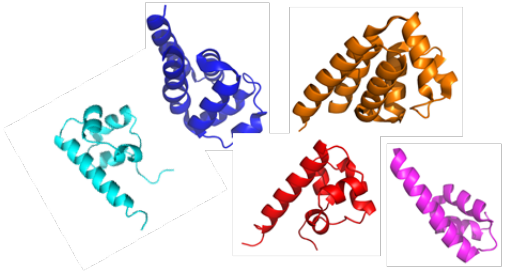

Epitope-focused vaccine design to elicit HR2/MPER antibodies

BDBV-MPER template

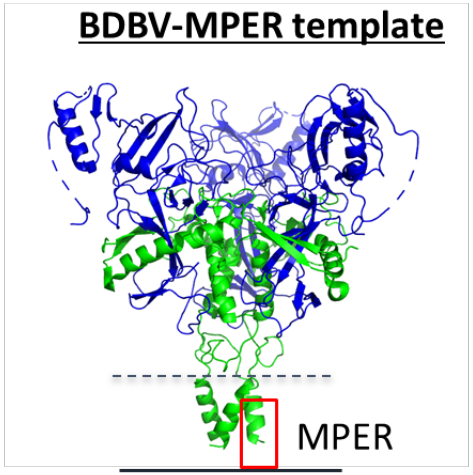

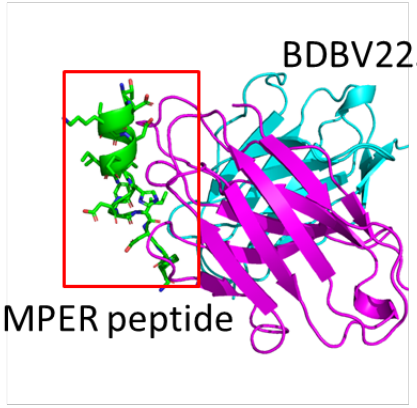

Rosetta immunogen design

Rosetta Commons

Sidechain Grafting
Backbone Grafting
FoldFromLoops
(1. Gen.)

PDB crystal structures
< 2.5 A resolution
E. coli expressed

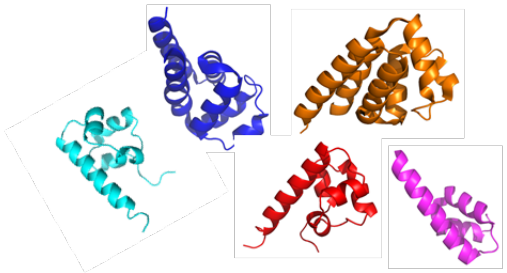

Immunogen testing

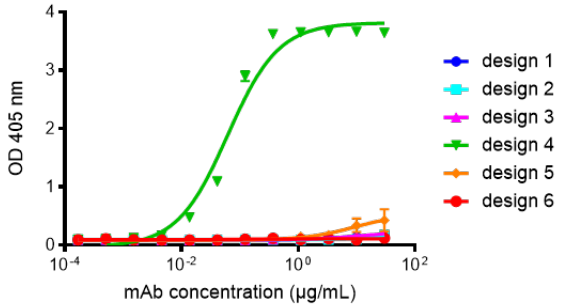

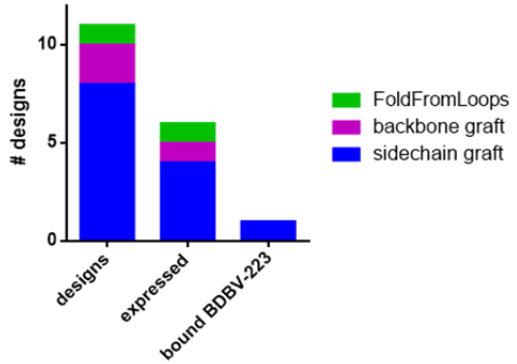

^{1}H-^{15}N HSQC spectrum showing the assignment for the MPER immunogen

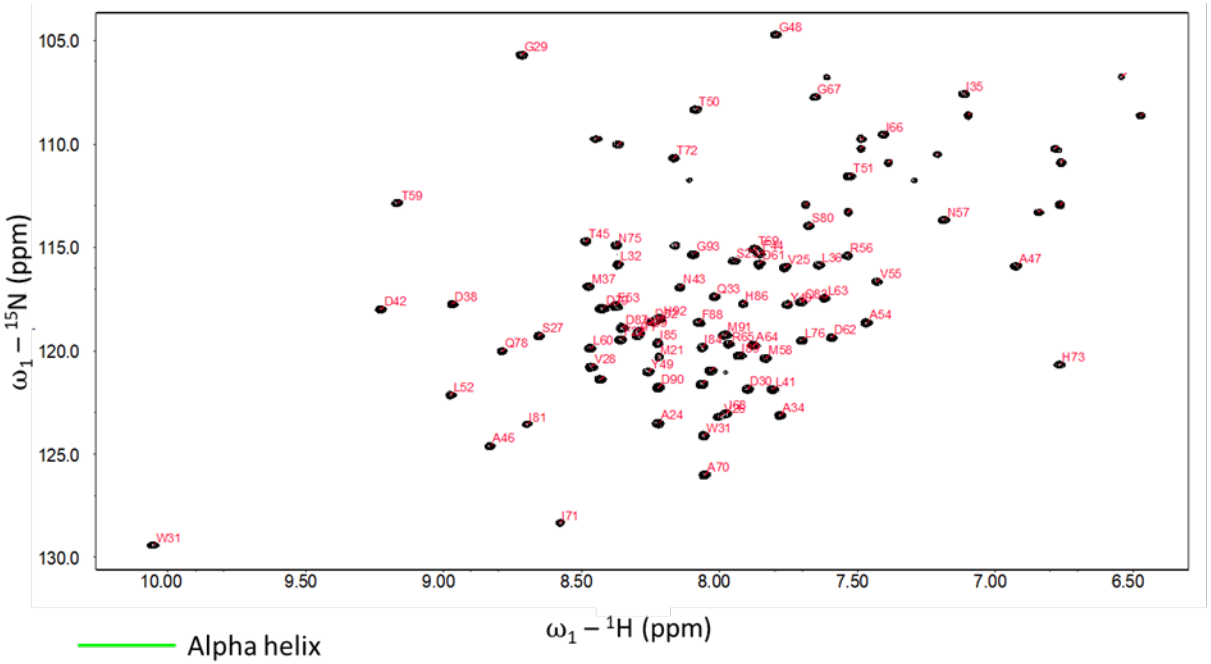

NMR

Rosetta

Alpha helix

Beta sheet

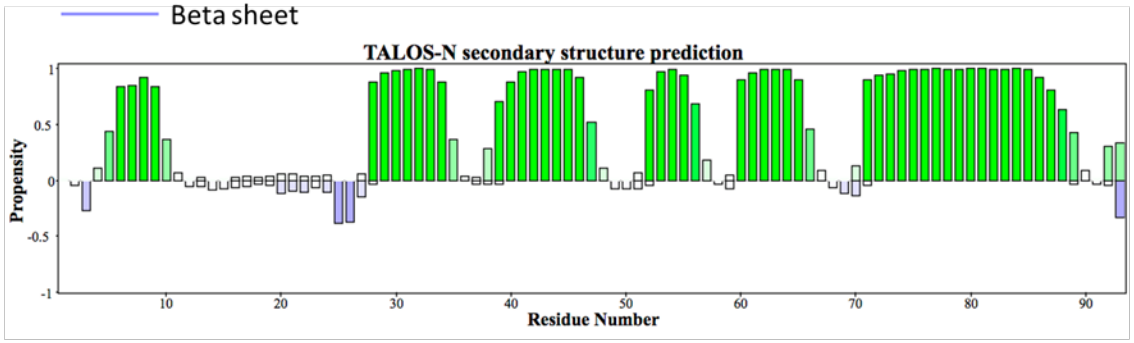

Presentation on Self-Assembling Particle Platform

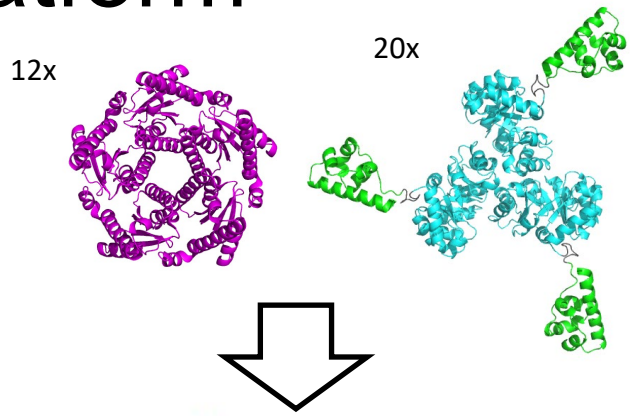

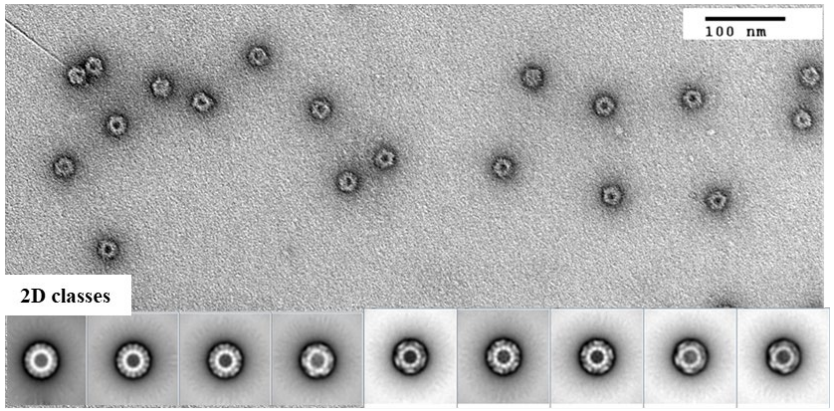

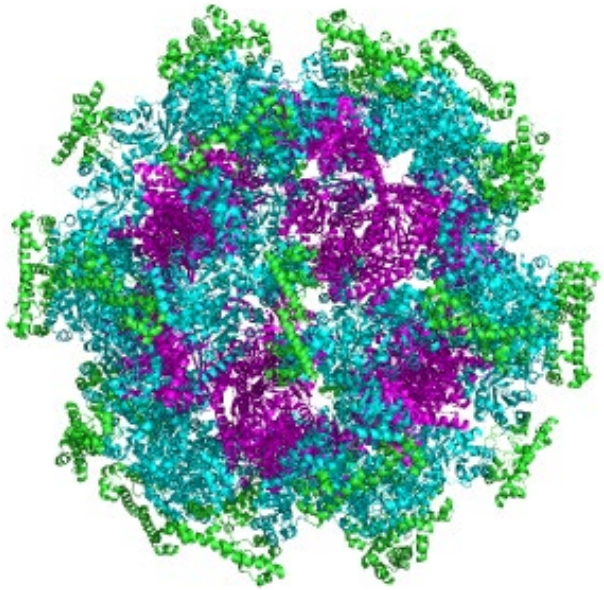

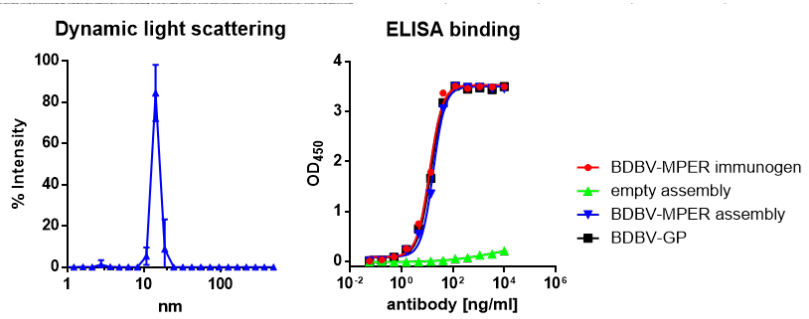

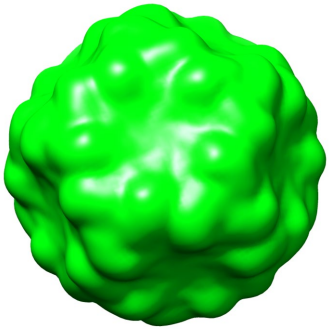

Rosetta Antibody Design biased to only create Human-Like Antibodies

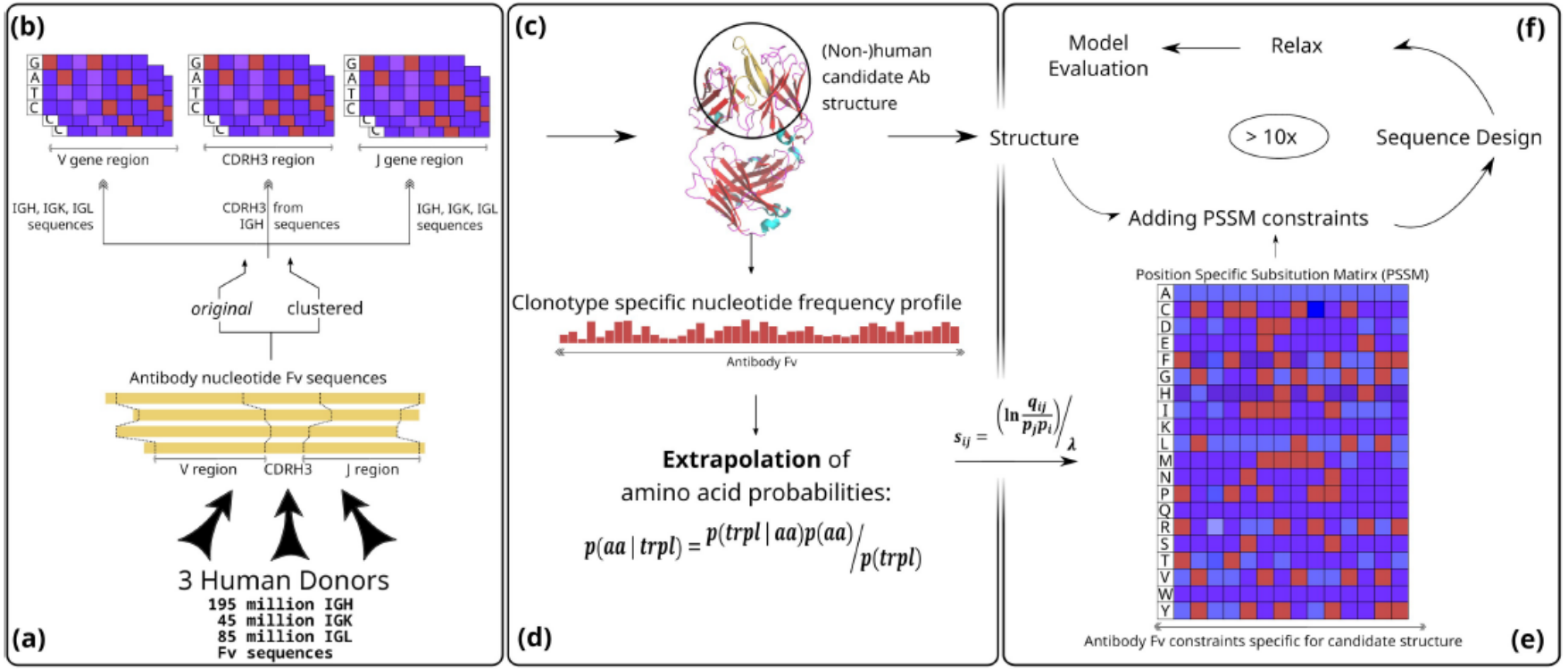

Nucleotide Frequency Assessment | Human antibody sequence space | Structural design of human-like antibodies

Schmitz, S., Schmitz, E. A., Crowe, J. E., Jr., & Meiler, J. (2022). The human antibody sequence space and structural design of the V, J regions, and CDRH3 with Rosetta. *MAbs, 14(1), 2068212. https://doi.org/10.1080/19420862.2022.2068212*

Robust deep learning-based protein sequence design using ProteinMPNN

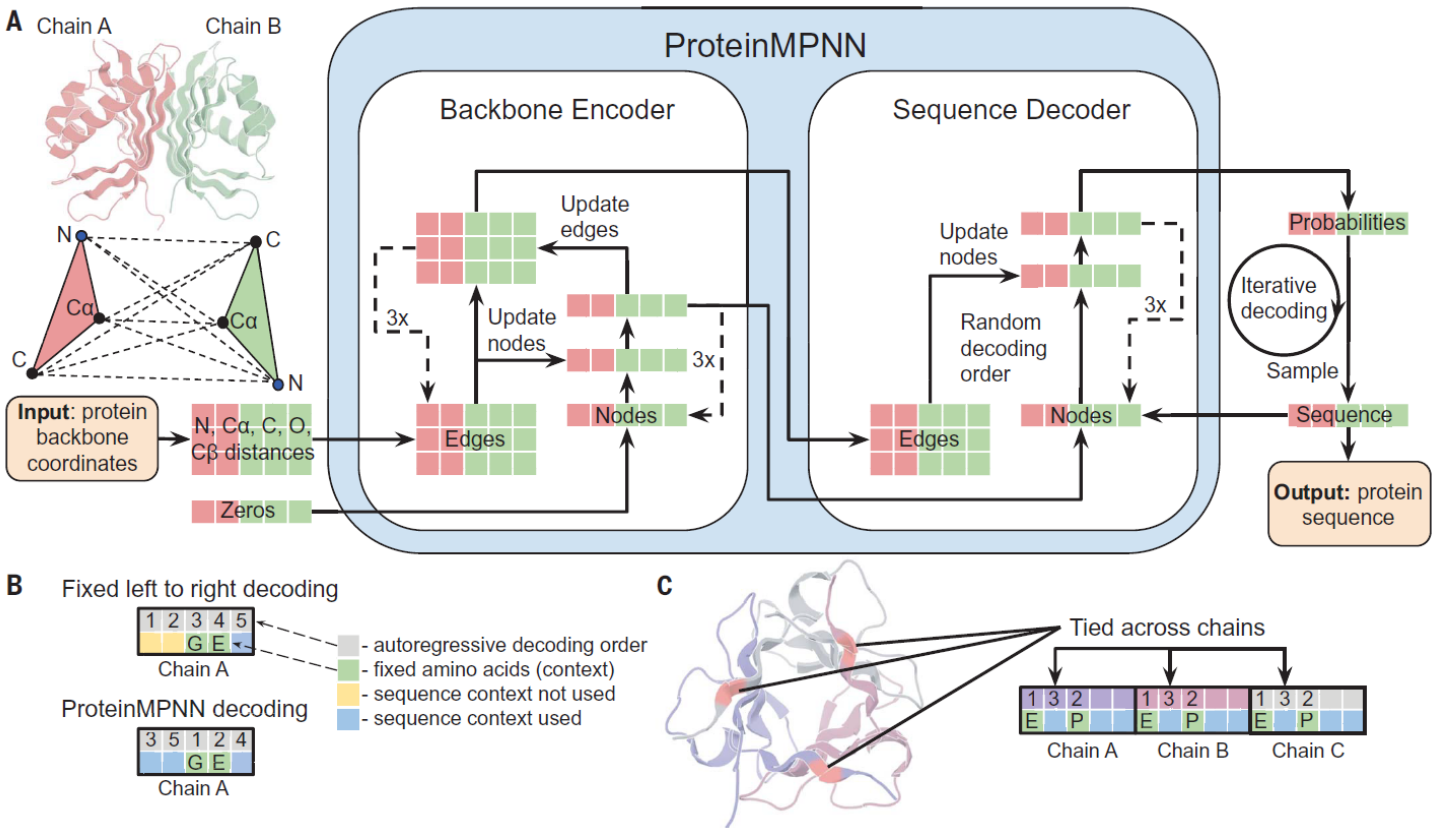

J. Dauparas, I. Anishchenko, N. Bennett, H. Bai, R. J. Ragotte, L. F. Milles, B. I. M. Wicky, A. Courbet, R. J. de Haas, N. Bethel, P. J. Y. Leung, T. F. Huddy, S. Pellock, D. Tischer, F. Chan, B. Koepnick, H. Nguyen, A. Kang, B. Sankaran, A. K. Bera, N. P. King and D. Baker; "Robust deep learning-based protein sequence design using ProteinMPNN"; *Science;* ***2022; Vol. 378 (6615): p. 49-56.***

De novo Protein Design by Deep Network Hallucination

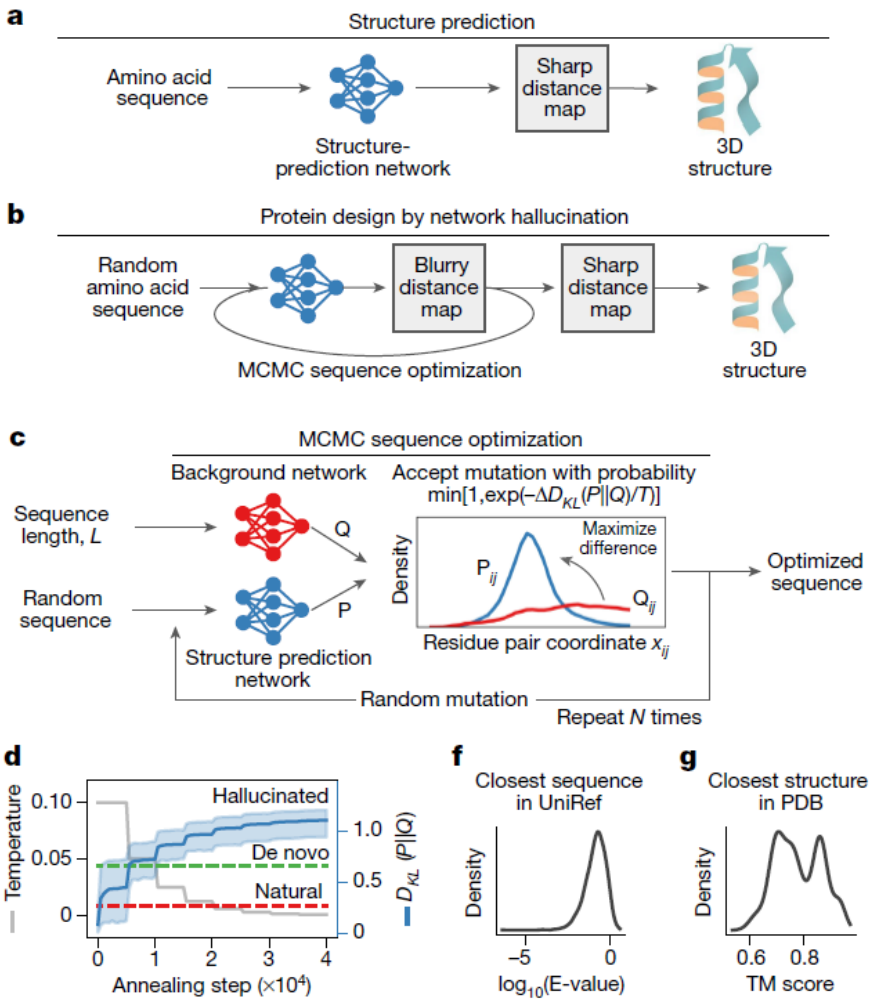

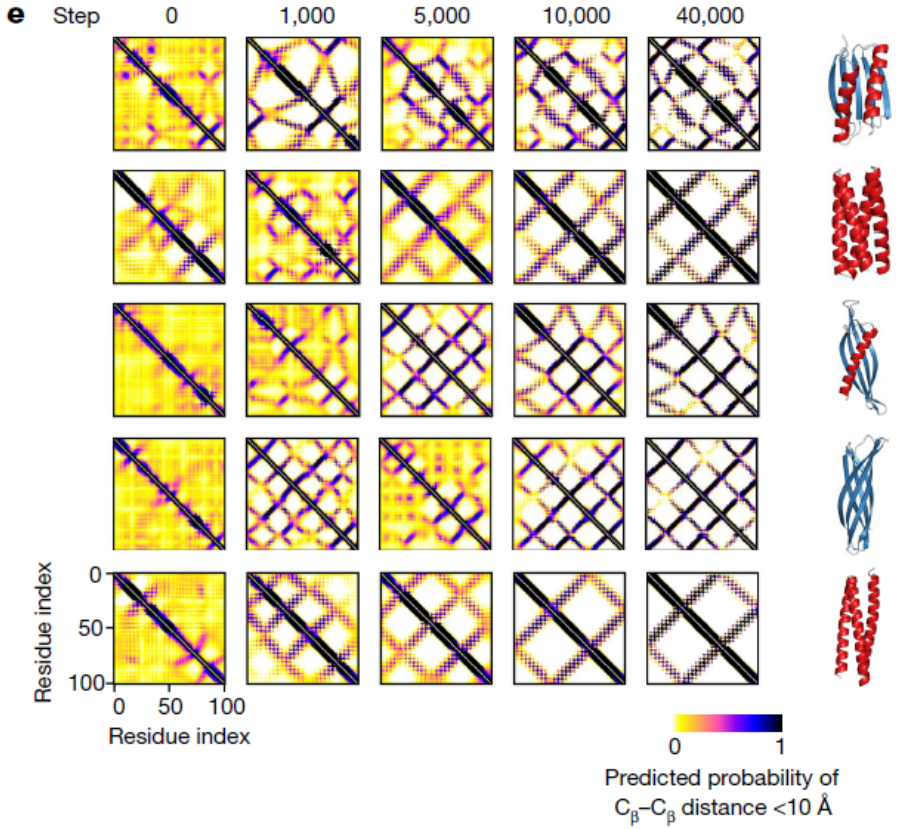

I. Anishchenko, S. J. Pellock, T. M. Chidyausiku, T. A. Ramelot, S. Ovchinnikov, J. Hao, K. Bafna, C. Norn, A. Kang, A. K. Bera, F. DiMaio, L. Carter, C. M. Chow, G. T. Montelione and D. Baker; "De novo protein design by deep network hallucination"; *Nature;* ***2021; Vol. 600 (7889): p. 547-552.***

Anchor extension: a structure-guided approach to design cyclic peptides

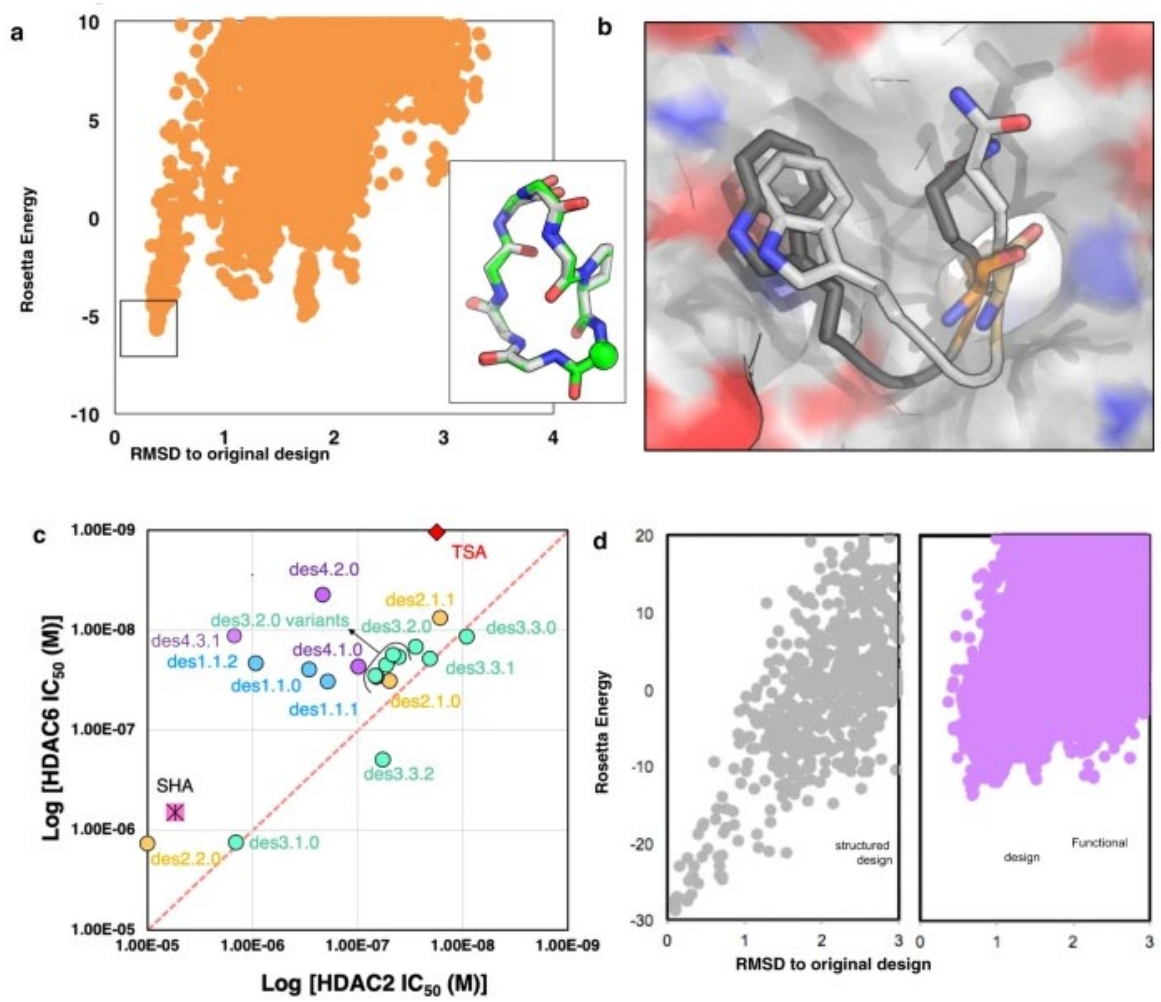

P. Hosseinzadeh, P. R. Watson, T. W. Craven, X. Li, S. Rettie, F. Pardo-Avila, A. K. Bera, V. K. Mulligan, P. Lu, A. S. Ford, B. D. Weitzner, L. J. Stewart, A. P. Moyer, M. Di Piazza, J. G. Whalen, P. J. Greisen, D. W. Christianson and D. Baker; "Anchor extension: a structure-guided approach to design cyclic peptides targeting enzyme active sites"; *Nat Commun;* ***2021; Vol. 12 (1): p. 3384.***

Design of protein-binding proteins from the target structure alone

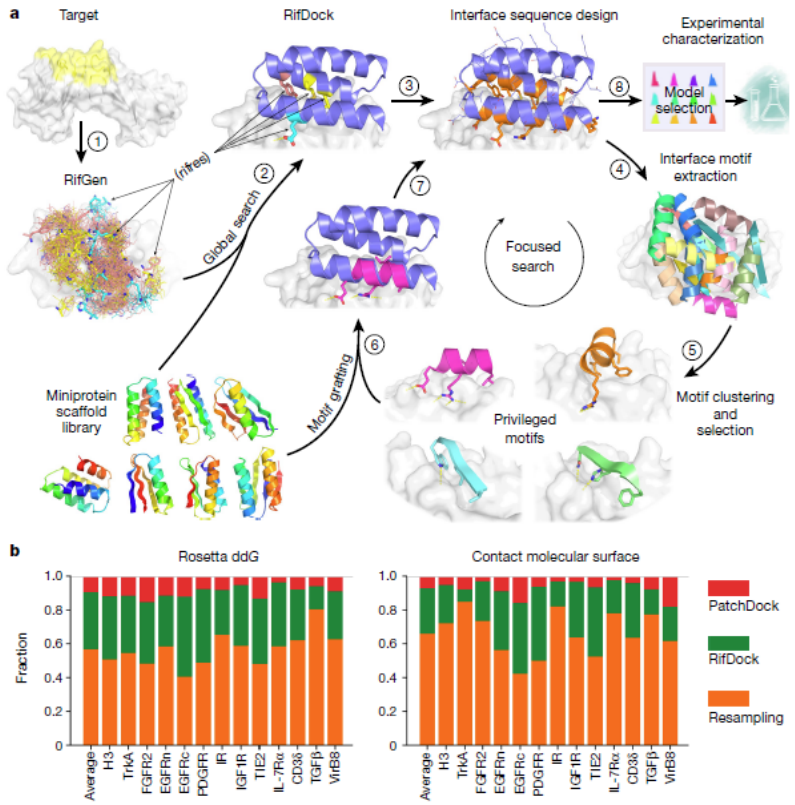

Fig. 1 | Overview of the de novo protein binder design pipeline. a, Schematic of our two-stage binder design approach. In the global search stage, billions of disembodied amino acids are docked onto the selected region of the target protein surface using RifGen, the favourable interacting amino acids are stored as rifres (step 1), and miniprotein scaffolds are then docked on the target guided by these favourable side-chain interactions (step 2). The interface sequences are then designed to maximize interactions with the target (step 3). In the focused search stage, interface structural motifs are extracted and clustered (steps 4 and 5). These privileged motifs are then used to guide another round of docking and design (steps 6 and 7). Designs are then selected for experimental characterization based on computational metrics (step 8). See Extended Data Fig. 1 for a more detailed flow chart of the de novo binder design pipeline. **b**, Comparison of the sampling efficiency of PatchDock, RifDock and resampling protocols. Bar graph shows the distribution over the three approaches of the top 1% of binders based on Rosetta dd*G* and contact molecular surface values after pooling equal-CPU-time dock-and-design trajectories for each of the 13 target sites and averaging per-target distributions (Methods).

Cao, L. X., Coventry, B., Goreshnik, I., Huang, B. W., Sheffler, W., Park, J. S., Jude, K. M., Markovic, I., Kadam, R. U., Verschueren, K. H. G., Verstraete, K., Walsh, S. T. R., Bennett, N., Phal, A., Yang, A., Kozodoy, L., DeWitt, M., Picton, L., Miller, L., . . . Baker, D. (2022). Design of protein-binding proteins from the target structure alone. *Nature, 605(7910), 551-+.*

Design of peptide-drug conjugate ligands of the kappa-opioid receptor

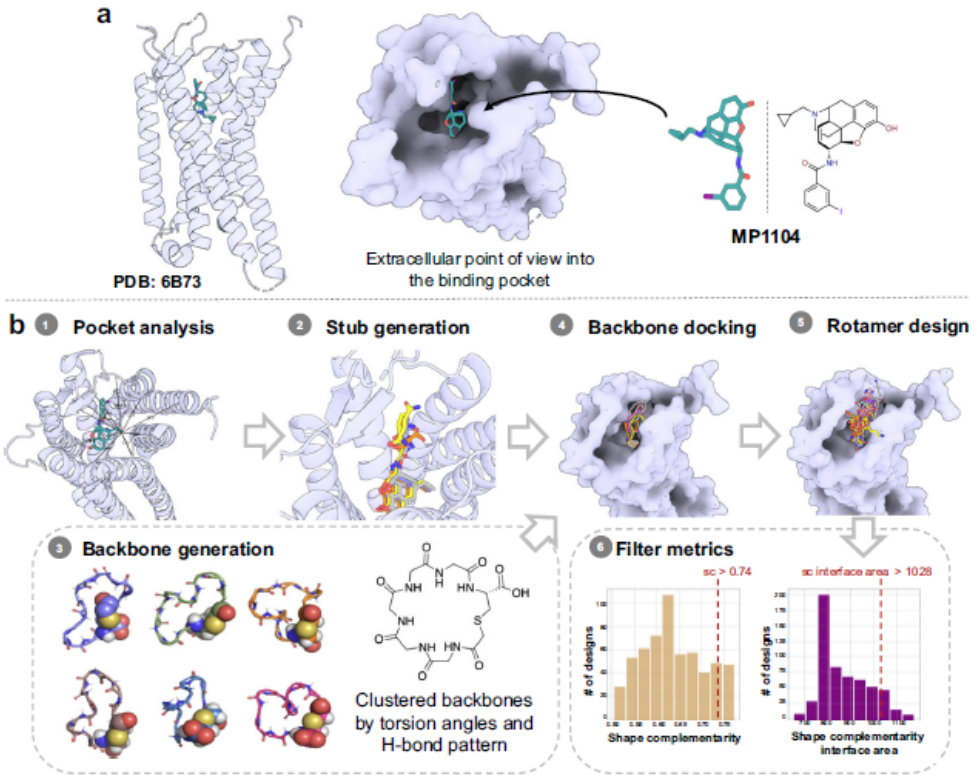

Fig. 1 | Strategy for the computational design of thioether macrocyclized peptide–small molecule conjugates targeting KOR. a 3D human KOR structure with small molecule agonist MP1104 was used as the starting template (PDB: 6B73). **b** Workflows for computational peptide–small molecule conjugate design: (1) Measurement of the pocket area (934 Å3) narrowed down the size of macrocycles to focus on 5- and 6-mer cyclic peptides. (2) Generation of small molecules with two additional amino acids, which were sampled and scored for optimal dimer sequence (select dipeptide modified small molecules: Gray: `CVV-D-Phe-Thr`; Yellow: `CVV-D-Phe-Gln`; Orange: `CVV-D-Phe-Ser`; CVV corresponds to N-cyclopropylmethyl-epoxy morphinan small molecule stub). (3) Generation of a comprehensive library of 5- and 6-mer thioether cyclized peptides clustered via torsion angle and hydrogen bond pattern. (4) Docked structure of thioether macrocyclized hexamers through coordinate-guided transformation of the backbone C-termini to the generated anchor N-termini. (5) Rotamer design to optimize the interface interactions of the backbones. (6) Design filtering based on shape complementarity and interface area as representative examples for interface metrics; dashed red line represents 90th percentile cut-off values.

Muratspahic, E., Deibler, K., Han, J., Tomasevic, N., Jadhav, K. B., Olive-Marti, A. L., Hochrainer, N., Hellinger, R., Koehbach, J., Fay, J. F., Rahman, M. H., Hegazy, L., Craven, T. W., Varga, B. R., Bhardwaj, G., Appourchaux, K., Majumdar, S., Muttenthaler, M., Hosseinzadeh, P., . . . Gruber, C. W. (2023). Design and structural validation of peptide-drug conjugate ligands of the kappa-opioid receptor. *Nat Commun, 14(1), 8064.*

How Stable Diffusion works in a Nutshell

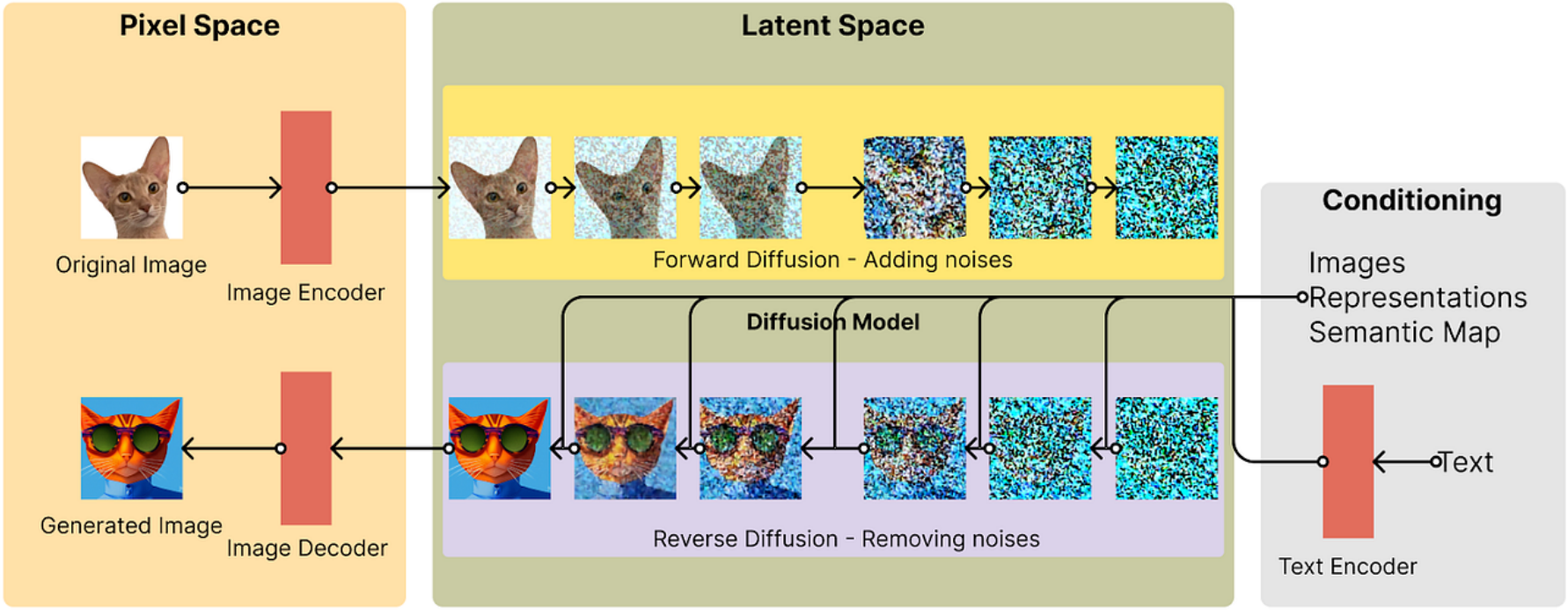

RFDiffusion for (Cyclic) Peptides

Normal positional embedding

0	1	2	3	4	5	6	7
-1	0	1	2	3	4	5	6
-2	-1	0	1	2	3	4	5
-3	-2	-1	0	1	2	3	4
-4	-3	-2	-1	0	1	2	3
-5	-4	-3	-2	-1	0	1	2
-6	-5	-4	-3	-2	-1	0	1
-7	-6	-5	-4	-3	-2	-1	0

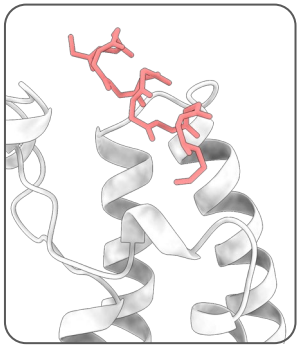

Cyclic positional embedding

0	1	2	3	-4	-3	-2	-1
-1	0	1	2	3	-4	-3	-2
-2	-1	0	1	2	3	-4	-3
-3	-2	-1	0	1	2	3	-4
-4	-3	-2	-1	0	1	2	3
3	-4	-3	-2	-1	0	1	2
2	3	-4	-3	-2	-1	0	1
1	2	3	-4	-3	-2	-1	0

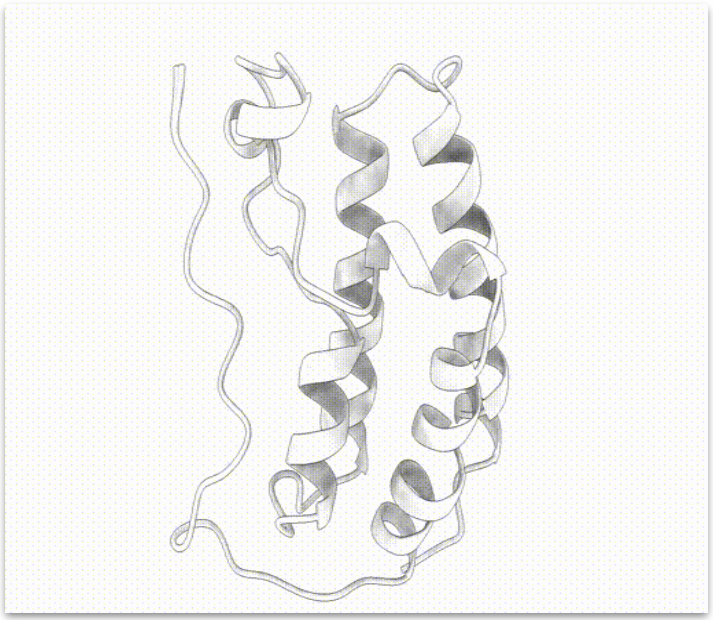

Max Beining, Clara Schoeder, Jens Meiler

RFDiffusion for (Cyclic) Peptides

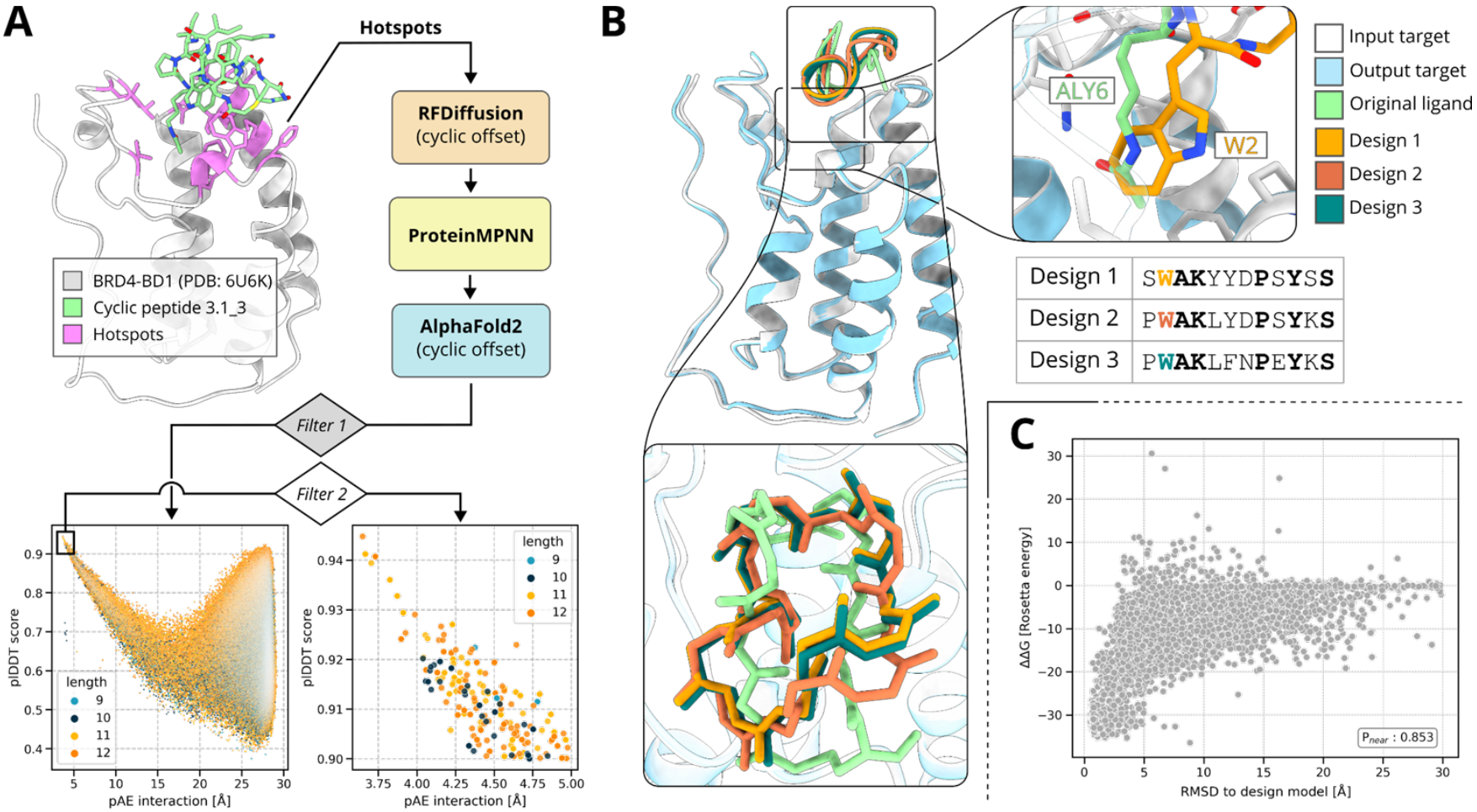

Generalized biomolecular modeling and design with RoseTTAFold All-Atom

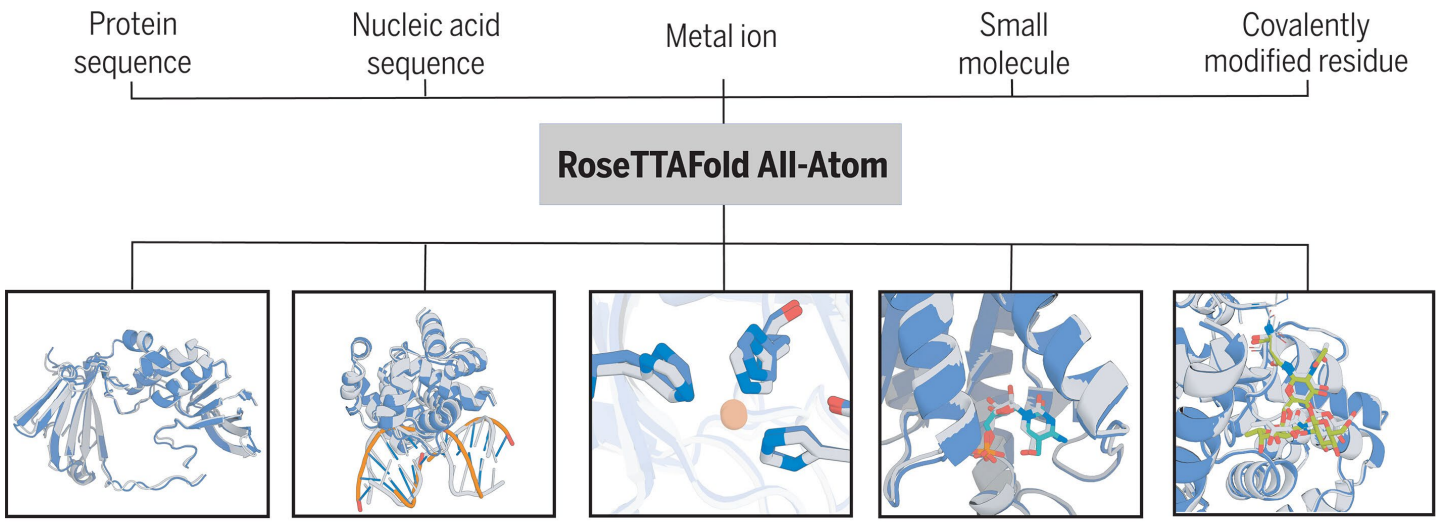

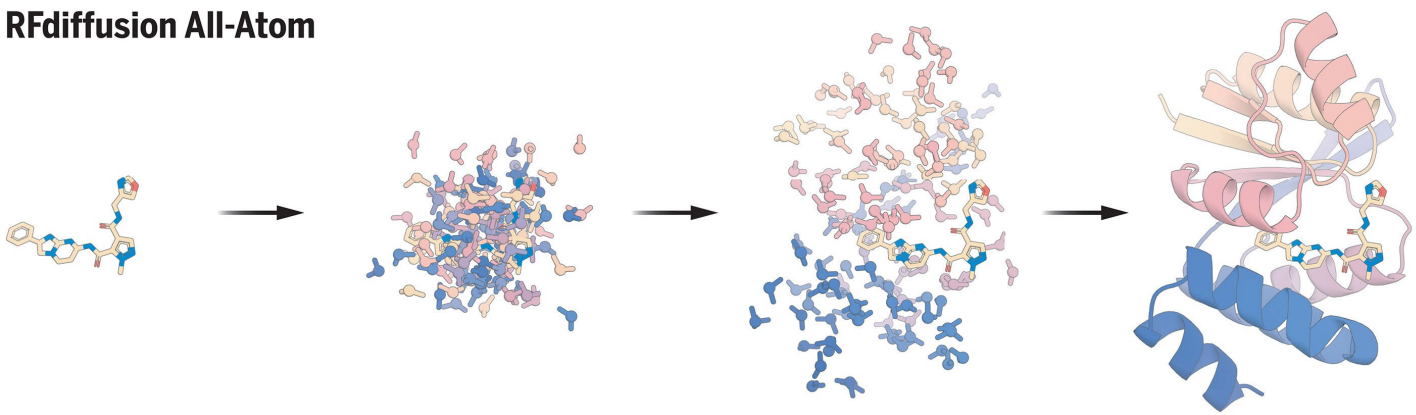

Krishna, R., Wang, J., Ahern, W., Sturmfels, P., Venkatesh, P., Kalvet, I., Lee, G. R., Morey-Burrows, F. S., Anishchenko, I., Humphreys, I. R., McHugh, R., Vafeados, D., Li, X., Sutherland, G. A., Hitchcock, A., Hunter, C. N., Kang, A., Brackenbrough, E., Bera, A. K., . . . Baker, D. (2024). Generalized biomolecular modeling and design with RoseTTAFold All-Atom. *Science, 384(6693), eadl2528.*

Acknowledgements

Current Members:
Abdullah Al Mamun
Alexander Fürll
Alican Gulsevin
Anja Landsmann
Benjamin Brown
Brennica Marlow
Carie Fortenberry
Carissa Li
Chris Jurich
Chris Moth
Claiborne Tydings
Cristina Martina
Davide Sala
Eli McDonald
Elleansar Okwei
Fabian Liessmann
Felipe Engelberger
Gustavo Araiza
Hope Woods
Jannis De Riz
Kaitlyn V. Ledwitch
Katherine Larochelle
Kortney Melancon
Kristina Vogel
Lance Liu
Lunkas v. Bredow
Mateusz Sklodowski
Moritz Ertelt
Michael Pritchard
Nathan Bloodworth
Oanh Vu
Paul Eisenhuth
Qianzhen Shao
Robert Mann
Rocco Moretti
Shannon Smith
Souhrid Mukherjee
Taylor Jones
Thomas Scott
Tracy Tang
Victoria Most
Vivian Ehrlich
Yidan Tang

Selected Alumni:
Annalen Bleckmann
Alex Sevy
Axel Fischer
Bian Li
Brett Kroncke
Brian Bender
Brian Weiner
Clara Schoeder
David Nannemann
Diego del Alamo
Georg Kuenze
Jeff Mendenhall
Jordon Willis
Julia Koehler Leman
Liz Dong Nguyen
Mariusz Butkiewicz
Nathan Alexander
Nils Woetzel
Nina Bozhanova
Steffen Lindert
Will Lowe

Collaborators: Jim Crowe, Heidi Hamm, Jeff Conn, Craig Lindsley, Seva Gurevich, Hassane Mchaourab, Dave Weaver, Ambra Pozzi, Chuck Sanders, Annette Beck-Sickinger, Daniel Huster, Christine Lovly, Carlos Arteaga

Funding: NIH NIGMS R01GM080403, NIH NIAID U19 AI117905, NIH NILBI R01HL122010, NSF CISE 1629811, NIH NIAID R01AI141661, NIH NCI R01CA227833, NIH NCI R01CA224899, NIH NIDA R01DA046138, NIH NIGMS R01GM129261, NIH NHGRI 3U01HG007674, BAYER, Boehringer Ingelheim, Alexander von Humboldt Foundation